IDEA

Innovations Deserving
Exploratory Analysis Programs

Highway IDEA Program

Performance Evaluation of 3-D Basalt Fiber Reinforced Concrete & Basalt Rod Reinforced Concrete

Final Report for Highway IDEA Project 45

Prepared by:
V Ramakrishnan and Neeraj S. Tolmare, South Dakota School of Mines & Technology, Rapid City, SD
Vladimir B. Brik, Research & Technology, Inc., Madison, WI

November 1998

TRANSPORTATION RESEARCH BOARD
OF THE NATIONAL ACADEMIES

IDEA PROGRAM FINAL REPORT
Contract No. NCHRP-45

IDEA Program
Transportation Research Board
National Research Council

November 1998

PERFORMANCE EVALUATION OF 3-D BASALT FIBER REINFORCED CONCRETE & BASALT ROD REINFORCED CONCRETE

V. Ramakrishnan
Neeraj S. Tolmare
South Dakota School of Mines & Technology, Rapid City, SD

Principal Investigator: Vladimir B. Brik
Research & Technology, Inc., Madison, WI

INNOVATIONS DESERVING EXPLORATORY ANALYSIS (IDEA) PROGRAMS MANAGED BY THE TRANSPORTATION RESEARCH BOARD (TRB)

This NCHRP-IDEA investigation was completed as part of the National Cooperative Highway Research Program (NCHRP). The NCHRP-IDEA program is one of the four IDEA programs managed by the Transportation Research Board (TRB) to foster innovations in highway and intermodal surface transportation systems. The other three IDEA program areas are Transit-IDEA, which focuses on products and results for transit practice, in support of the Transit Cooperative Research Program (TCRP), Safety-IDEA, which focuses on motor carrier safety practice, in support of the Federal Motor Carrier Safety Administration and Federal Railroad Administration, and High Speed Rail-IDEA (HSR), which focuses on products and results for high speed rail practice, in support of the Federal Railroad Administration. The four IDEA program areas are integrated to promote the development and testing of nontraditional and innovative concepts, methods, and technologies for surface transportation systems.

For information on the IDEA Program contact IDEA Program, Transportation Research Board, 500 5th Street, N.W., Washington, D.C. 20001 (phone: 202/334-1461, fax: 202/334-3471, http://www.nationalacademies.org/trb/idea)

PERFORMANCE EVALUATION OF 3-D BASALT FIBER REINFORCED CONCRETE & BASALT ROD REINFORCED CONCRETE

TABLE OF CONTENTS

LIST OF PHOTOGRAPHS

LIST OF SKETCHES

LIST OF TABLES

LIST OF FIGURES

Appendix A

Appendix B

Appendix C

GLOSSARY

The following is a glossary of terms for fiber reinforced concrete (FRC) used in this report.

0.1 GENERAL TERMS

Aspect Ratio - The ratio of length to diameter of the fiber. Diameter may be equivalent diameter.
Balling - When fibers entangle into large clumps or balls in a concrete mixture.
Collated - Fiber bundled together either by cross-linking or by chemical or mechanical means.
Equivalent Diameter - Diameter of a circle with an area equal to the cross-sectional area of the fiber.
Fiber content - The weight of fibers in a unit volume of concrete.
Fibrillated - A fiber with branching fibrils.
First Crack - The point on the flexural load-deflection or tensile load-extension curve at which the form of the curve first becomes nonlinear.
Hairline Crack – Cracks with widths less than 0.1 mm (0.0039 inches) are termed as hairline cracks.
First Crack Deflection - The deflection value on the load deflection curve at the first crack.
First Crack Strength - The stress obtained when the load corresponding to first crack is inserted in the formula for modulus of rupture given in ASTM Test Method C 78.
First Crack Toughness - The energy equivalent to the area of the load deflection curve up to the first crack.
Flexural Toughness - The area under the flexural load-deflection curve obtained from a static test of a specimen up to a specified deflection. It is an indication of the energy absorption capability of a material.
Toughness Indices - The numbers obtained by dividing the area under the load-deflection curve up to a specified deflection by the area under the load-deflection curve up to "First Crack" as given in ASTM C 1018.
Toughness Index, I_5 - The number obtained by dividing the area up to 3.0 times the first crack deflection by the area up to the first crack of the load deflection curve, as given in ASTM C 1018.
Toughness Index, I_{10} - The number obtained by dividing thc area up to 5.5 times the first crack deflection by the area up to the first crack of the load deflection curve, as given in ASTM C 1018
Toughness Index, I_{20} - The number obtained by dividing the area up to 10.5 times the first crack deflection by the area up to the first crack of the load deflection curve, as given in ASTM C 1018
Residual Strength Factor $R_{5,10}$ - The number obtained by calculating the value of $20(I_{10}-I_5)$, as given in ASTM C 1018.
Residual Strength Factor $R_{10,20}$ - The number obtained by calculating the value of $10(I_{20}-I_{10})$, as given in ASTM C 1018.
Flexural Toughness Factor (JCI) - The energy required to deflect the fiber reinforced concrete beam to a mid point deflection of 1/150 of its span.
Equivalent Flexural Strength (JCI) - It is defined by

$$F_c = T_b \times s/\delta_{tb} \times b \times d^2$$

where

F_c = equivalent flexural strength, psi
T_b = flexural toughness, inch-lb
s = span, inches
δ_{tb} = deflection of 1/150 of the span, inches
b = breadth at the failed cross-section, inches
d = depth at the failed cross-section, inches

Impact Strength - The total energy required to break a standard test specimen of a specified size under specified impact conditions, as given by ACI Committee 544.
Monofilament - Single filament fiber.
Static Modulus - The value of Young's modulus of elasticity obtained from measuring stress-strain relationships derived from other than dynamic loading.
High Performance Concrete - In this report, High Performance Concrete is defined as a concrete with highly enhanced (or improved) desirable properties for the specific purpose and function for which it is

used. It need not necessarily be high-strength concrete. High performance concrete may have one or more of the following properties enhanced: ductility, fatigue strength, durability, impact resistance, toughness, impermeability and wear resistance.
Whitetopping - Whitetopping is concrete placed over asphalt where the concrete thickness is 101 (4 inch) or more mm thick.
Ultra-Thin Whitetopping - Ultra-Thin Whitetopping is concrete placed over asphalt where the concrete is less than 101 mm (4 inch) thick.

0.2 ACRONYMS USED

ACI - American Concrete Institute
CFP - Collated Fibrillated Polypropylene
FRC - Fiber Reinforced Concrete
LS - Low Slump
NMFRC - Non-Metallic Fiber Reinforced Concrete. This acronym refers only to Polyolefin Fiber Reinforced Concrete. These fibers were manufactured and purchased from 3M for the purpose of this study.
NMFRS - Non-Metallic Fiber Reinforced Shotcrete
PFRC - Polypropylene Fiber Reinforced Concrete
PCC - Portland Cement Concrete
SFRC - Steel Fiber Reinforced Concrete.
SNFRC - Synthetic Fiber Reinforced Concrete
SIFCON - Slurry Infiltrated Fiber Concrete
SIMCON - Slurry Infiltrated Mat Concrete

0.3 ASTM SPECIFICATIONS

A 820 - Specification for Steel Fibers for Fiber Reinforced Concrete
C 31 - Practices for Making and Curing Concrete Test Specimens in the Field
C 39 - Test Method for Compressive Strength of Cylindrical Concrete Specimens
C 78 - Test Method for Flexural Strength of Concrete (Using Simple Beam with Third-point Loading)
C 94 - Specification for Ready-Mixed Concrete
C138 - Test for Unit Weight, Yield and Air Content (gravimetric) of concrete
C 143 - Test Method for Slump of Portland Cement Concrete
C 172 - Method of Sampling Freshly Mixed Concrete
C 173 - Test Method of Air Content of Freshly Mixed Concrete by the Volumetric Method
C 231 - Test Method for Air Content of Freshly Mixed Concrete by the Pressure Method
C 469 - Test Method for Static Modulus of Elasticity and Poisson's Ratio of Concrete in Compression
C 995 - Test Method for Time of Flow of Fiber Reinforced Concrete Through Inverted Slump cone
C1018 - Test Method for Flexural Toughness and First Crack Strength of Fiber - Reinforced Concrete (Using beam with Third-point Loading)
C 1116 - Specification for Fiber Reinforced Concrete and Shotcrete

0.4 INTERNATIONAL STANDARDS

A - American Concrete Institute Committee 544 Fiber Reinforced Concrete
ACI 544.2R.89 Flexural Fatigue Endurance
Impact Resistance
Toughness

B - British Standards Institute
BS1881: Part 2, Methods of Testing Concrete-Vebe Test

C - Japanese Society of Civil Engineers
JSCE Standard III-1, Specification of Steel Fibers for Concrete, Concrete Library, No. 50, March 1983.
- JSCE-SF4 Standard for Flexural Strength and Flexural Toughness, "Method of Tests for Steel Fiber Reinforced Concrete," *Concrete Library of JSCE,* No. 3, June 1984, Japan Concrete Institute (JCI), pp. 58-66.
- "Standard Test Method for Flexural Strength and Flexural Toughness of Fiber Reinforced Concrete, (Standard SF4),"*JCI Standards for Test Methods of Fiber Reinforced Concrete,* Japan Concrete Institute, 1983, pp. 45-51.

EXECUTIVE SUMMARY

This report presents the experimental investigation carried out to evaluate the performance characteristics of basalt fiber reinforced concrete and basalt bar reinforced concrete. The fibers and bars were supplied by Research & Technology Inc., Madison, WI.

All the experiments were conducted following the ASTM standards. The test program was conducted for fresh and hardened concrete properties. The fresh concrete properties consisted of the following tests: slump, Vebe slump, Vebe time, concrete temperature, air content and unit weight. The hardened concrete properties determined were compressive strength, static modulus, flexural strength, load-deflection behavior, comparison of load-deflection curves, ASTM toughness indices, first crack toughness, post crack behavior, Japanese standard method for toughness indices and equivalent flexural strength.

The test results show that the basalt fiber can be easily mixed in the concrete without any balling, bridging or segregation. There was a noticeable increase in the post crack energy absorption capacity and ductility due to the addition of basalt fibers. The impact resistance increased as the fiber content increased.

Tests were also conducted on beams reinforced with basalt bars, which were supplied by the manufacturer. The load deflection curves were plotted and the toughness indices and first crack toughness were calculated in a similar way as the ASTM standards for the beams reinforced with basalt fibers. Toughness indices according to the Japanese Standard method and the equivalent flexural strength were also calculated.

Tests were conducted on beams reinforced with basalt bars, which were designed and cast in the lab. Strain across the depth of the beams was measured, using electrical resistance strain gauges. Deflection was measured, using a magnetic dial gauge. The tests indicated that there was insufficient bond strength and the bars slipped gradually before the ultimate load was released. Beams with increased development lengths failed suddenly with breaking of rods. It was a sudden and brittle failure. The ultimate-load and cracking-load moments and the deflections of the basalt rod reinforced concrete beams were compared.

The tension tests were conducted on the basalt bars, and a cable, having two basalt bars twisted together. Graphs of stress vs. strain were plotted and the modulus of elasticity of the basalt bars was calculated.

1. INTRODUCTION

Plain concrete has two major deficiencies; a low tensile strength and a low strain at fracture. The tensile strength of concrete is very low because plain concrete normally contains numerous microcracks. It is the rapid propagation of these microcracks under applied stress that is responsible for the low tensile strength of the material. These deficiencies have led to considerable research aimed at developing new approaches to modifying the brittle properties of concrete.

Current research has developed a new concept to increase the concrete ductility and its energy absorption capacity, as well as to improve overall durability. This new generation technology utilizes fibers, which if randomly dispersed throughout the concrete matrix, provides better distribution of both internal and external stresses by using a three dimensional reinforcing network. (1,2,3)

The primary role of the fibers in hardened concrete is to modify the cracking mechanism. By modifying the cracking mechanism, the macro-cracking becomes micro-cracking. The cracks are smaller in width; thus reducing the permeability of concrete and the ultimate cracking strain of the concrete is enhanced. The fibers are capable of carrying a load across the crack. A major advantage of using fiber reinforced concrete (FRC) besides reducing permeability and increasing fatigue strength is that fiber addition improves the toughness or residual load carrying ability after the first crack. Additionally, a number of studies have shown that the impact resistance of concrete can also improve dramatically with the addition of fibers.

Combining the technical benefits and in place costs, FRC has been found to meet the prerequisites of value engineering for use, particularly in airport and highway pavements, in bridge deck overlays, curtain walls, sewer pipes and precast concrete products (2). Fibers have also been used in shotcrete for rockfill stabilization, tunnel linings and dome structures. FRC had been used extensively in overlays and repairs of airport pavements and bridge decks.

FRC composites are almost ideal materials for repair, rehabilitation, retrofit and renovation of the world's deteriorating infrastructure. Concrete fiber composites technology has grown over the last three decades into a mature industry. The purpose of this paper is to review the current research on basalt fiber reinforced concretes.

2. LITERATURE

2.1 LITERATURE REVIEW

The addition of fibers in concrete matrix has many important effects. Most noticeable among the improved mechanical properties of fiber reinforced concrete are its superior fracture resistance and resistance to impact and impulsive or dynamic loads. Secondly they impart additional strength under all modes of loading which include, direct tension, shear, flexural and torsion loading. The degrees of improvement of the mechanical characteristics of fiber reinforced concrete (FRC), are influenced by specimen size, loading configuration, size and type of fibers (4,5,6).

Even though reinforcing a brittle matrix with discrete fibers is an age old concept, modern-day use of fibers in concrete started in the early 1960s. In the beginning, only straight steel fibers were used. The major improvement occurred in the areas of ductility and fracture toughness, even though some flexural strength increases were observed. The law of mixtures was applied to analyze the fiber contributions.

Fibers have been produced from steel, plastic, glass and natural materials in various shapes and sizes. Fibers for commercial application of FRC have been of great variety including (7);

- Differing materials: steel, glass, polypropylene, polyolefin and cellulose are representative of the metallic, mineral, synthetic and natural fiber types.
- Differing amounts: ranging from relatively high fiber additions by volume to low-volume concentrations, with high, being considered in the range of 3 to 12 percent, intermediate in the range of 1 to 3 percent, and low in the range of 0.1 to 1 percent, based on the total volume of concrete produced.
- Differing fiber geometry: prismatic, round or flat, with deformations throughout or at the ends, irregular cross sections, fibrillated monofilament or bundles of fibers, fine (small effective diameter fibers of relatively high aspect (length to diameter) ratios, or coarse fibers of lower aspect ratios).

2.2 CURRENTLY USED FIBERS

2.2.1 Steel Fibers

The majority of the applications with steel fibers in the United States, has been with mixes using normal weight concrete. For straight steel fibers, the primary factors that controlled the properties of the composite were fiber volume fraction and aspect ratio of the fibers. The amount of fiber used ranged from 89 to 119 kg/m^3 (150 to 200 lb/cu. yard) of concrete. The major problems encountered in the early stages were difficulty in mixing and workability. At higher volume fractions, fibers were found to ball up during the mixing process. This process called balling was found to occur frequently for longer fibers. The size of the coarse aggregate was normally restricted to facilitate the use of short fibers and to avoid balling. Additionally, the mortar fraction of concrete was increased to combat the balling problem. There was always a reduction in workability with the addition of fibers. This tends to affect the quality of concrete in place, especially for higher fiber volume fractions (8 to 13).

2.2.2 Carbon Fibers

Until mid 1980's the high cost of carbon fibers limited their use in portland cement composites. More recently, low cost carbon fibers have been manufactured with petroleum and coal pitch. Carbon fibers are very light with a specific gravity of about 1.9 and inert to most of the chemicals. Even though their cost is higher than polymeric fibers, carbon fibers have potential for special applications that require high tensile and flexural strength. Carbon fibers are available in strands (tows) that can contain up to 12,000 individual filaments and have elastic modulus as high as steel and are two to three times stronger than steel.(2,14,15)

2.2.3 Glass Fibers

Experiments using glass fibers have been conducted in the United States since the early 1950's as well as in the United Kingdom and in Russia (15,16). Applications of fiber reinforced concrete investigated since the mid 1960's have included road and floor slabs, topping layers, refractory materials, and some precast concrete products. Glass fibers are primarily used for glass fiber reinforced cement (GFRC) sheets (16 to 21).

2.2.4 Synthetic Fibers

Synthetic fibers are most commonly added to concrete for slab-on-grade construction to reduce early plastic shrinkage cracking and increase impact and abrasion resistance and toughness. The fibers also can be added to precast concrete to improve resistance to handling stresses, to pumped concrete to improve cohesiveness, and to shotcrete, to reduce rebound and material waste.

Synthetic fibers are mainly polypropylene fibers and their use started since the early 1960's. The common forms of these fibers are smooth mono-filamented, twisted, fibrillated and tri-dimensional mat. Polypropylene fibers are hydrophobic, so they don't absorb water and have no effect on the mixing water requirements. It has a low density and is also chemically inert.

The major shortcomings of polymeric fibers are low modulus of elasticity, poor bond with cement matrix, combustibility, and low melting point. Their bond to cement matrix is improved by twisting several fibers together or by treating the fiber surface.

The latest development in the field of synthetic fibers is polyolefin fibers, with low aspect ratio similar to steel fibers for use in concrete. These fibers are available in various lengths and diameters and their addition will improve the structural properties of concrete like the steel fibers. They can be mixed with concrete in large quantities, as much as 20 % (by volume) without causing any balling, segregation or increase in air entrainment in concrete. It is possible to produce high volume fiber reinforced concrete using the regular concrete mixture proportions including coarse aggregates whereas high volume fiber concrete using steel fibers are produced using cement slurry instead of regular concrete. There are a number of advantages for polyolefin fibers, such as no corrosion potential, chemical inertness, and no hazardous or nuisance conditions when fibers become loose or protrude from the concrete surface. Unlike steel fibers, these fibers are non-magnetic and non-corrosive.

2.2.5 Basalt Fibers

Basalt fibers are manufactured in a single-stage process by melting pure raw material. They are environmentally safe and non-toxic, possess high heat stability and insulating characteristics and have an elastic structure. When used for composite materials, they provide unique mechanical properties. They can be easily processed into fabric with high reliability.

The tensile strength of continuous basalt fibers is about twice that of E-glass fibers and the modulus of elasticity is about 15-30% higher. Basalt fibers in an amorphous state exhibit higher chemical stability than glass fibers. When exposed to water at 70^0 C (158^0 F), basalt fibers maintain their strength for 1200 hours, whereas the glass fibers do so only for 200 hours.

2.2.6 Basalt Rod Reinforced Concrete

An exhaustive literature survey showed no data on basalt rod reinforced concrete.

3. PERFORMANCE EVALUATION OF 3-D BASALT FIBER REINFORCED CONCRETE

3.1 PROBLEM STATEMENT

Basalt fibers have been used in Russia for some time. However this technology is now being experimented in the United States of America. Before beginning the production and use of these fibers commercially, it was necessary to investigate the fiber in detail.

Therefore this investigation was undertaken to provide the needed information about the influence of various parameters on performance characteristics of basalt fiber reinforcement.

3.2 RESEARCH OBJECTIVES

The primary objective of this investigation was to determine the various parameters influencing the performance and properties of basalt fiber reinforced concrete specimens made of different fiber dosages. And these properties were compared with those of control (plain) concrete. The following tests were carried out to achieve the primary objective.

- The properties of fresh concretes with and without fibers.
- The properties of hardened concretes such as compressive strength, static modulus, static flexure strength, unit weight and impact strength.
- The toughness indices by the ASTM method with the help of load deflection curves.
- The flexural toughness factor and equivalent flexural strength by the Japanese Standard method.
- The variation of fresh and hardened concrete properties with respect to dosage of fibers.
- To compare the load deflection curves for various dosages of fibers.

3.3 MATERIALS

Fibers: The fibers used in this investigation were basalt fibers, which were supplied by Research & Technology Inc. The information about the fibers, as provided by the manufacturer is as follows:
Diameter of fiber = 12 μm (0.0005 in)
Length of fiber (Average) = 13 mm (0.52 in)
Cement: Type I/II normal portland cement satisfying ASTM C 150 requirements was used. The cement was supplied by Dacotah Cement, Rapid City, South Dakota.
Coarse Aggregate: The coarse aggregate used was crushed limestone, obtained from a local source in Rapid City, South Dakota. The maximum size of the aggregate used was 19 mm (0.75in) with absorption of 0.45%.
Fine Aggregate: The fine aggregate used was natural sand with a water absorption coefficient of 1.6%. Both the coarse and fine aggregates were according to the grading requirements of ASTM C33.
Water: The water used was tap water from the Rapid City, S. D. Municipal water supply system.

3.4 MIXES

A total of 5 mixes were done for the basalt fiber. The dosages of fibers added to the concrete were 0.1, 0.25, 0.4, 0.5 % by volume. The water cement ratio was kept constant at 0.5 for all the mixes. The mix proportions and designations are given in Table 1. One mix was done as control (plain) mix.

3.5 MIXING PROCEDURE

Mixing for the first two mixes was done in a batch of 2 cubic feet, whereas for the other three mixes, 2.5 cubic feet was batched out. All mixing was done in a nine cubic feet capacity mixer. The fibers were weighed accurately and kept in a separate plastic container. First the buffer mix was done. Then coarse aggregates were put in the mixer. Then the sand and two thirds of the water were added and mixed for one minute. Cement was then added along with the remaining one third of the water. Then the fibers were added and the ingredients mixed for three minutes, which was followed by a three minute rest period and a final mixing was done for 2 minutes so that the fibers distributed properly.

3.6 TEST SPECIMENS

The following specimens were cast from each mix:

- Six -- 101 x 101 x 356 mm (4inx 4in x 14in) beams – For Static Flexural Test.
- Six – 152 x 304 mm (6in x 12in) cylinders – For Compressive Strength and Static Modulus.
- Six – 152 x 63 mm (6in. dia. x $2^1/_2$in) cylinders – For Impact Test.

The specimens were cast according to the ASTM standards and covered with plastic sheets for 24 hrs at room temperature. They were then placed in a lime saturated water tank maintained at 22^0C (72^0 F). They remained in water till they were tested for 7 and 28 day strengths.

3.7 TESTS FOR FRESH CONCRETE

The freshly mixed concrete was tested for slump (ASTM C143), air content (ASTM C231), fresh concrete unit weight (ASTM C138), concrete temperature and Vebe time. No balling or segregation was observed even after the addition of larger quantities of fibers.

3.8 TESTS FOR HARDENED CONCRETE

3.8.1 Static Modulus and Compressive Strength

Cylinders were tested for static modulus (ASTM C469) and compressive strength (ASTM C39) at 7 days and 28 days.

3.8.2 Static Flexure Test

Beams were tested at 7 and 28 days for the static flexural strength (ASTM C1018). The span length was 300mm(12 in). This test is a deflection controlled test. The rate of deflection was kept in the range of 0.005 to 0.01mm(0.0002 to 0.0004 in) per minute as per ASTM C1018. The load at first crack and the maximum load reached were noted for every beam. From the load and deflections obtained, load-deflection curves were drawn from which the toughness indices and the residual strength factors by ASTM method and equivalent flexural strength by the Japanese Standard method were calculated.

The test apparatus used for the deflection measurement was according to ASTM standards. A specially designed frame was used to mount the dial gauge. This frame was supported only at the four points, which are on the neutral axis above the supports. The dial gauge was fixed such that it was touching the center point of the bottom surface. This arrangement enabled us to measure the true deflection excluding any extraneous deformations due to crushing of concrete at supports and load points, and any deformations and strains induced in the testing frame. Because the deflection is measured at the center point, any slight warping or twisting of beam will not affect true deflections measured. Hence the deflections measured were the true deflections of the beam. (5)

3.8.3 Impact Test

The specimens were tested for impact at 28 days by the drop weight test method (ACI 544). In this test method, the equipment consisted of a standard manually operated 4.55 kg (10 lbs) weight with an 0.45m (18") drop, a 63 mm (2.5") in diameter hardened steel ball, a flat steel base plate with a positioning bracket and four positioning lugs. The specimen was placed on the base plate with its rough surface facing upwards. The hard steel ball was placed on the top of the specimen and the compactor was placed with its base on the steel ball. The test was performed on a flat rigid surface to minimize the energy losses. The hammer was dropped consecutively, and the number of blows required to cause the first visible crack on the specimens was recorded. The impact resistance of the specimen to ultimate failure was also recorded by the number of blows required to open the crack sufficiently so that the pieces of the specimen were touching at least three of the four positioned lugs on the base plate.

3.9 FRESH CONCRETE PROPERTIES

Room temperature, humidity and concrete temperature were recorded to ensure that all the mixes were carried out under similar conditions. The room temperature and humidity varied in the range of 18^0C to 26^0C (65^0F to 80^0F) and 25% to 35% respectively. The concrete temperature range was 20^0C to 24^0C (68^0F to 76^0F). The unit weights of fiber concrete and plain concrete were approximately the same and no noticeable change was observed due to addition of fibers. The fresh concrete properties are given in Table 2.

3.9.1 Workability

Two tests were performed to determine the workability of the mixes; slump (consistency) and Vebe time along with the Vebe slump (consolidation). These test results indicate that satisfactory workability can be maintained even with the addition of the fibers. The test results indicate that the slump and Vebe slump decreases with the addition of fibers, whereas the Vebe time increases with the addition of the fibers. Vebe time measures the workability of concrete based on the energy needed to compact the concrete. The concrete started to harden in about 40 to 45 minutes. The fibers mixed well and were uniformly distributed throughout the concrete. Overall, there was no balling, bleeding or segregation. Even though the slump values show the decreasing trend with the addition of the fibers, no difficulty was encountered in placing and consolidating the concrete with the use of the table vibrator.

3.9.2 Air Content

The air content ranged from 1.8% to 2.6%. It was constant at 2.2% for three of the mixes. No air-entraining agent was used. Therefore the measured air is considered as entrapped air.

3.10 HARDENED CONCRETE PROPERTIES

3.10.1 Compressive Strength and Static Modulus Test

The results of the compressive strength are tabulated in Table 3A and 3B. There is little or no variation in the compressive strength. Compressive strength depends on water cement ratio and air content. If the water cement ratio is less, compressive strength will be more. Likewise, if the air content is more, the compressive strength will be less.

A ductile mode of failure, as compared to plain concrete's brittle failure, was observed while testing for compressive strength. The plain concrete cylinder failed fully shattering into pieces with a loud noise, whereas the fiber reinforced concrete cylinders continued to sustain the load and underwent deformation without totally breaking into pieces. The change of mode of failure from a brittle type to a ductile type is an important contribution due to the addition of fibers.

The static modulus test served primarily as a means of quality control. The results indicate that the mixes were reasonably consistent and the addition of fibers had no effect on the static modulus. The comparison of compressive strength for the plain concrete and fiber concretes is shown in the form of a bar chart in Fig. 1.

3.10.2 Static Flexural Strength

The static flexural strength test results, the first crack load, first crack deflection, ultimate load and flexural stress are given in Table 4A and 4B. When the fiber concrete beams are loaded in flexure, the behavior is more or less linear up to the first crack and then the curve is significantly non-linear and reaches its peak at the ultimate strength or at the maximum sustainable static load. One factor that significantly influences the flexure test is the fiber volume.

The mode of failure was a simultaneous yielding of the fibers and the matrix. The cracks were prevented from propagating until the composite ultimate stress was reached. The load deflection curves indicate a ductile behavior and large energy absorption. Fibers when added in significant volume fractions, increase the first crack and ultimate flexural strengths of concrete. The flexural strengths are compared in Fig. 2.

3.10.3 Load Deflection Behavior

The area under the curve represents the energy absorbed by the beam. Load deflection curves for both the pre first crack and post first crack data, were drawn. Toughness indices and the residual strength indices were calculated by using these curves.

3.10.4 Flexural Toughness (Energy Absorption)

Toughness or energy absorption of concrete is increased considerably by the addition of fibers (2). Toughness index is the measure of the amount of energy required to deflect the 100 mm (4in) beam in the modulus of rupture test. The most important variable governing the toughness index of fiber reinforced concrete is the fiber efficiency. Other parameters influencing the toughness index are the position of the crack, the fiber type, aspect ratio, volume fraction and the distribution of fibers. Fiber efficiency is controlled by the resistance of the fiber to pull out from the matrix, which is developed as a result of the bond strength at the fiber matrix interface. The advantage of pullout type of failure of fiber is that, it is gradual and ductile, compared to a more rapid and catastrophic failure, which may occur, if fibers are brittle and fail in tension with little or no elongation. The fiber pullout or fracture depends on the yield strength of the fibers, the bond and anchorage between the matrix and the fiber.

Toughness index (ASTM C1018) is a dimensionless parameter, which defines or finger prints the shape of the load deflection curve. Indices have been defined on the basis of three service levels, identified as the multiples of the first crack deflection. The index is computed by dividing the total area under the load deflection curve up to the first crack deflection. The toughness index I_5 is calculated at three times the first crack deflection. Likewise I_{10}, I_{20} and I_{30} are the indices up to 5.5, 10.5 and 15.5 times the first crack deflection respectively (5). The toughness indices and the residual strength indices are shown in the form of bar charts in Fig. 3A, 3B, 3C and 3D. The toughness index ratio is shown in Fig. 3E and 3F. The toughness indices are tabulated in Tables 5A and 5B. The load deflection curves plotted for both 7 and 28 day results are shown in Appendix A.

3.10.5 Japanese Standard Method of Calculating Flexural Toughness Factor and Equivalent Flexural Strength

In addition to the toughness indices, the equivalent flexural strength (F_e) as specified by the Japanese Society of Civil Engineers (JSCE) was calculated for all the specimens. (5)

The Japanese Toughness Test takes into account the absorbed energy up to the deflection of L/150th of the span. The equivalent flexural strength was calculated using the following equation.

$$F_e = T_b * L/\delta t_b * b * h^2$$

where F_e = equivalent flexural strength

T_b= flexural toughness, (in-lb)

L= span in inches

δt_b = deflection of L/150th of the span

b = width of failed cross section in inches

h = depth of failed cross section in inches

The Japanese flexural toughness factors and equivalent flexural strength were also calculated. The results are tabulated in Tables 6A and 6B. The results clearly indicate that the toughness increases with the increase in the fiber dosage. Comparative bar chart of the Japanese toughness indices is shown in Fig. 4A and the equivalent flexural strength in Fig. 4B.

3.10.6 Impact Strength

The drop weight test (ACI committee 544) was used in this investigation. This is a very simple and inexpensive test that can be done anywhere including in the field. If more specimens are tested, the mean values indicate qualitatively a good index of the impact resistance of the material.

The impact test was done for 28 days strength, for both plain and fiber reinforced specimens. The results prove that the fiber concrete had greater impact resistance compared to the plain concrete. Impact strength increases with the increase in the fiber content. The age of the specimen also affects the impact strength.

The results clearly indicate the increase in number of blows for the increase in the fiber dosage. The results are tabulated in Table 7 and a comparative bar chart is also shown in Fig. 5.

3.11 CONCLUSIONS

- Satisfactory workability can be maintained, with the addition of basalt fibers, up to 0.5% by volume.
- Larger quantities of fibers, compared to polypropylene fibers, could be added without causing any balling or segregation.
- The performance of basalt fiber reinforced concrete is similar to that of the polypropylene fiber reinforced concrete currently being used in the market.
- Compared to the control (plain) concrete, there was considerable increase in the toughness and impact strengths.
- The most important contribution due to the addition of fibers, is the change of mode of failure from a brittle to ductile failure, when subjected to compression, bending and impact.

3.12 RECOMMENDATIONS

Based on the observations from earlier research conducted using polypropylene fibers, it is suggested that the length of the fibers be increased to 50mm (2in) for a more efficient performance.

Table 1:Mix Proportions for Basalt Fiber Reinforced Concrete

For 0.057 m^3 (2.0 $ft.^3$)

Mix Degn.	Water Cement Ratio	Fibers kg(lbs)	Fibers Vol %	Weight in kg(lbs) Cement kg(lbs)	Coarse Agg. kg(lbs)	Fine Agg kg(lbs)	Water kg(lbs)
B1	0.5	......	......	20.85 (45.2)	53.1 (117)	53.1 (117)	10.25 (22.6)
B2	0.5	0.68 (1.5)	0.5	20.85 (45.2)	53.1 (117)	53.1 (117)	10.25 (22.6)

For 0.071 m^3 (2.5 $ft.^3$)

B3	0.5	0.54 (1.12)	0.4	25.68 (56.5)	66.5 (146.3)	66.5 (146.3)	12.83 (28.3)
B4	0.5	0.43 (0.94)	0.25	25.68 (56.5)	66.5 (146.3)	66.5 (146.3)	12.83 (28.3)
B5	0.5	0.17 (0.38)	0.1	25.68 (56.5)	66.5 (146.3)	66.5 (146.3)	12.83 (28.3)

Basic Mix Proportions for one m^3 (yd^3)

Cement kg(lbs)	Water kg(lbs)	Fine Agg. kg(lbs)	Coarse Agg. kg(lbs)	Water Cement Ratio
361.9 (610)	188 (305)	937.4 (1580)	937.4 (1580)	0.5

Table 2:PROPERTIES OF FRESH CONCRETE

Mixture Type	Mixture Designation	Slump (inches)	Vebe Time (secs)	Vebe Slump (inches)	Air Content (%)	Unit Weight (lb/ft^3)	Concrete Temp. (^0F)	Remarks
Plain	B1	1.5	3	1	1.8	150.4	78.8	
BFRC	B2	0.25	9	0	2.6	147.6	78.8	Some of the fibers were added along with the aggregates.
BFRC	B3	0.375	5	0.125	2.2	146.8	75.2	Balling or Segregation of Fibers did not occur
BFRC	B4	1	3	0.25	2.2	148	77	
BFRC	B5	1.5	2	2	2.2	149.6	77	
BRRC	BR-1	3	--	--	2	147.2	78.1	
BRRC	BR-2	2.75	--	--	2	147.6	78.2	

Conversion Factors:

25.4 mm = 1 in.
$^0C = (^0F - 32)/1.8$
1 kg/m^3 = 0.0625 lb/ft^3

TABLE 3A: CYLINDER COMPRESSIVE STRENGTH & ELASTIC MODULUS -- 7 DAYS

Mix Type	Specimen #	Age (Days)	Dimensions		Unit Weight	Static Modulus	Compressive Strength
			Length	Diameter	lb/ft^3	(10^6 psi)	(psi)
Plain	B1C1	7	12.0	6.0	150.3	4.8	5040
	B1C2	7	12.0	6.0	151.1	4.9	5160
	B1C3	7	---	---	---	---	---
	Average				150.7	4.8	5100
BFRC	B2C1	7	12.0	6.0	150.3	4.7	5680
	B2C2	7	12.0	6.0	150.8	4.9	5670
	B2C3	7	---	---	---	---	---
	Average				150.6	4.8	5675
BFRC	B3C1	7	12.0	6.0	150.8	4.9	4970
	B3C2	7	12.0	6.0	148.4	4.8	5030
	B3C3	7	12.0	6.0	150.4	4.8	5010
	Average				149.9	4.8	5000
BFRC	B4C1	7	12.0	6.0	150.4	4.9	5170
	B4C2	7	12.0	6.0	150.8	4.7	4530
	B4C3	7	12.0	6.0	149.9	4.9	4820
	Average				150.3	4.8	4840
BFRC	B5C1	7	12.0	6.0	150.4	4.9	5040
	B5C2	7	12.0	6.0	150.4	4.9	4750
	B5C3	7	12.0	6.0	150.1	4.7	4980
	Average				150.3	4.8	4920

Conversion Factors:

1 MPa = 145 psi
1 kg = 2.2 lbs
25.4 mm = 1in.
1 kg/m^3 = 0.0625 lb/ft^3

TABLE 3B: CYLINDER COMPRESSIVE STRENGTH & ELASTIC MODULUS -- 28 DAYS

Mix Type	Specimen #	Age (Days)	Dimensions		Unit Weight	Static Modulus	Compressive Strength
			Length	Diameter	lb/ft^3	(10^6 psi)	(psi)
Plain	B1C4	28	12.0	6.0	150.7	5.3	6330
	B1C5	28	12.0	6.0	148.0	4.3	6480
	---	---	---	---	---	---	---
	Average		12.0	6.0	149.4	4.8	6405
BFRC	B2C4	28	12.0	6.0	148.0	4.8	6680
	B2C5	28	12.0	6.0	148.0	4.8	6600
	---	---	---	---	---	---	---
	Average		12.0	6.0	148.0	4.8	6640
BFRC	B3C4	28	12.0	6.0	147.0	5.3	5930
	B3C5	28	12.0	6.0	148.0	4.7	6280
	B3CS	28	12.0	6.0	147.5	4.3	5860
	Average		12.0	6.0	147.5	4.8	6020
BFRC	B4C4	28	12.0	6.0	147.9	4.7	6040
	B4C5	28	12.0	6.0	148.0	4.8	6100
	B4CS	28	12.0	6.0	147.0	4.8	6300
	Average		12.0	6.0	147.6	4.8	6150
BFRC	B5C4	28	12.0	6.0	147.8	4.8	5980
	B5C5	28	12.0	6.0	147.4	5.0	6020
	B5CS	28	12.0	6.0	147.8	4.7	6030
	Average		12.0	6.0	147.7	4.8	6010

Conversion Factors:

1 kg/m^3 = 0.0625 lb/ft^3
1 Mpa = 145 psi
25.4 mm = 1 in.

TABLE 4A: FIRST CRACK STRENGTH AND MAXIMUM FLEXURAL STRENGTH -- 7 DAYS

Mixture Type	Specimen #	Age (Days)	First Crack Load (lbs)	First Crack Deflection (inches)	First Crack Stress (psi)	Maximum Load (lbs)	Flexural Strength (psi)
Plain	B1B1	7	4096	---	819	4096	820
	B1B2	7	4932	---	950*	4932	950*
	B1B3	7	4393	---	850	4393	850
	Average				835		835
BFRC	B2B1	7	4000	0.0018	772	4340	840
	B2B2	7	3500	0.0009	679	3903	760
	B2B3	7	3000	0.0007	597	3968	790
	Average				683		795
BFRC	B3B1	7	3600	0.002	691	4669	900
	B3B2	7	3200	0.0019	613	4552	870
	B3B3	7	4000	0.002	766	4240	810
	Average				690		860
BFRC	B4B1	7	4000	0.0021	770	4583	880
	B4B2	7	4000	0.0023	767	4737	910
	B4B3	7	4000	0.0022	767	4580	880
	Average				768		890
BFRC	B5B1	7	3600	0.0027	693	4225	810
	B5B2	7	3200	0.0024	611	3900	745
	B5B3	7	3200	0.0019	614	3942	755
	Average				639		770

* - This value is considered as an outlayer as per statistical considerations, and is omitted in calculating the average.

Conversion Factors:

1 MPa = 145 psi
1 kg = 2.2 lbs
25.4 mm = 1in.

Table 4B:FIRST CRACK STRENGTH AND MAXIMUM FLEXURAL STRENGTH -- 28 DAYS

Mixture Type	Specimen #	Age (Days)	First Crack Load (lbs)	First Crack Deflection (inches)	First Crack Stress (psi)	Maximum Load (lbs)	Flexural Strength (psi)
Plain	B1B4	28	4723	---	888.2	4723.0	890
	B1B5	28	5650	---	1061.5*	5650.0	1060*
	B1B6	28	4846	---	909.1	4846.0	910
	Average		5073		895.0	5073.0	895
BFRC	B2B4	28	3600	0.0014	677.0	4230.0	795
	B2B5	28	3600	0.0013	679.0	4760.0	900
	B2B6	28	3600	0.0011	679.0	4390.0	830
	Average		3600	0.001267	678.3	4460.0	840
BFRC	B3B4	28	3600	0.0014	677.0	4712.0	890
	B3B5	28	4000	0.0015	751.0	4864.0	910
	B3B6	28	4000	0.0015	752.0	4792.0	900
	Average		3867	0.001467	726.7	4789.3	900
BFRC	B4B4	28	4450	0.0014	836.0	4450.0	840
	B4B5	28	4437	0.0016	833.8	4437.0	830
	B4B6	28	4955	0.0015	930.7	4955.0	930
	Average		4614	0.0015	866.8	4614.0	900
BFRC	B5B4	28	4618	0.0012	867.2	4618.0	870
	B5B5	28	4396	0.0011	825.5	4396.0	830
	B5B6	28	4713	0.0013	885.5	4713.0	890
	Average		4576	0.0012	859.4	4575.7	860

*- This value is considered as an outlayer as per statistical considerations, and is omitted in calculating the average.

Conversion Factors:

25.4 mm = 1 in.
1 kg = 2.2 lbs
1 MPa = 145 psi

TABLE 5A: ASTM- TOUGHNESS INDICES -- 7 DAYS

Mixture Type	Specimen #	First Crack Toughness (inch-lbs)	Toughness Indices			Toughness Ratios		Residual Strength Indices	
			I5	I10	I20	I10/I5	I20/I10	$R_{5,10}$	$R_{10,20}$
Plain	B1B1	---	---	---	---	---	---	---	---
	B1B2	---	---	---	---	---	---	---	---
	B1B3	---	---	---	---	---	---	---	---
	Average								
BFRC	B2B1	4.1	4.3	7.6	11.6	1.8	1.5	66.6	39.7
	B2B2	1.7	4.8	9.0	15.2	1.9	1.7	84.8	61.4
	B2B3	1.2	5.0	9.6	17.1	1.9	1.8	92.6	74.2
	Average	2.4	4.7	8.8	14.6	1.9	1.7	81.3	58.4
BFRC	B3B1	4.1	4.3	6.6	8.7	1.5	1.3	46.0	20.5
	B3B2	3.6	4.6	8.6	14.5	1.9	1.7	79.2	59.0
	B3B3	4.3	4.6	8.0	10.9	1.7	1.4	67.2	29.4
	Average	4.0	4.5	7.7	11.4	1.7	1.5	64.1	36.3
BFRC	B4B1	4.9	4.0	6.0	8.1	1.5	1.3	40.2	20.5
	B4B2	5.0	4.6	7.7	10.2	1.7	1.3	62.4	24.1
	B4B3	5.1	4.4	8.2	14.2	1.9	1.7	75.8	59.2
	Average	5.0	4.4	7.3	10.8	1.7	1.5	59.5	34.6
BFRC	B5B1	5.0	5.1	9.4	15.6	1.9	1.7	87.2*	31.4
	B5B2	4.3	4.6	8.4	13.8	1.8	1.7	72.0	30.6
	B5B3	3.6	4.6	8.7	15.2	1.9	1.7	70.0	30.9
	Average	4.3	4.7	8.8	14.8	1.9	1.7	71.0	31.0

Conversion Factor:
1 in-lb = 0.113 Nm

* - This value is considered as an outlayer as per statistical considerations, and is omitted in calculating the average.

TABLE 5B: ASTM- TOUGHNESS INDICES -- 28 DAYS

Mixture Type	Specimen #	First Crack Toughness (inch-lbs)	Toughness Indices				Toughness Ratios			Residual Strength Indices	
			I5	I10	I20	I30	I10/I5	I20/I10	I30/I20	$R_{5,10}$	$R_{10,20}$
Plain	B1B4	---	---	---	---	---	---	---	---	---	---
	B1B5	---	---	---	---	---	---	---	---	---	---
	B1B6	---	---	---	---	---	---	---	---	---	---
	Average										
BFRC	B2B4	2.6	6.8	13.8	24.4	30.5	1.7	1.7	1.0	140.0	76.8
	B2B5	2.7	5.2	13.8	20.4	23.2	1.9	1.6	1.1	172.0	66.0
	B2B6	2.3	5.6	10.6	18.1	22.4	1.8	1.6	1.1	100.0	69.0
	Average	2.5	5.9	12.7	21.0	25.4	1.8	1.6	1.1	137.3	70.6
BFRC	B3B4	2.1	5.1	8.8	15.3	15.9	2.0	1.8	1.3	97.9	65.0
	B3B5	2.8	4.9	9.0	14.3	15.8	2.6	1.5	1.1	98.8	53.0
	B3B6	2.2	5.0	9.1	14.1	15.5	1.9	1.7	1.2	99.0	50.0
	Average	2.4	5.0	9.0	14.6	15.7	2.2	1.7	1.2	98.6	56.0
BFRC	B4B4	2.0	4.6	8.8	14.7	15.0	1.9	1.7	1.0	84.0	48.9
	B4B5	2.2	4.7	8.7	14.6	15.1	1.9	1.7	1.0	80.0	47.2
	B4B6	2.0	4.8	8.9	14.8	14.9	1.9	1.7	1.0	82.0	47.8
	Average	2.1	4.7	8.8	14.7	15.0	1.9	1.7	1.0	82.0	48.0
BFRC	B5B4	1.8	4.0	8.0	11.7	13.6	2.0	1.5	1.2	80.9	37.7
	B5B5	2.0	4.1	8.4	11.9	13.8	2.0	1.4	1.2	83.5	36.5
	B5B6	1.9	4.2	8.2	12.1	14.0	2.0	1.5	1.2	82.2	37.2
	Average	1.9	4.1	8.2	11.9	13.8	2.0	1.5	1.2	82.2	37.1

Conversion Factor:
1 in-lb = 0.113 Nm

TABLE 6A: JAPANESE STANDARD- TOUGHNESS & EQUIVALENT FLEXURAL STRENGTH -- 7 DAYS

Mixture Type	Specimen #	Age (Days)	Toughness (inch-lbs)	Equivalent Flexural Strength (psi)
Plain	B1B1	7.0	---	---
	B1B2	7.0	---	---
	B1B3	7.0	---	---
	Average			
BFRC	B2B1	7.0	52.7	123.7
	B2B2	7.0	52.8	124.5
	B2B3	7.0	47.2	111.1
	Average		50.9	119.8
BFRC	B3B1	7.0	79.8	187.4
	B3B2	7.0	84.6	200.7
	B3B3	7.0	80.0	189.5
	Average		81.0	192.5
BFRC	B4B1	7.0	49.0	186.0
	B4B2	7.0	51.5	189.0
	B4B3	7.0	48.6	188.0
	Average		49.7	187.7
BFRC	B5B1	7.0	31.6	172.0
	B5B2	7.0	32.0	171.0
	B5B3	7.0	30.0	173.0
	Average		31.2	172.0

Coversion Factors:

1 MPa = 145 psi
1 in-lb = 0.113 Nm

TABLE 6B:JAPANESE STANDARD-TOUGHNESS & EQUIVALENT FLEXURAL STRENGTH -- 28 DAYS

Mixture Type	Specimen #	Age (Days)	Toughness (inch-lbs)	Equivalent Flexural Strength
Plain	B1B4	28	---	---
	B1B5	28	---	---
	B1B6	28	---	---
	Average			
BFRC	B2B4	28	83.0	201.0
	B2B5	28	75.0	182.0
	B2B6	28	83.0	207.0
	Average		80.3	197.0
BFRC	B3B4	28	80.0	191.0
	B3B5	28	94.0	225.0
	B3B6	28	81.0	194.0
	Average		85.0	209.0
BFRC	B4B4	28	69.6	220.0
	B4B5	28	67.2	219.0
	B4B6	28	68.1	218.0
	Average		68.3	219.0
BFRC	B5B4	28	59.6	204.0
	B5B5	28	58.2	205.0
	B5B6	28	56.3	209.0
	Average		58.0	206.0

Conversion Factors:

1 MPa = 145 psi
1 in-lb = 0.113 Nm

TABLE 7: IMPACT TEST RESULTS -- 28 DAYS

Mixture Type	Age (Days)	Specimen #	Number of Blows to		Difference in no. of blows from first crack to failure
			First Crack	Failure	
Plain	28	B1-1	77.0	80.0	3.0
	28	B1-2	55.0	61.0	6.0
	28	B1-3	23.0	27.0	4.0
	28	B1-4	14.0	18.0	4.0
		Average	42.3	46.5	4.3
BFRC	28	B2-1	13.0	44.0	31.0
	28	B2-2	8.0	59.0	51.0
	28	B2-3	26.0	63.0	37.0
	28	B2-4	9.0	27.8	18.8
		Average	14.0	48.5	34.5
BFRC	28	B3-1	8.0	49.7	41.7
	28	B3-2	12.0	77.0	65.0
	28	B3-3	107.0	116.0	9.0
	28	B3-4	108.0	127.0	19.0
	28	B3-5	59.0	72.0	13.0
	28	B3-6	14.0	34.0	20.0
		Average	51.3	79.3	28.0
BFRC	28	B4-1	26.0	90.0	64.0
	28	B4-2	98.0	106.0	8.0
	28	B4-3	40.0	57.0	17.0
	28	B4-4	30.0	52.0	22.0
	28	B4-5	62.0	81.0	19.0
	28	B4-6	18.0	28.0	10.0
		Average	45.7	69.0	23.3
BFRC	28	B5-1	40.0	62.0	22.0
	28	B5-2	43.0	59.0	16.0
	28	B5-3	36.0	49.0	13.0
	28	B5-4	54.0	96.0	42.0
	28	B5-5	54.0	77.0	23.0
	28	B5-6	48.0	64.0	16.0
		Average	45.8	67.8	22.0

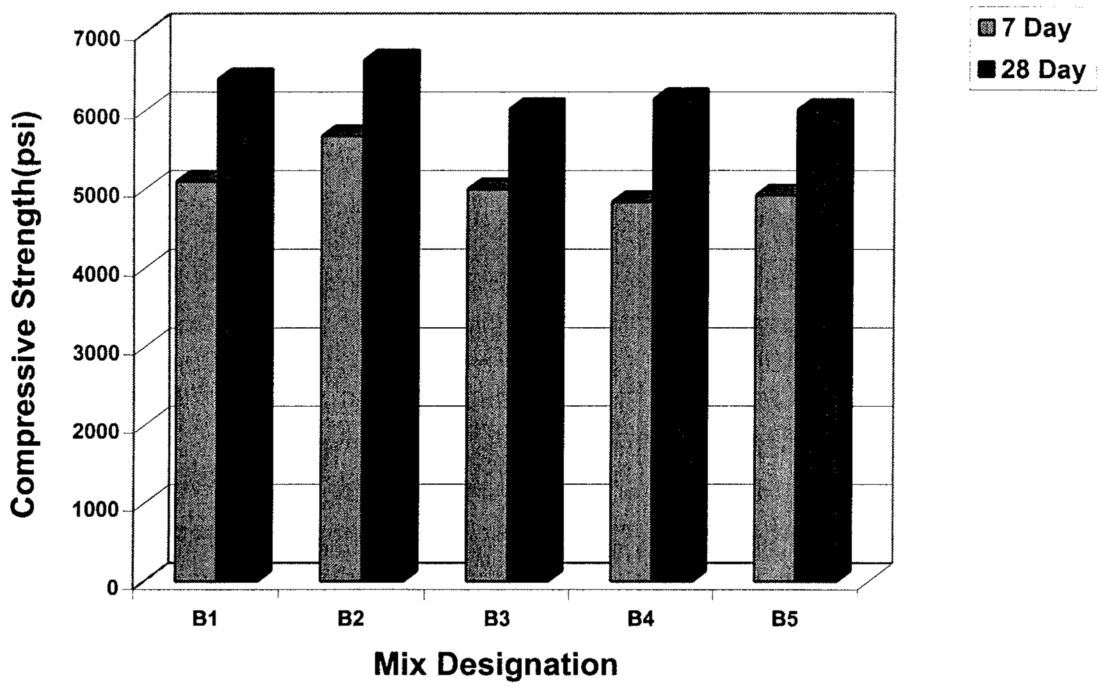

Fig. 1 Comparison of Compressive Strength

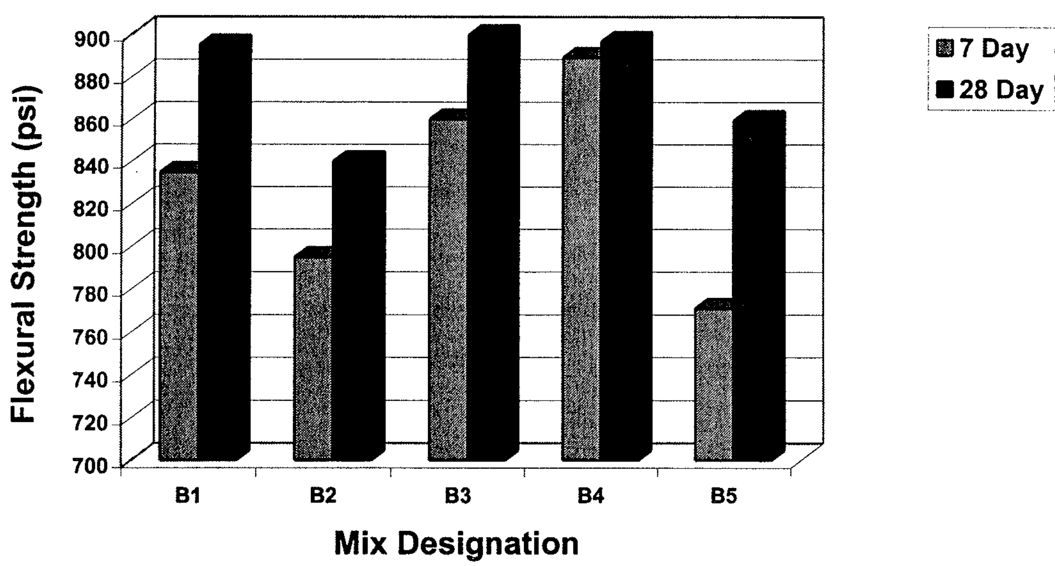

Fig. 2 Comparison of Flexural Strength

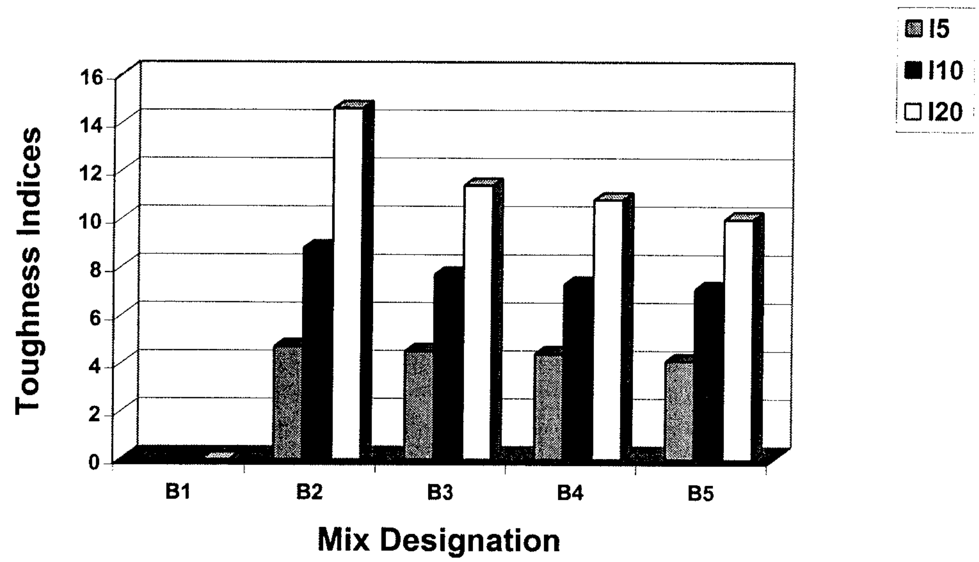

Fig. 3A Comparison of Toughness Indices (7 Day)

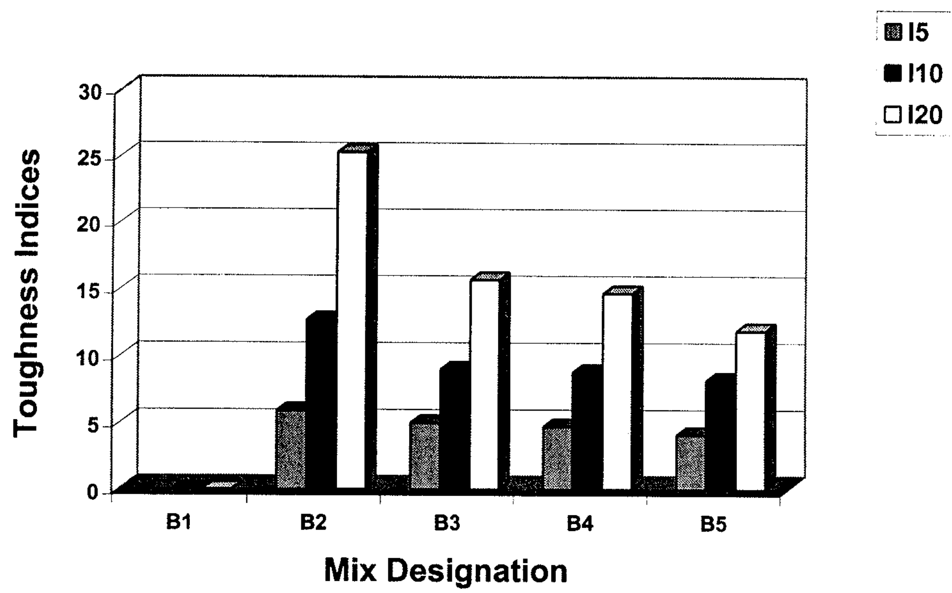

Fig. 3B Comparison of Toughness Indices (28 Day)

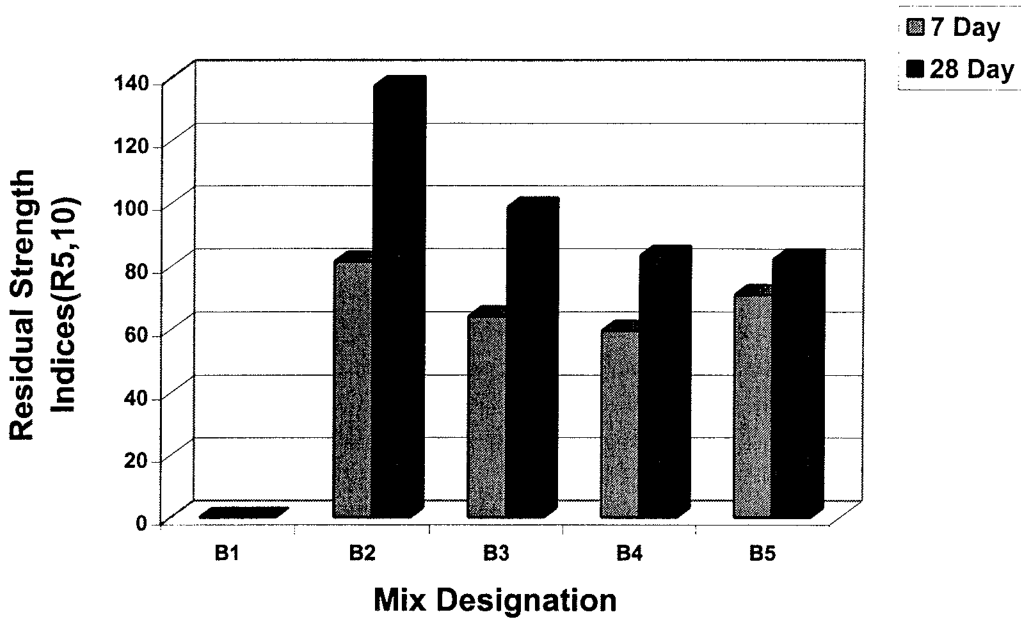

Fig. 3C Comparison of Residual Strength Indices R(5,10)

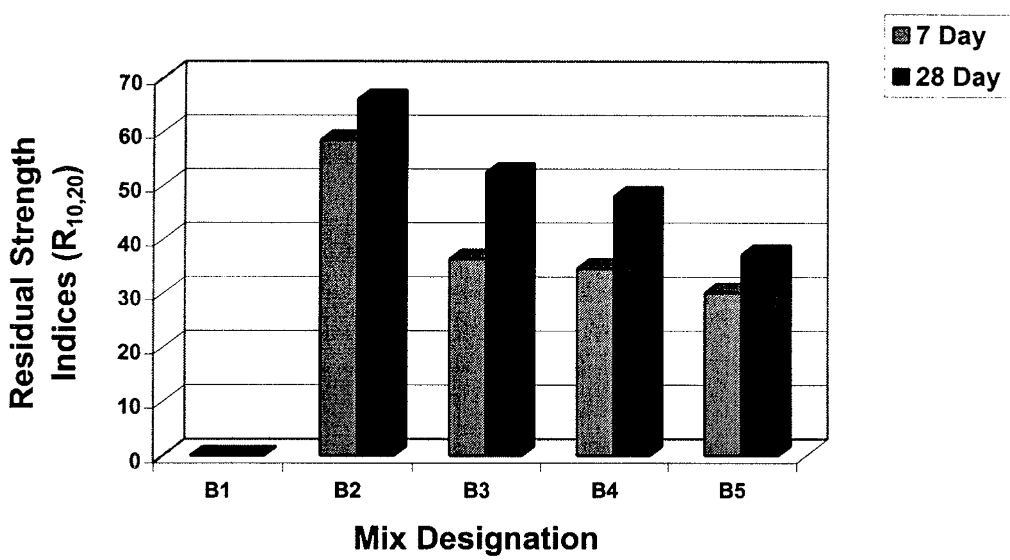

Fig. 3D Comparison of Residual Strength Indices (R10,20)

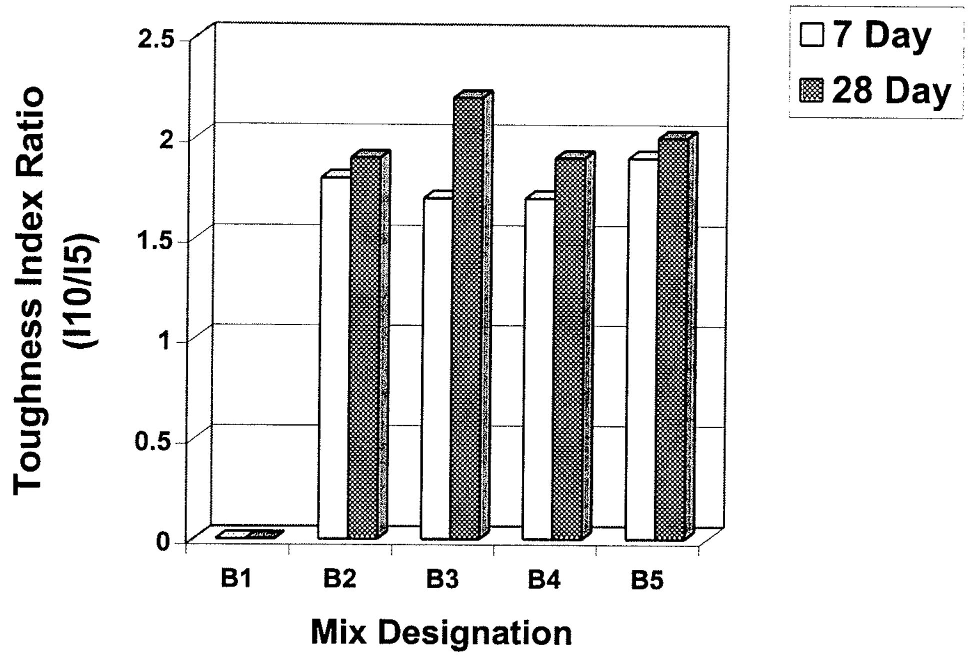

Fig. 3E Comparison of Toughness Index Ratio (I10/I5)

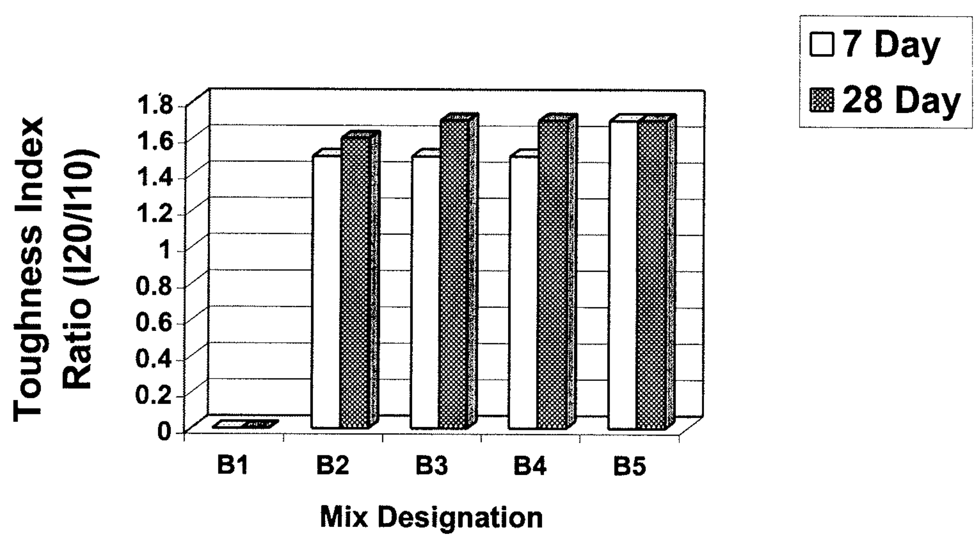

Fig. 3F Comparison of Toughness Index ratio (I20/I10)

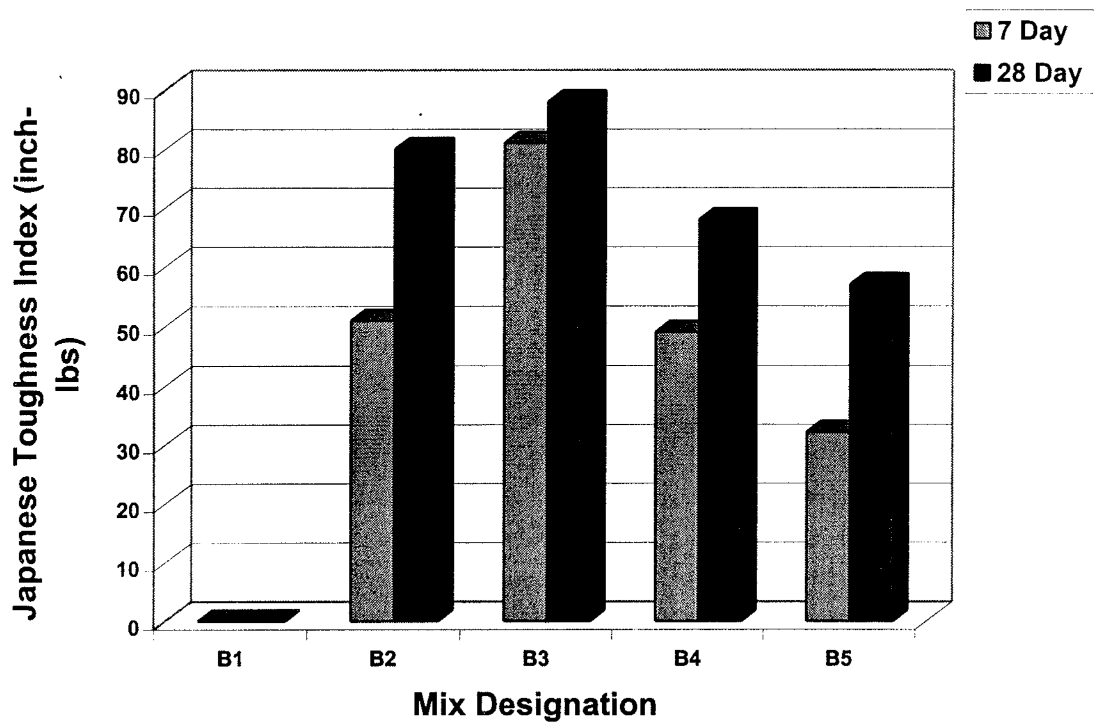

Fig. 4 Comparison of Japanese Toughness Index

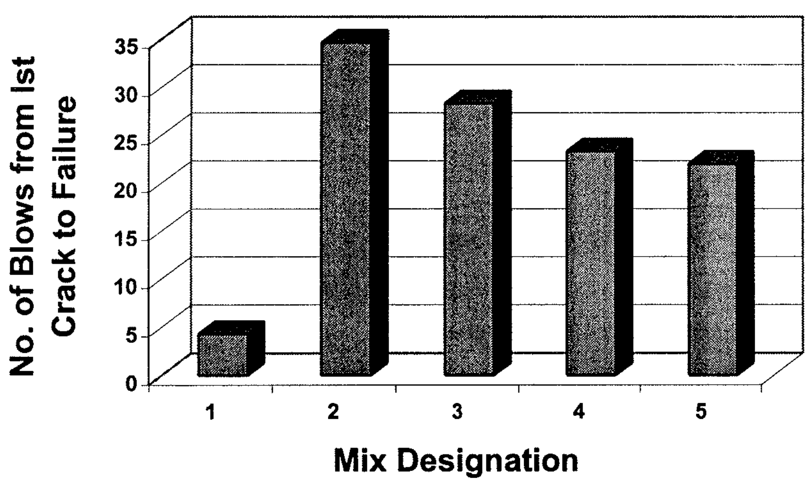

Fig. 5 Impact Test Results (28 Day)

4. TENSION TEST FOR BASALT ROD

4.1 TENSION TEST

The tension test was done on basalt bars, with 14.25mm (0.56in.) and 6mm (0.24in.) in diameter and also on a cable, 6mm (0.24in.) in diameter. The description of the test is as follows.

4.1.1 Tension Test On Basalt Bar With 14.25mm(0.56in.) Diameter:

The bar was tested for tension on the Tinius Olsen Machine, which has a load capacity of 181, 818 kg (400,000 lbs). The test set-up is shown in Photo 1. Two electrical strain gauges with a gauge factor of 2.07 ± 0.5 %, were used to measure the strain in the bar. The bar failed at a load of 23636 kg (52,000 lbs). Mega-Dac data acquisition software was used for the test. The ultimate tensile strength of the bar is 1458 MPa (211,382 psi). The static modulus of elasticity is 62,069 MPa (9×10^6 psi). The type of failure was brittle and the bar did not yield. Photo 2 shows the bar at failure in the machine. It splintered into small bundles of fibers. The results are tabulated in Table 8 and the stress strain curves drawn for the bar are shown in Fig. 6 and 7. Photo 3 shows the failed specimen with the end anchorages.

4.1.2 Tension Test On Basalt Bar With 6mm (0.24in.) Diameter and Basalt Cable With 0.24in. Diameter:

For the tension test of the 6mm (0.24in.) diameter bar, and the 6mm (0.24in.) diameter cable, steel anchorages with rough grooves on the inside, were designed for a better bond. These grooves were cleaned with acetone to remove all the oil and dust. Then the basalt bar was roughened with a sand-paper and small grooves were made in the bar for a better bond with the anchorages. Then one end of the bar was fit into the anchorage and structural epoxy was poured into it, which had a curing agent (25% by weight of the epoxy) to speed up the curing process. The epoxy used was 815 resin. This mixture along with the bar was allowed to set for a period of 48 hrs. Then the process was repeated for the other end of the bar. The same procedure was adopted for the cable.

Due to the small size of the bar and the cable, strain gauges could not be fixed on them. Both the bar and the cable were tested on the same Tinius Olsen Machine. The 6mm (0.24in.) diameter bar failed at a load of 2043 kg (4494 lbs). The ultimate tensile strength for this bar is 707.5 MPa (102,595 psi). Photo 4 shows the failed specimen. The failure was brittle and the bar splintered into small bundles of fibers without yielding.

The cable is made of two basalt bars with a diameter of 3mm (0.12in.), twisted together. The 6mm (0.24in.) diameter cable failed at a load of 439.5 kg (967 lbs). The ultimate tensile strength of the cable is 308 MPa (44,640 psi). Photo 5 shows the failed specimen. The cable broke into two pieces without any splintering of the fibers, unlike both the bars.

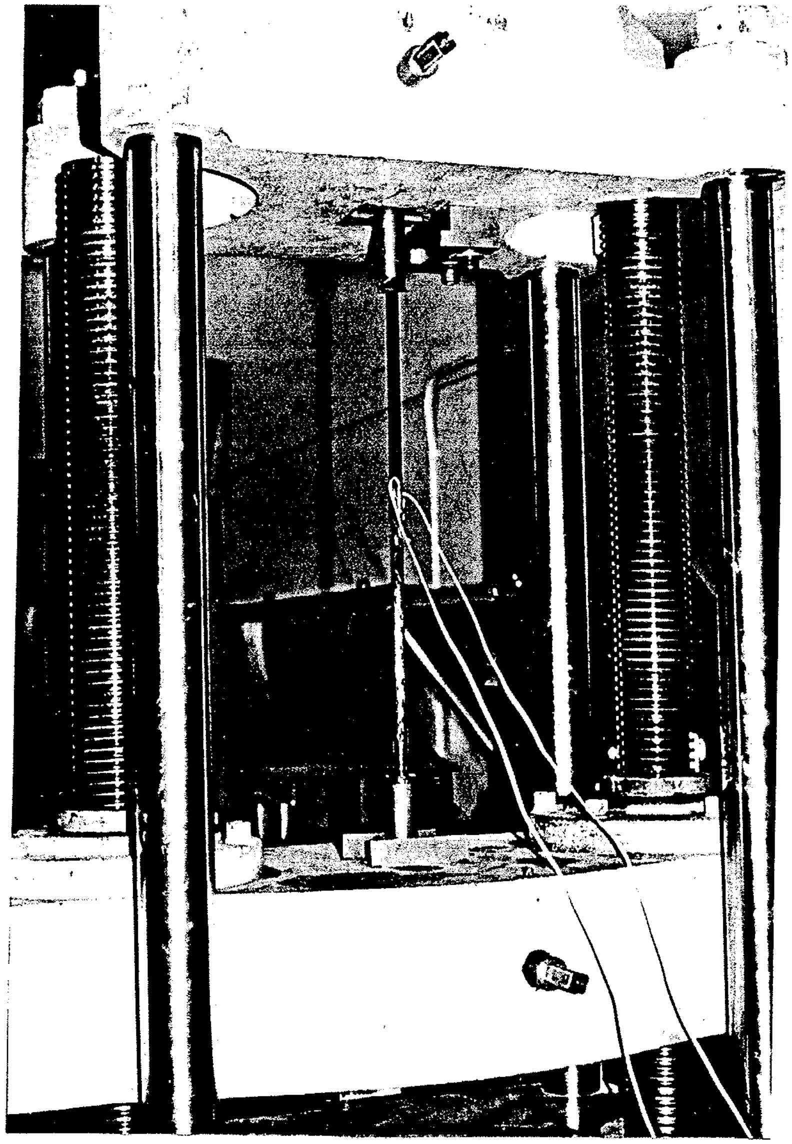

Photo 1 Test set-up

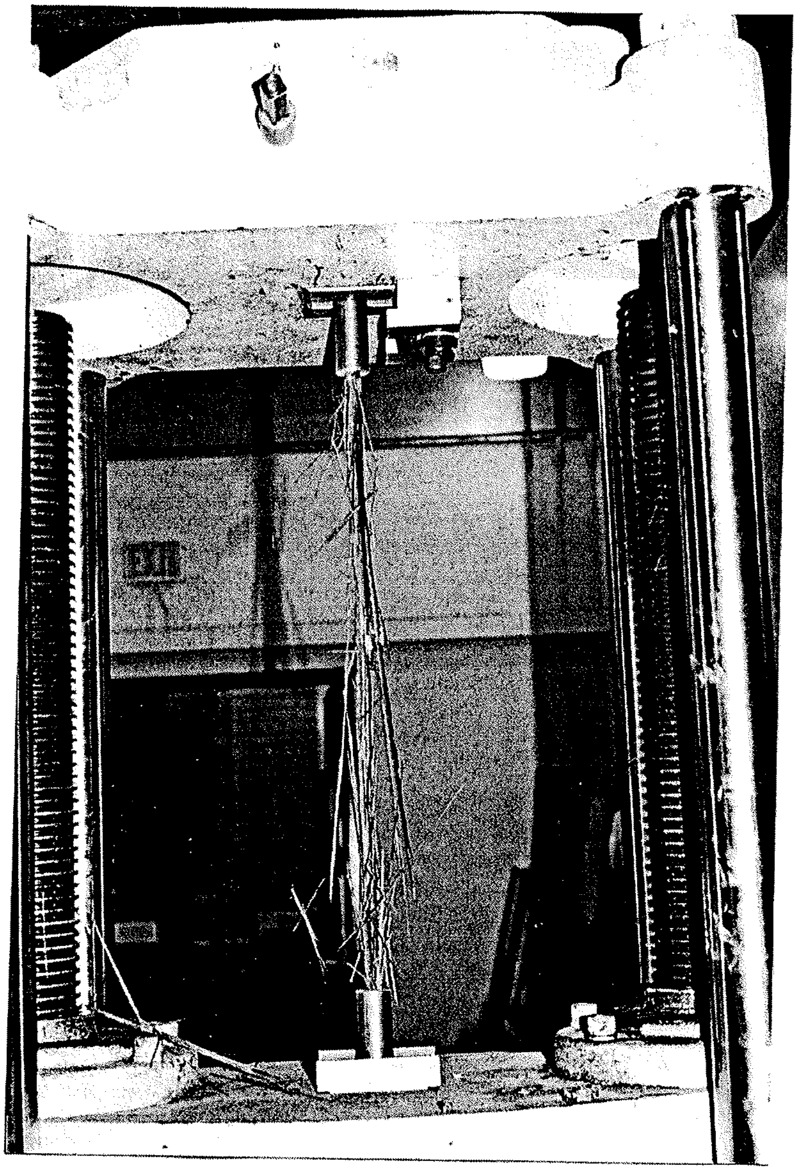

Photo 2 Specimen at failure in the machine
Diameter of bar = 14.25mm(0.56 in.)

Photo 3 Failed specimen with anchorages
The bar splintered into small bundles of fibers.

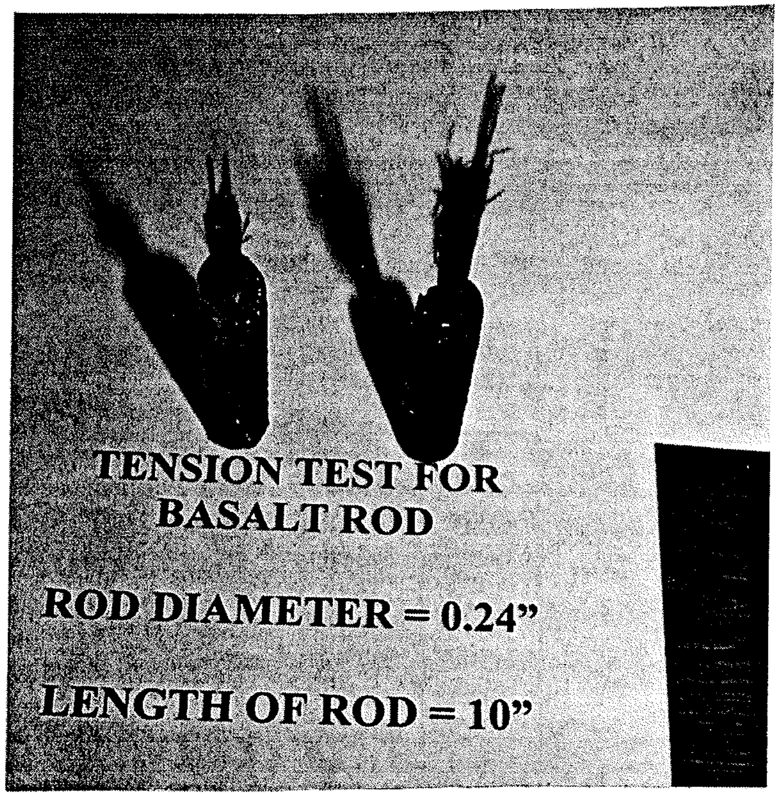

Photo 4 Failed specimen
Diameter of bar = 6mm(0.24 in.)

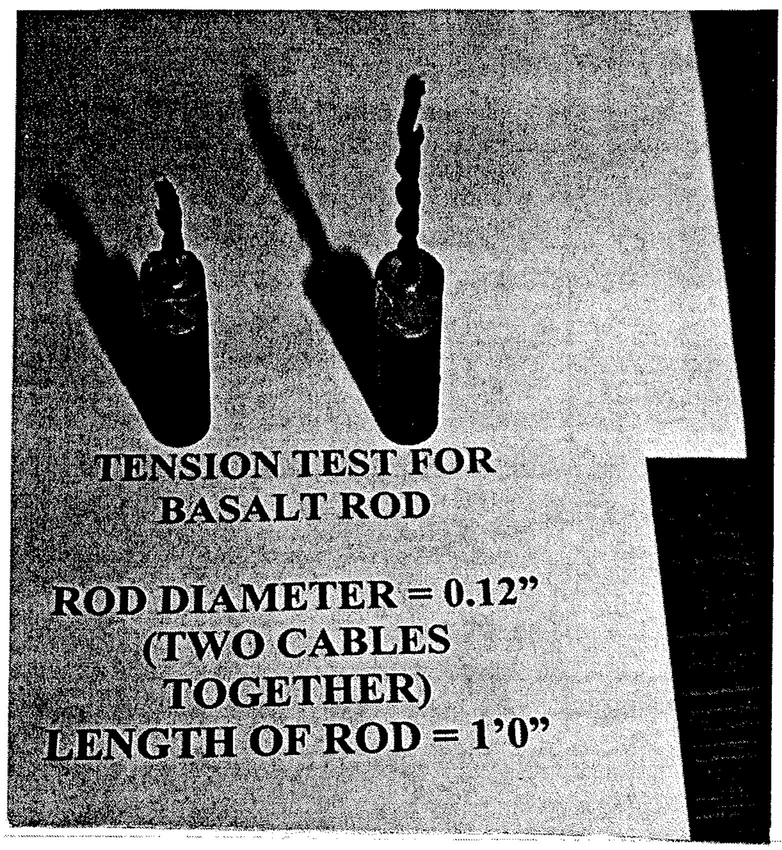

Photo 5 Failed specimen
Diameter of cable = 6mm(0.24in.)

Table 8:Tension Test for Basalt Rod
Diameter of Rod = 0.56in.
Strain Gauge Factor = 2.07

Load (lbs)	Stress (psi)	Strain1	Strain2
0	0	0	0
2000	8130	947	949
4000	16260	1850	1797
6000	24390	2792	2798
8000	32520	3561	3570
10000	40650	4550	4561
12000	48780	5449	5464
14000	56910	6329	6334
16000	65040	7271	7280
18000	73170	8192	8198
20000	81300	9054	9068
22000	89430	9941	9967
24000	97560	10888	10889
26000	105691	11879	11881
28000	113821	12831	12840
30000	121951	13790	13794
32000	130081	14658	14700
34000	138211	15704	15699
36000	146341	16600	16666
38000	154471	17661	17663
40000	162601	18532	18538
42000	170731	19471	19482
44000	178861	20491	20492
46000	186991	21582	21683
48000	195121	22491	22498
50000	203252	23491	23581
52000	211382	24571	24580

Conversion Factors:

1 MPa = 145 psi
1 kg = 2.2 lbs
25.4mm = 1in.

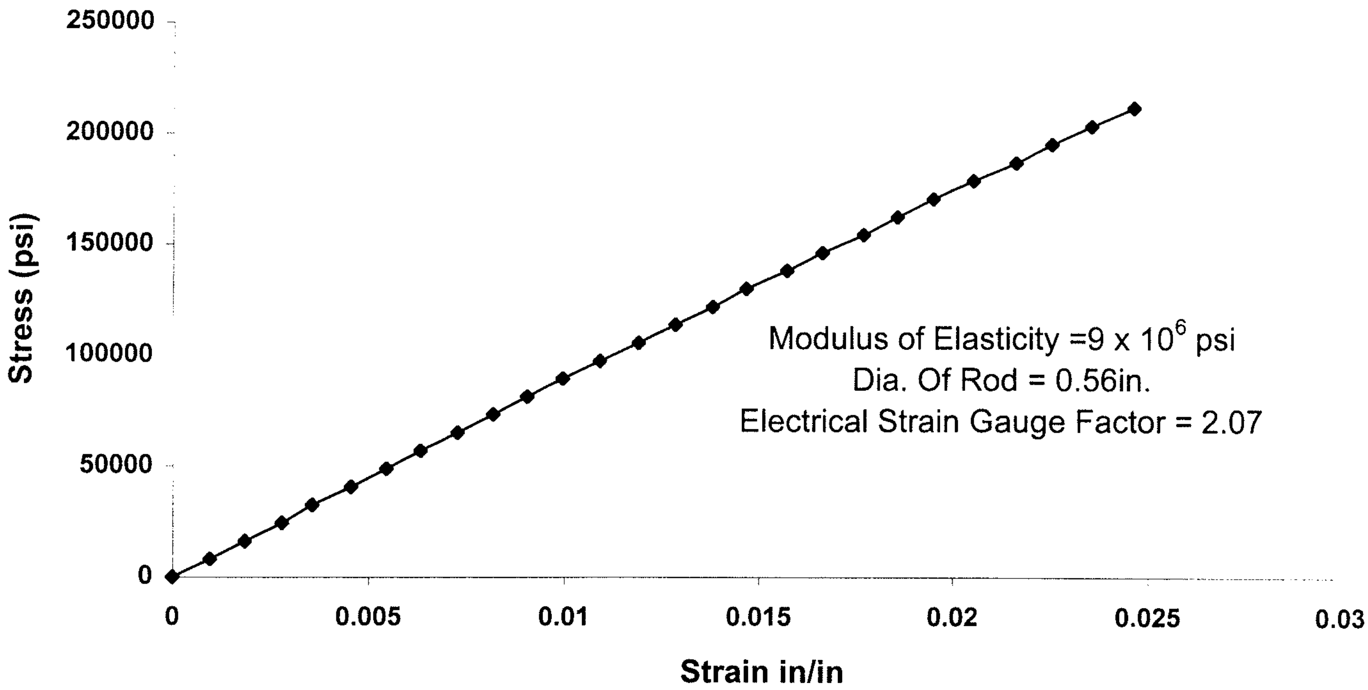

Fig. 6 Tension Test for Basalt Rod (No.1)

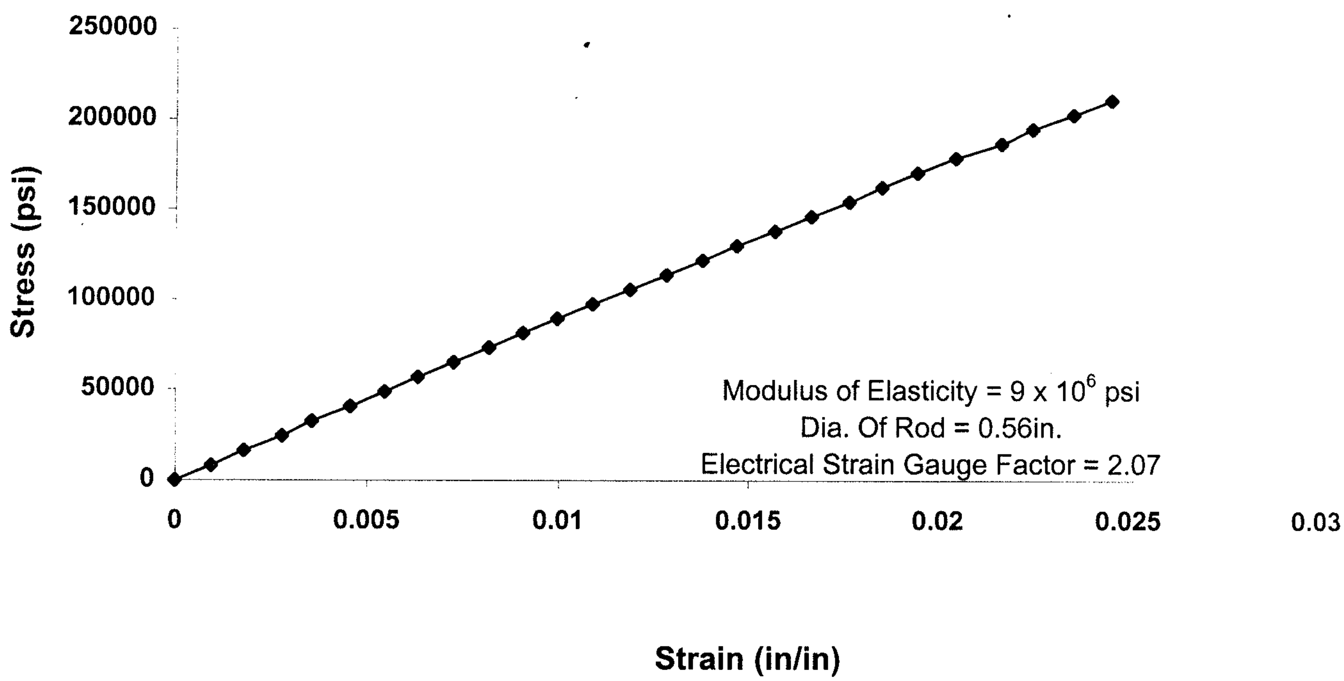

Fig. 7 Tension Test for Basalt Rod (No. 2)

5. CONCRETE REINFORCED WITH BASALT FIBER COMPOSITE REBARS

5.1 PROBLEM STATEMENT

The innovative aspect of this project is the detailed study of non-corrosive, basalt fiber composite rebar. This rebar consists of 80% fibers and has a tensile strength three times that of the steel bar. It is made, by utilizing a resin (epoxy) binder. Basalt fiber composite rebars have the potential to replace steel in reinforced concrete structures exposed to salt water, ocean climate, etc. wherever the corrosion problem exists. This advantage alone could warrant a sufficient argument for substitution of the basalt rebar on a large scale. Other advantages of the basalt rebar are that its weight is one-third of the weight of steel and the thermal expansion coefficient is very close to that of concrete. The high mechanical performance/price ratio of basalt fiber composite rebar, combined with corrosion resistance to alkaline attack are further reasons for replacing steel in concrete by basalt fiber composite rebar. There is no published information available on the behavior of the basalt fiber composite rebar and, therefore, there is a need for this research.

5.2 OBJECTIVE

This investigation was undertaken to evaluate the performance of concrete reinforced with basalt fiber composite rebars. The following were the objectives of the research.

- To determine the ultimate failing load.
- To study the load-deflection behavior.
- To observe the bond strength.
- To measure the strain in the concrete.
- To study the mode of the failure.

5.3 RESEARCH PROGRAM

In all, eleven beams reinforced with basalt rebars were tested. Research & Technology Inc supplied five beams and six beams were designed and cast in the lab. The beams that were designed and cast in the lab are referred to as BRC-A to F in the discussion, whereas the beams supplied by the manufacturer are referred to as BRC-1 to 5. Three plain concrete (control) beams were also supplied which are referred to as P1-3.

The concrete beams reinforced with basalt bars were tested in bending. Load deflection behavior was studied by measuring the true deflections. Strain across the depth of the beam was measured using the Mega-Dac data acquisition software. Beams with increased development lengths were also tested.

5.4 BASALT BAR REINFORCED CONCRETE BEAMS (DESIGNED AND CAST IN THE LAB)

Six beams were designed and cast in the lab for the investigation. Photo 6 shows the casting of the beam in the lab. Needle vibrator was used to consolidate the concrete. Table 9 gives the mix proportions, used for the beams.

The details of BRC-A and B are as follows. These beams were reinforced with two basalt bars with 14.25mm (0.56in) diameter, placed at the bottom, with a cover of 25.4mm (1in). The distance between the bars was kept to175mm (7in) for the beam, BRC-A and 125mm (5 in) for BRC-B. The distance of the reinforcement from the sides of the mould was kept to 64mm (2.5in). The cover for the reinforcement was maintained by 25.4mm (1in) wooden spacers, placed at regular intervals over the length of the bars. Care was taken to prevent the spacers from moving, by tying them to the mould by binding wires. Sketch 1 shows these details. Two other beams, BRC-C and D were also cast. They had an increased cover of 87mm (3.5in) for the reinforcement. Sketch 2 shows the details of these beams.

The details of the remaining two beams, BRC-E and F are as follows. BRC-E was reinforced with two basalt bars of 14.25mm (0.56in) diameter and, BRC-F with two basalt bars of 5mm (0.2in) diameter. The cover was maintained at 25.4mm (1in) and 18.8mm (0.75in) respectively with the help of wooden spacers. The bars along with the spacers were tied to the bottom of the mould with the help of binding wires for maintaining the correct cover. The bars were kept at a distance of 25.4mm (1in) from the sides of the mould. Sketch 3 shows these details. The details of beams BRC-A to F are tabulated in Table 10.

5.4.1 Design of Beams

The design details of the beam BRC-A are as follows:

Notation:

a = lever arm, mm(in.)
Abr = area of tension reinforcement, mm^2 ($in.^2$)
b = width of member, mm(in.)
d = distance of extreme compression fiber to centroid of tension reinforcement, mm (in.)
fc' = compressive strength of concrete, MPa (psi)
fr = modulus of rupture, MPa (psi)
fyb = yield strength of basalt reinforcement, MPa (psi)
l = span length of beam, mm(in.)
M. R = Moment of resistance, N.m (in-lb)
W = Load kg (lbs)

Data:

fc'	= 36.8MPa(5334 psi)
fyb	= 1458MPa(211,382 psi)
Length of Bar	= 1.2m(4ft.)
Diameter of Bar	= 14.3mm(0.562in.)
Beam Size	= 300mm x 300mm x 1.3m(12in x 12in x 51in)
No. of Bars Used	= 2
Area of Reinforcement	= 2 x (π/4) x $(14.3)^2$ = 321mm^2(0.496 in^2)
Effective Depth (d)	= 279mm(11in.)

a = (Abr x fyb)/(0.85 x fc' x b)
= (321 x 1458)/(0.85 x 36.8 x 300)
= 49.9mm(1.96in.)
Jd = {d – (a/2)}
= 279 – (49.9/2)
= 254mm(10in.)

On similar lines, beams BRC-B, C and D were designed.

5.4.2 Calculation of Ultimate and Cracking moments for the beam

5.4.2.1 Ultimate Moment for BRC-A

Actual Bending Moment = (3Wl)/14
(Measured Ultimate Load = 71.2 KN (16,000 lbs) ....Ref. Table 10a
= (71.2 x 1.067) x 3 / 14
= 16.27KN.m(12.0 k-ft.)
Moment of resistance = A_{br} x F_{yb} x (d – a/2)

= 119.8 KNm (88.35 k-ft.)

The calculated ultimate moment is much higher than the actual moment at maximum load. This indicates that the beam did not reach its ultimate load, as there was a bond slip in the reinforcing bars. Table 10a shows the comparison of the measured and calculated ultimate moments for beams BRC-B to F.

5.4.2.2 Cracking Moment for BRC-A

Actual Bending Moment = (3Wl)/14
at cracking load
(Measured Cracking Load = 66 KN (15,000 lbs) ....Ref. Table 10a
= (66 x 1.067) x 3 / 14
= 15.25 KNm (11.25 k-ft)

Calculated Cracking Moment = (fr x Ig) / y_t
fr = 7.5 x sqrt (f'c)
= 7.5 x 5.8
= 3.77MPa(547psi)
Ig = (bxd^3) / 12
= (300×300^3) / 12
= 675×10^6 mm^4 (1728 in^4)
y_t = 150mm(6 in.)
∴ Moment = ($3.77 \times 675 \times 10^6$) / 150
= 17.82 KNm (13.14 k-ft.)

The calculated cracking moment of the beam is close to the actual cracking moment, which also indicates, that the beam did not reach its ultimate moment after cracking, as the reinforcing bars experienced a slip. Table 10a shows the comparison of the measured and calculated cracking moments for beams BRC-A to F. Table 10b shows the measured deflections at first crack and ultimate loads for beams BRC-A to F.

5.5 TESTING OF THE BASALT REINFORCED CONCRETE BEAMS (BRC-A TO F)

The beams were tested after 14 day curing period. The test set-up is as shown in Photo 7. Five strain gauges were fixed for measuring the strain variation along the depth of the beam. Photo 8 shows the electrical strain gauges fixed on the beam. Sketch 3a shows the details of the position of strain gauges on beams BRC-C and D. Deflections were measured during the test, with the help of a dial-gauge (Photo 9). The load-deflection curves for BRC-A and B are shown in Fig. B1 and B2 in Appendix B. The load-deflection curves for BRC-C and D are also plotted, and are shown in Fig. B3 and B4 in Appendix B. The measured deflection values are tabulated in Tables B1 and B2 in Appendix B.

Photo 10 shows the close-up of the cracked beam, still carrying the maximum load. Fig. B5 and B6 show the load deflection curves for the beams, BRC-E and F. Load versus strain graphs were plotted, and are shown in Fig. B7 through B16 in Appendix B.

5.6 MEASUREMENT OF SLIP OF REINFORCEMENT

Photo 11 shows a close-up of the beam after failure which shows a single crack instead of multiple cracking which indicates slip of the reinforcing bars. After the testing was done and the beams failed, the edges were cut using a diamond tipped saw and the slip in the bars was measured. Photo 12 shows the maximum width of the crack was 50mm (2in) and Photo 13 shows the close-up of the slip of the reinforcement.

The concrete beam was cut at the corners, on the same side of a bar with the help of a diamond tipped saw, in such a way that the ends of the bar at both the ends were exposed. Photos 14 and 15 show the slip of the reinforcement at the left end and the right end of the same beam, respectively. Sketch 4 shows the details of the slip.

Care was taken to prevent the bar from being damaged while cutting and not to damage the concrete near the exposed reinforcement.

After carefully removing the cut concrete, the slip of the basalt bar was clearly visible at both the ends with a distinct mark left in the concrete at the original placing of the reinforcement. Photo 16 shows another view of the slip in the reinforcement after testing. Then the slip distance was measured using an accurate measuring scale. The slip for the beam BRC-A, at the left end, was 25mm (1in) and 29mm (1.141in) at the right end. The total slip was 54mm (2.141in). The slip for beam BRC-B, was 17mm (0.7in) at both the ends with a total slip of 34mm (1.4in).

The overall test results indicate that there was insufficient bond strength and the bars slipped gradually before the ultimate load was reached. Two beams, BRC-E and F, were tested with increased development lengths. The spans for the beams were 0.75m (30in) and 0.9m (36in) respectively. Beam BRC-E failed in flexure, but at a higher load than beams BRC-A to D, due to the increased development length, whereas beam BRC-F, failed suddenly with the breaking of the reinforcement. It was a sudden and brittle failure. The measured and calculated ultimate and cracking loads, are compared in Table 10a.

5.7 BASALT BAR REINFORCED CONCRETE BEAMS (BEAMS SUPPLIED BY MANUFACTURER)

Research & Technology Inc. supplied 8 beams. Five beams (BRC-1 to 5), were reinforced with basalt fiber composite rebars. Four of these beams had 3-D basalt fiber reinforced concrete. Three beams (P1 to P3), were plain concrete (control) beams. The details of these beams are given in Table 11 and sketch 5 shows these details. The beams were tested in bending. The test set-up is shown in Photo 17. Electrical strain gauge was used to measure the strain. Photo 18 shows the close-up of the test set-up along with the electrical strain gauge. Three students required for noting down the results, are also seen in the photograph.

Deflections were measured using a dial-gauge. A specially designed frame was used to mount the dial gauge. Photo 18a shows the close-up of the frame. This frame was supported only at four points, which are on the neutral axis above the supports. The dial gauge was fixed such that, it was touching the center point of the bottom surface of the beam. This arrangement enabled the measurement of the true deflections, excluding deformations due to the crushing of concrete at the supports and load points. As the frame could move laterally, it took care of the deformations and strains induced in the frame. As the deflections were measured at the center point, any slight warping or twisting of the beam did not affect the true deflections measured.

The toughness indices, Japanese toughness indices, and the Equivalent flexural strength were calculated and the results are tabulated in Table 12. The comparative bar charts for these values are shown in Fig. 8 through 11. The measured load-deflection readings are given in Table C1 in Appendix C and the curves are shown in Fig. C1 through C5 in Appendix C. Two of the beams failed in flexure. Photos 19 and 20 show the flexural failure and Photo 20a shows the beams after the flexural failure. 20b shows the close-up of the flexural failures. The basalt rods are also visible in the photograph. Two beams failed in shear. Photo 21 shows the close-up of shear failure, whereas Photo 21a shows a general view of all the eight tested beams. The plain concrete beams failed by breaking into two pieces, unlike the basalt rod reinforced beam. One beam failed by secondary end splitting and the close-up is shown in Photo 21b. The reinforcing bars used in these beams had a tensile strength of 707.5 MPa (102,595 psi) which is low in comparison to the bars used to reinforce the beams designed and cast in the lab. These bars failed by breaking into two pieces at the ultimate load. Beams BRC-1,2,3 and 5 had small amount of fibers, due to which, a ductile failure was observed. In beam BRC-4, there were no fibers, hence a brittle failure was observed. Photo 22 shows close-up of the secondary shear failure.

All three plain concrete beams failed instantaneously, at the appearance of the first crack. The failure was brittle and sudden, whereas all the beams reinforced with the basalt rebars had a gradual failure after considerable amount of deflection. As expected, the addition of reinforcement, either in the form of small fibers or composite basalt rods, converted the brittle failure into a ductile failure.

The manufacturer supplied cylinders with 75mm (3in) diameter and 150mm (6in) height. Compression tests were done on these cylinders. Photos 23 and 23a show the failure of both the plain as well as basalt fiber reinforced cylinders. The plain cylinder failed by splitting into two pieces, whereas the reinforced cylinder did not.

The ultimate and cracking moments of the basalt rod reinforced beams, were also calculated and compared to those of the actual moments. Table 13 shows the actual and the calculated ultimate moments for the beams. The bending moments at which the bond slip occurred are given in Table 13. The results indicate a slip of the reinforcing bars.

5.8 CONCLUSIONS

- The tests indicated that there was insufficient bond strength and the bars experienced a gradual slip after the ultimate load was reached.
- The basalt bar had a very high tensile strength. The bar did not have a yield point and it had a brittle failure. It was a very sudden and explosive type of failure.
- The failure observed in the beams was a ductile failure, due to a gradual slip of the bars, thus preventing a brittle failure.
- The beams supplied by the manufacturer were reinforced with smaller diameter bars which did not have a high tensile strength in comparison to the bar used for reinforcing the beams designed and cast in the lab. These beams supplied by the manufacturer, failed at the ultimate load, by breaking into two pieces. The type of failure was of a brittle nature.
- The beams that were designed and cast in the laboratory failed in flexure, whereas the beams supplied by the manufacturer exhibited a primary failure in flexure and shear and a secondary failure in splitting.
- In general, it can be concluded that it is feasible to make concrete beams reinforced with basalt composite rebars. However, the bond between the bar and the concrete should be increased in order to increase the load carrying capacity of the beams, and hence the efficient use of basalt composite rebars.

5.9 RECOMMENDATIONS

- Roughening of the bar or having modulations on the surface is suggested for improving the bond with the concrete.

Using a different resin (epoxy) binder for increasing the roughness of the bar surface is also suggested.

Photo 6 Casting of Basalt Reinforced Concrete Beams

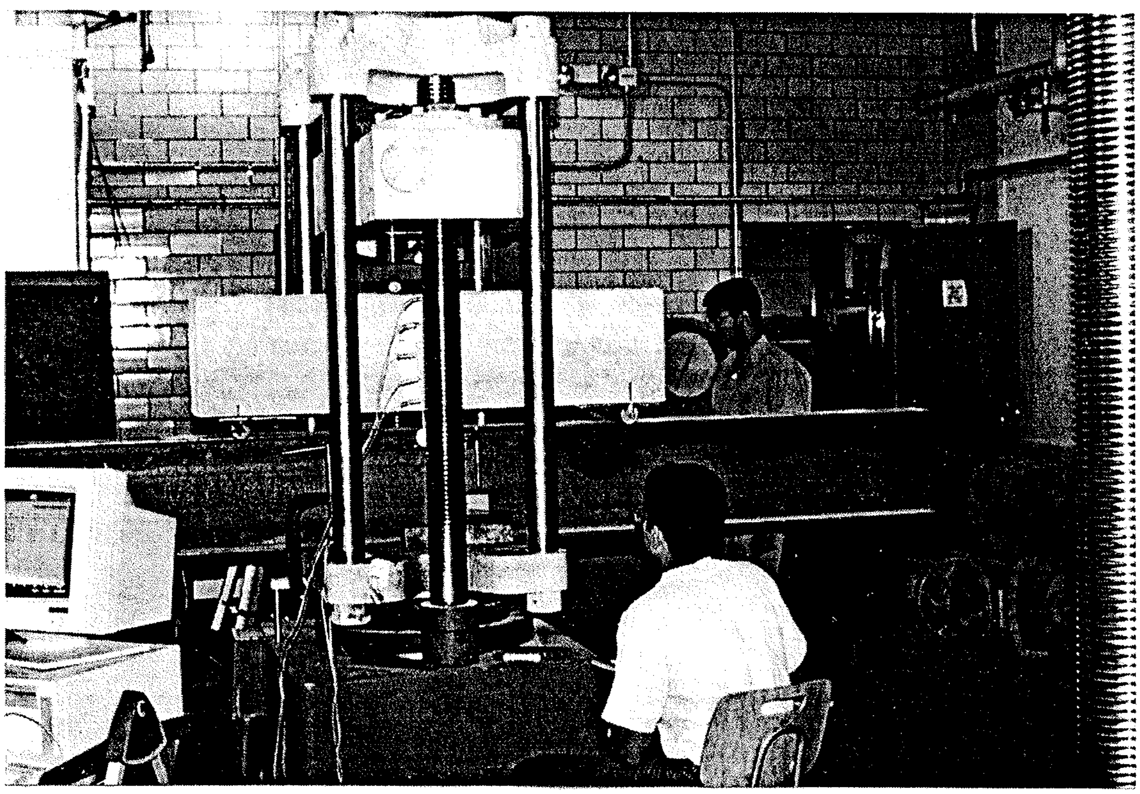

Photo 7 Test set-up for Basalt Reinforced Beam
Data Acquisition Software(Mega-Dac)seen in the picture

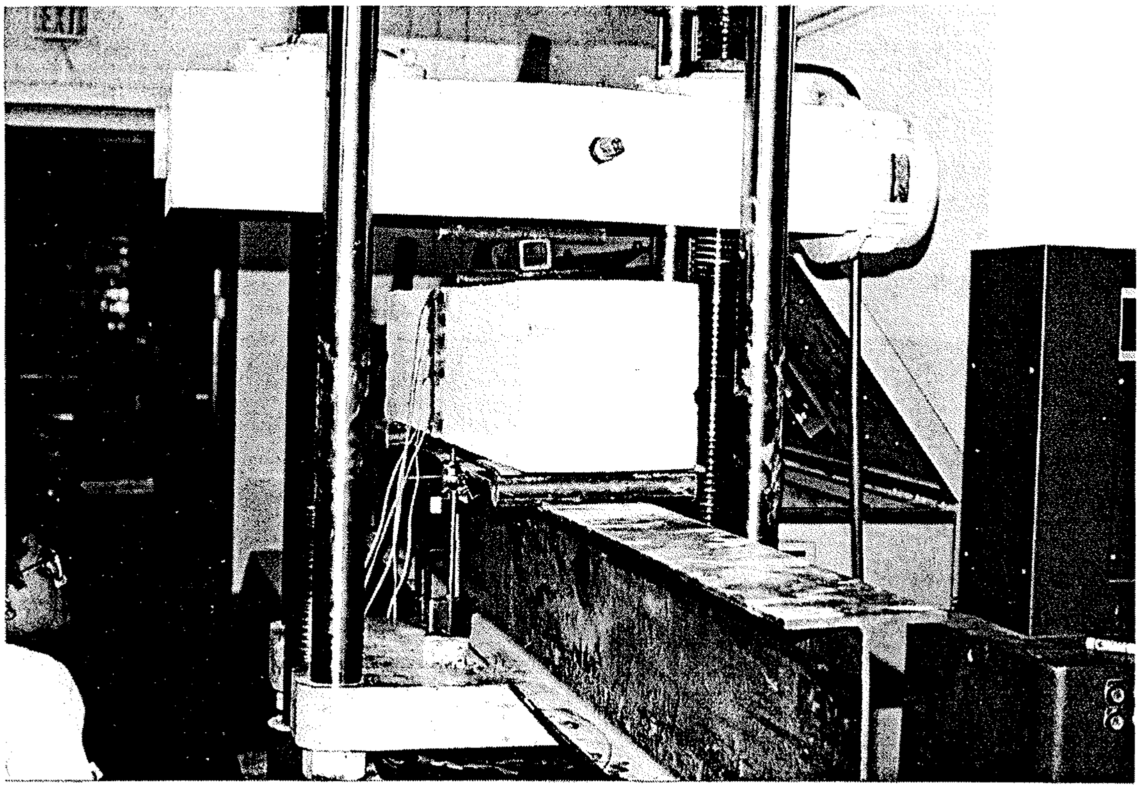

Photo 8 Test set-up for the Basalt Reinforced Concrete Beam Electrical Strain gauges seen in the photograph

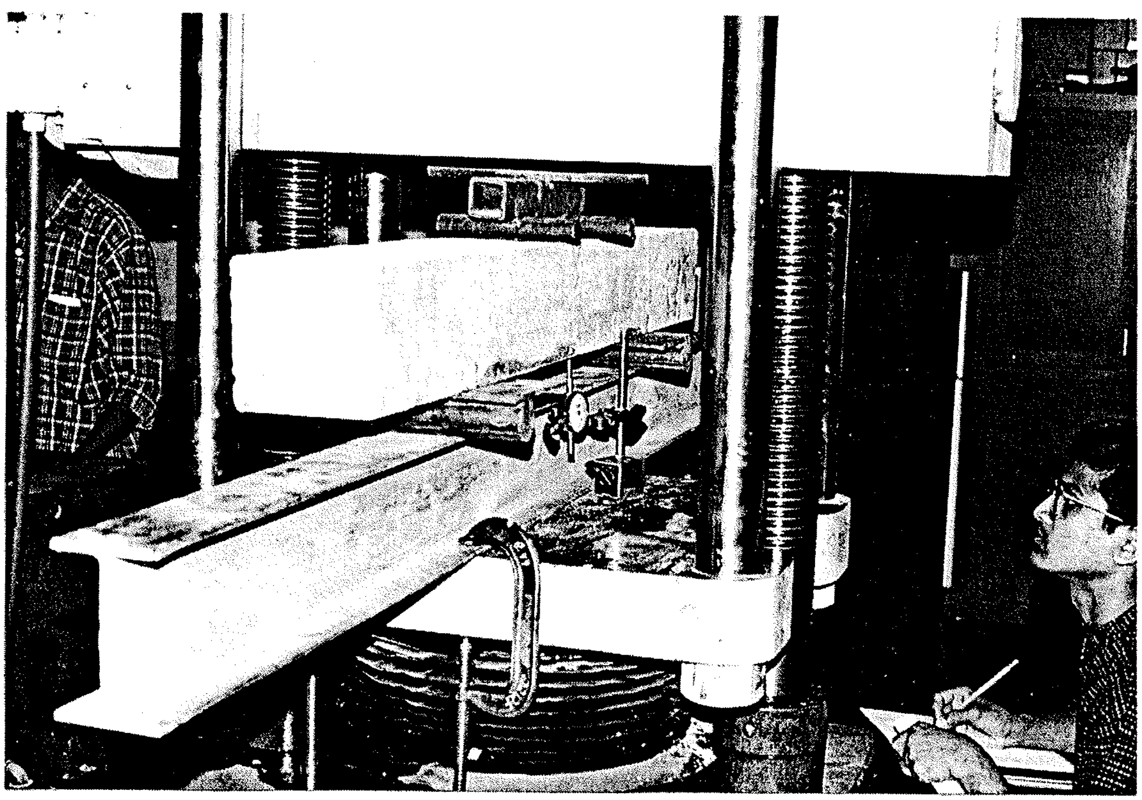

Photo 9 Deflection Measurement for Basalt Reinforced Concrete Beam

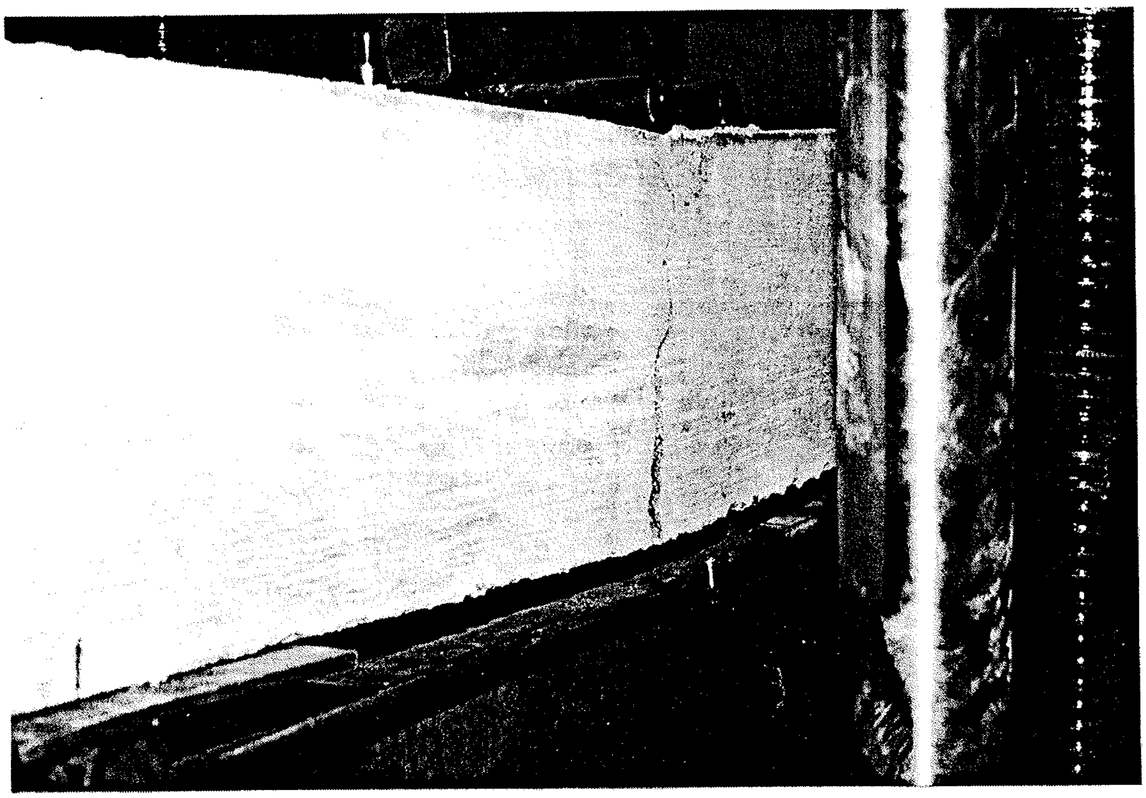

Photo 10 Close-up of cracked beam still carrying the maximum load

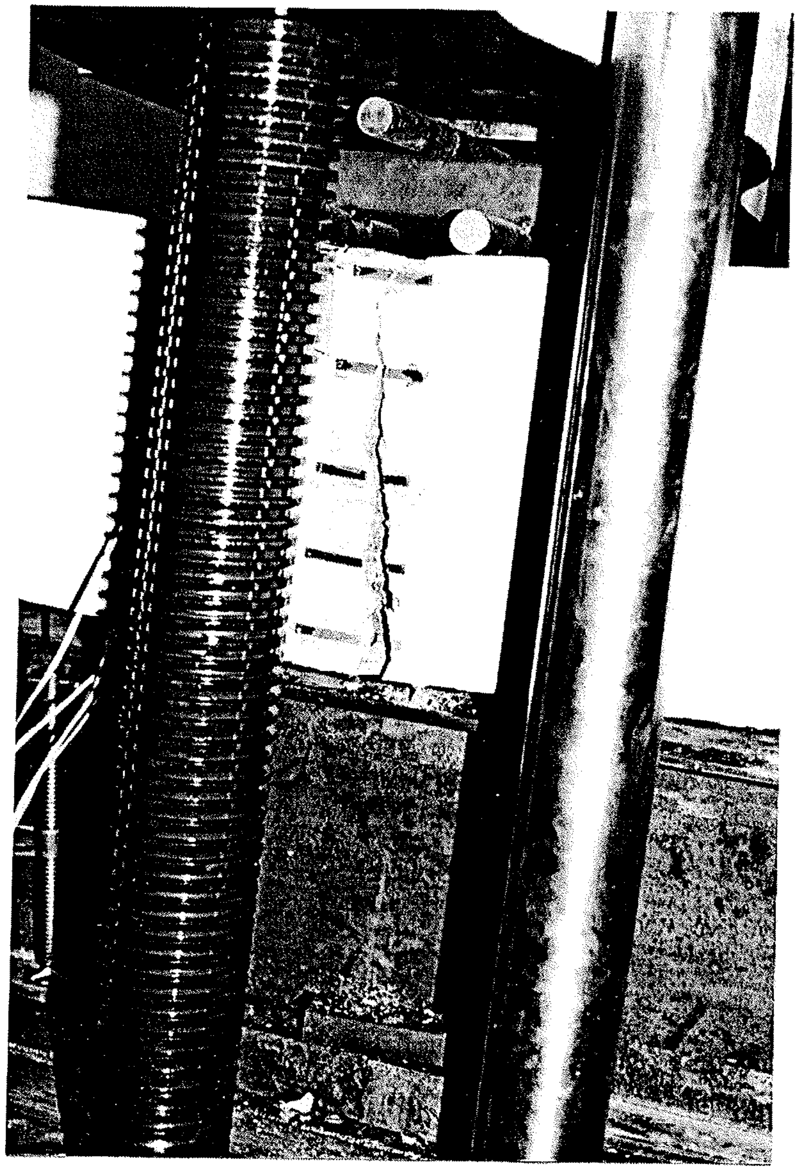

Photo 11 Close-up of beam after failure
A single crack instead of multiple cracking caused the failure.
This indicates bond slip.

Photo 12 Close-up showing maximum width of crack
Maximum crack width = 50mm(2 in.)

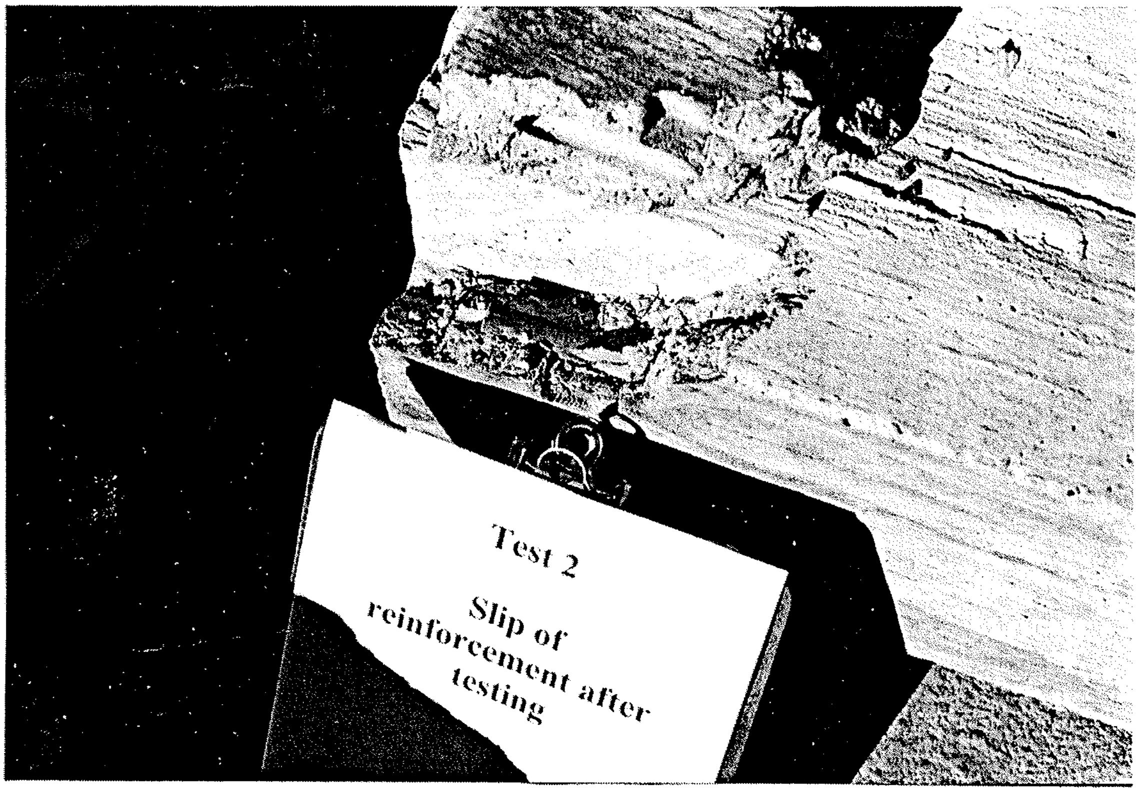

Photo 13 Close-up of slip of reinforcement

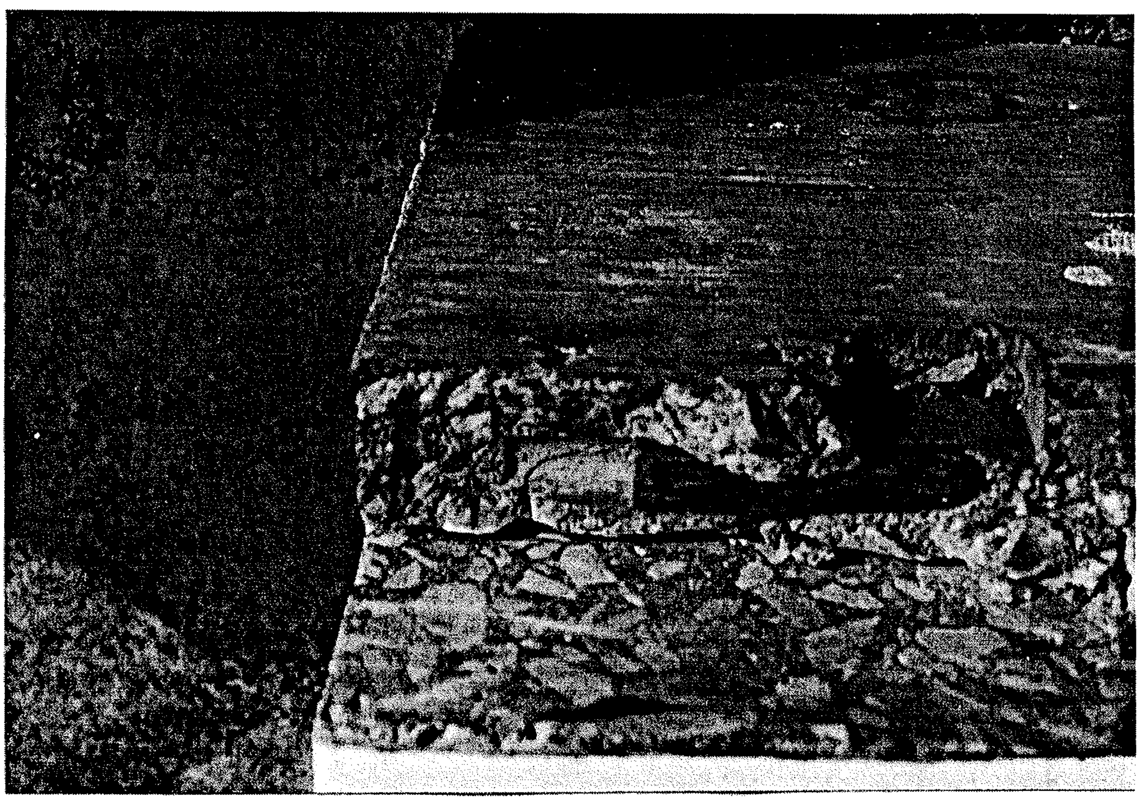

Photo 14 Slip of reinforcement at left end of the beam.

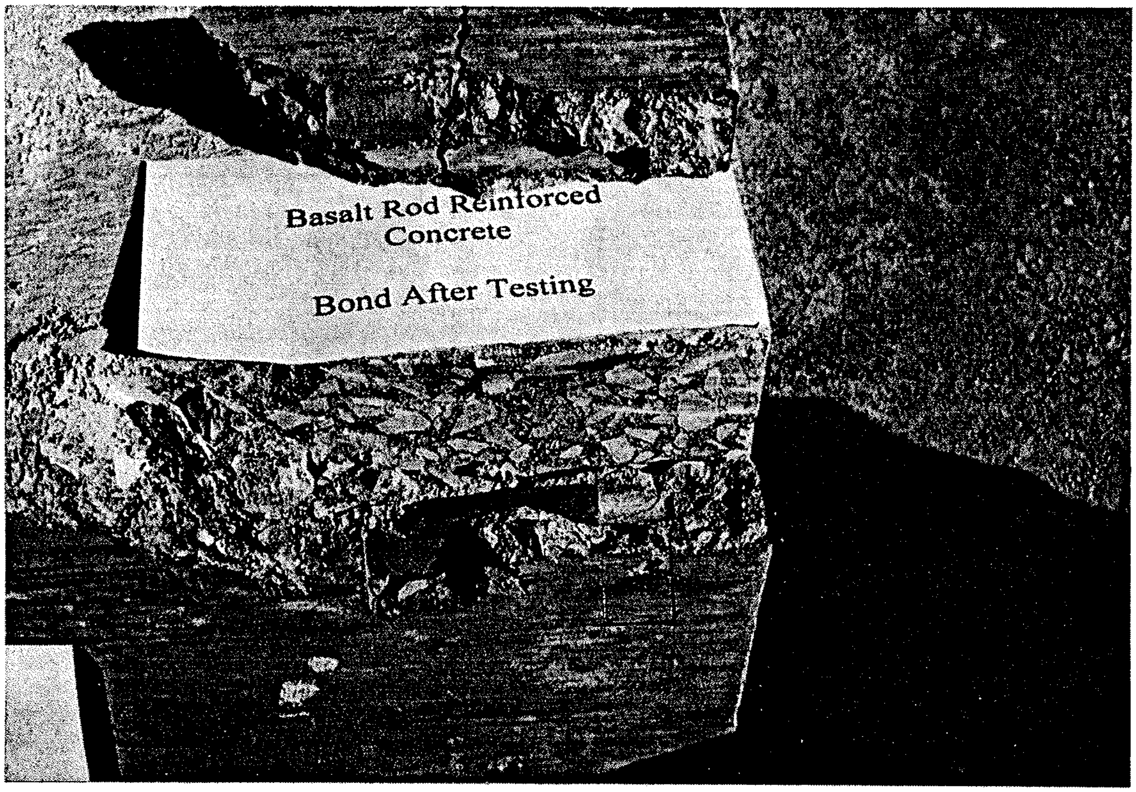

Photo 15 Slip of reinforcement at the right end of the beam.

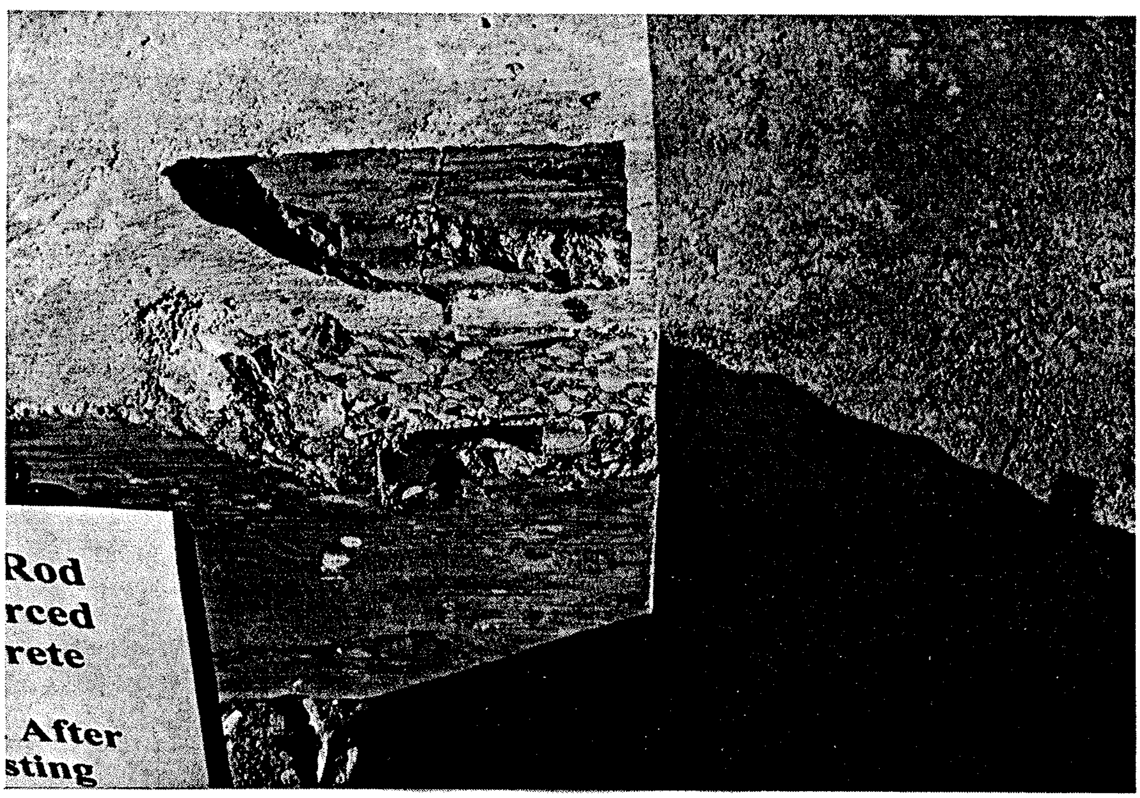

Photo 16 Another view of the slip of reinforcement after testing.

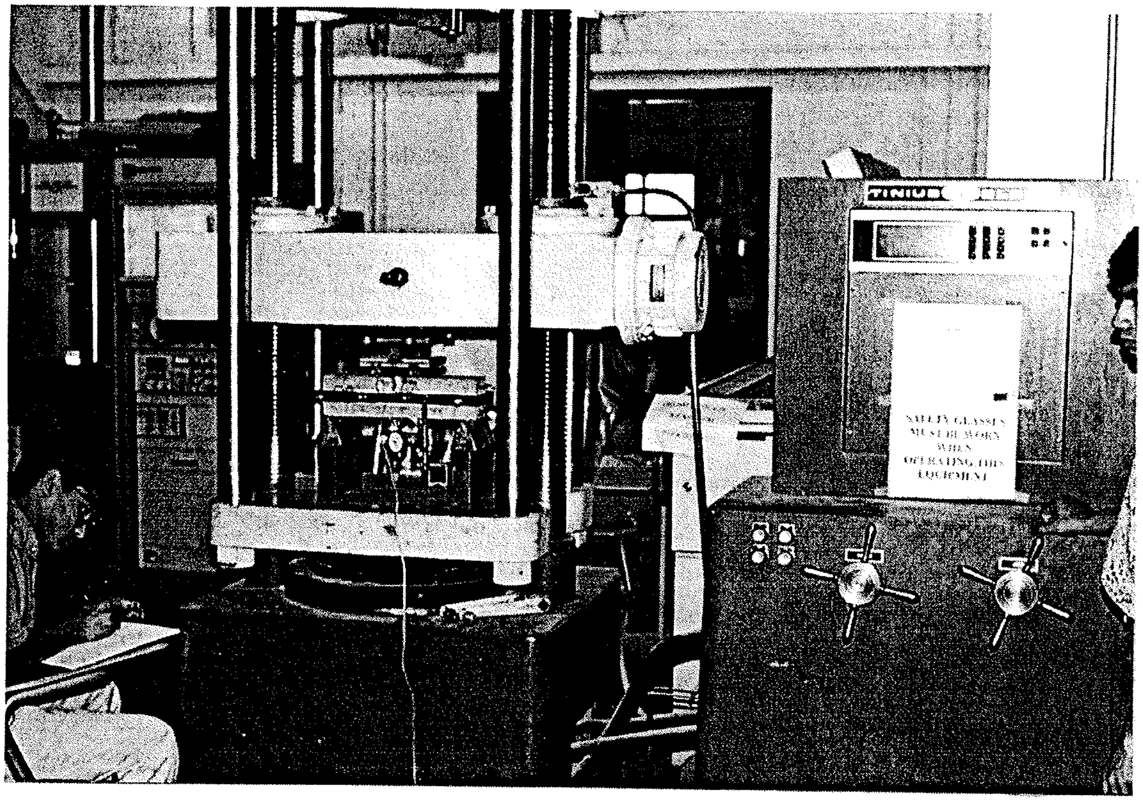

Photo 17 Close-Up of Test Set-Up with True Deflection Measuring Frame & Electrical Strain Gauge Lead Wire

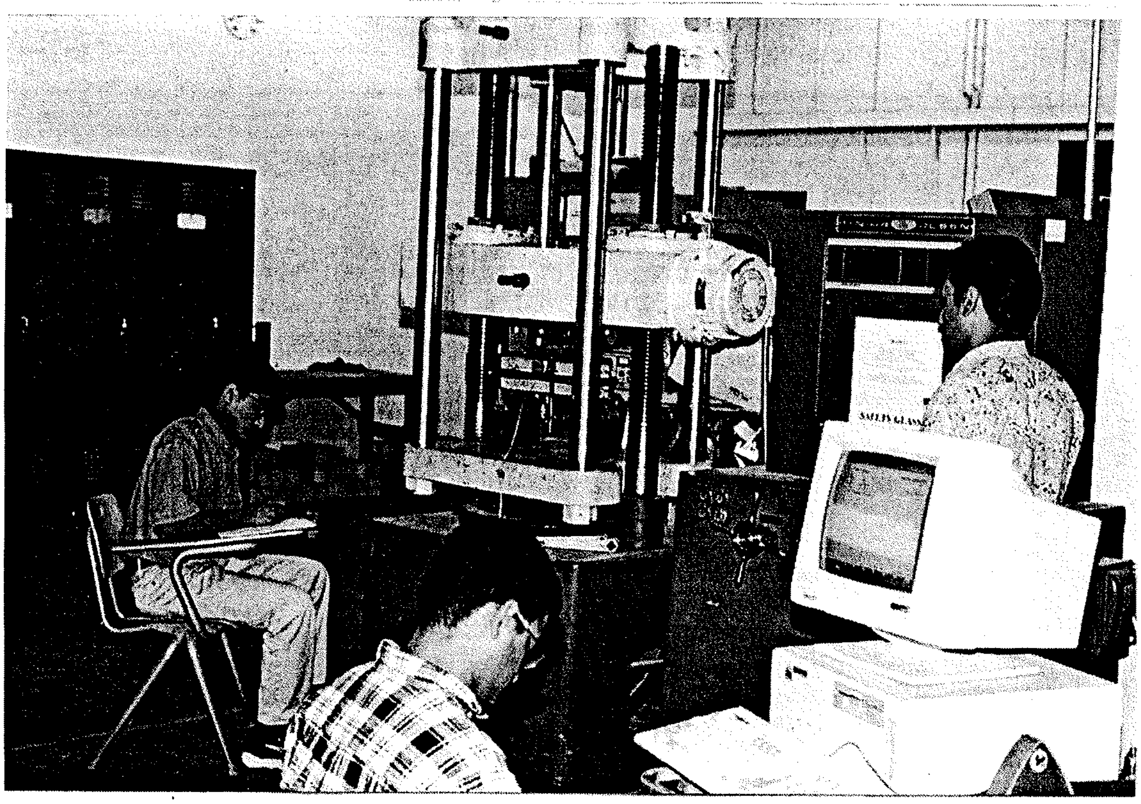

Photo 18 General View of Test Set-Up. Mega-Dac, LVDT Data Logger and the Students Recording the Data can be seen in the Photograph

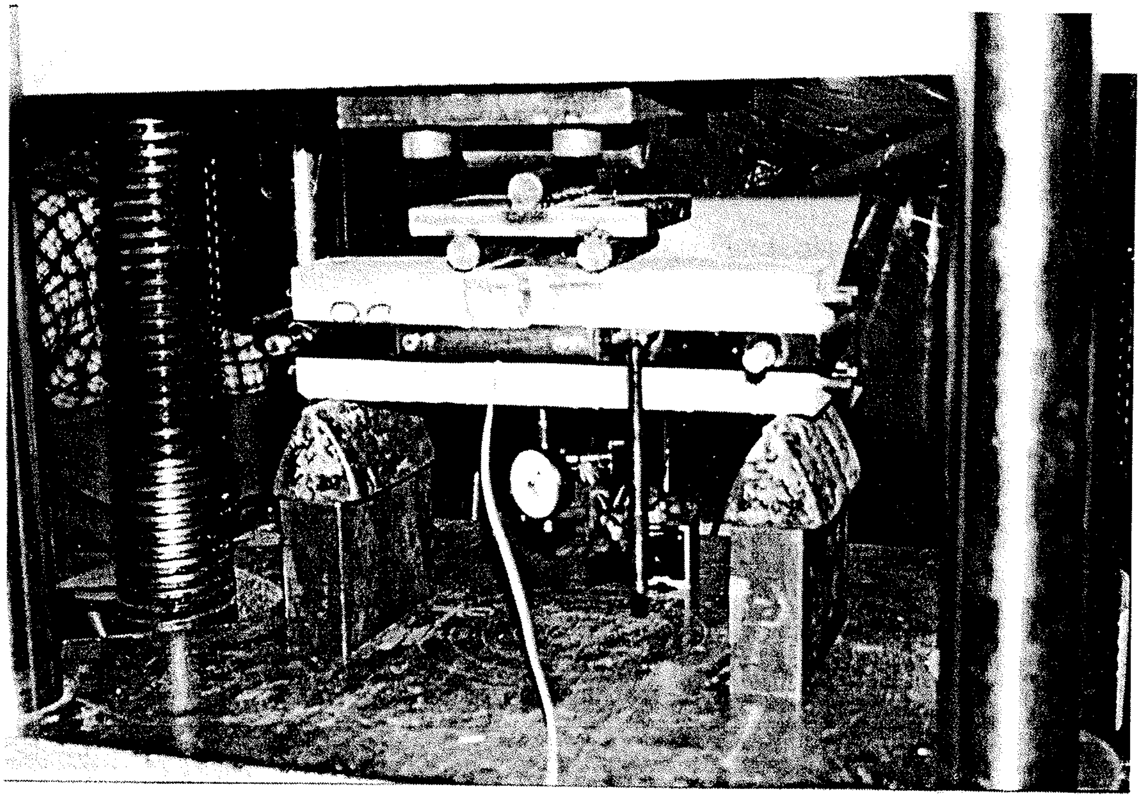

Photo 18a Close-Up of Test Set-Up.
True Deflection Measuring Frame is seen in the Photograph

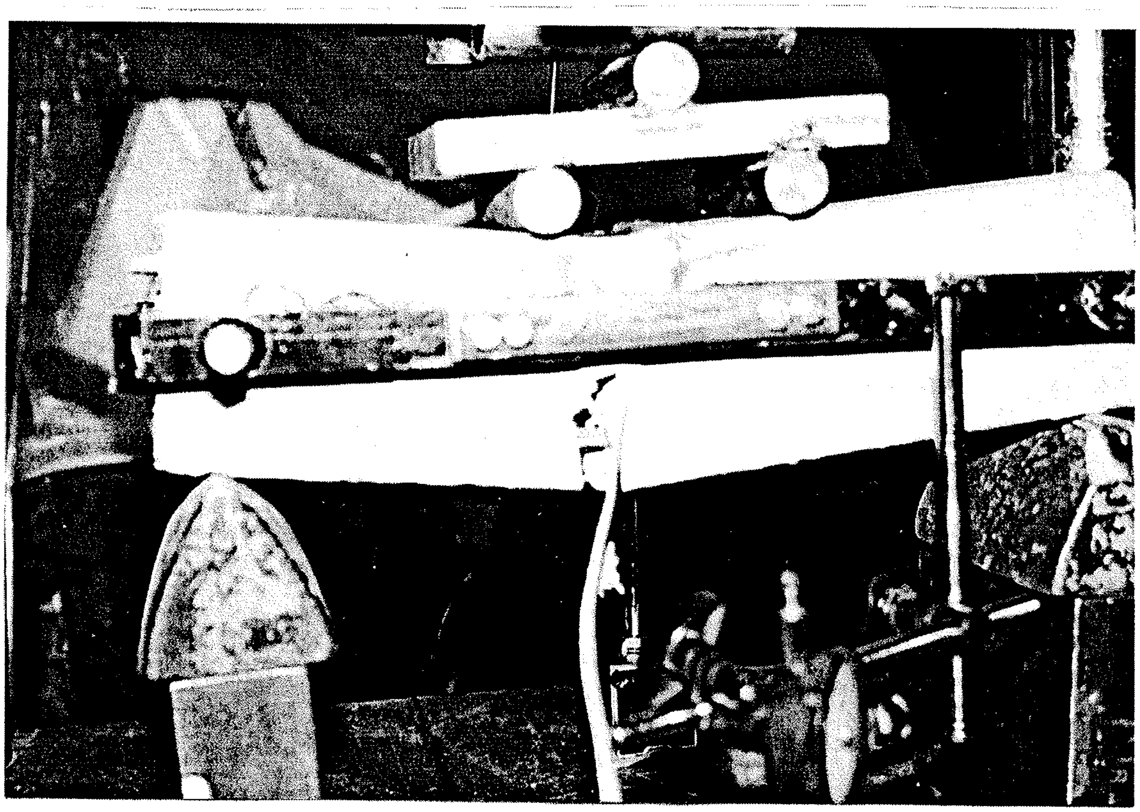

Photo 19 Typical Flexural Failure. (Close-Up)
Wide Crack is Visible in the Photograph

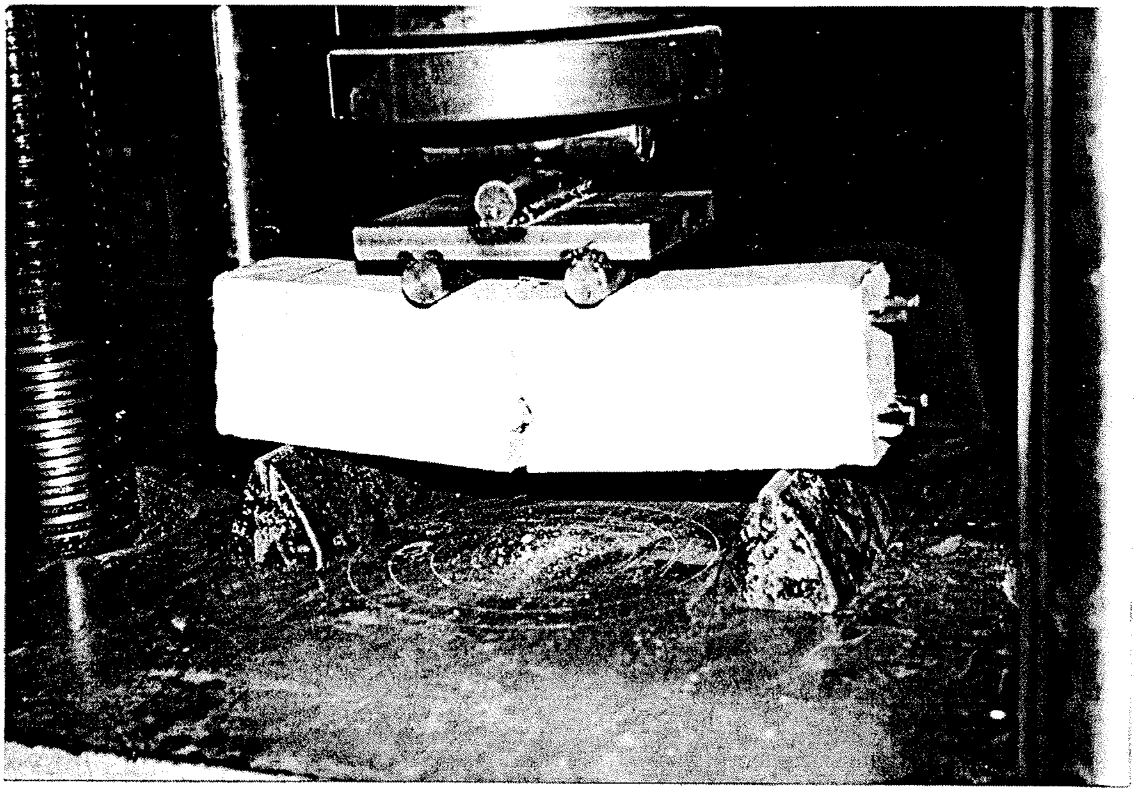

Photo 20 Test Set-Up, Without Deflection Gauge
Typical Flexural Failure

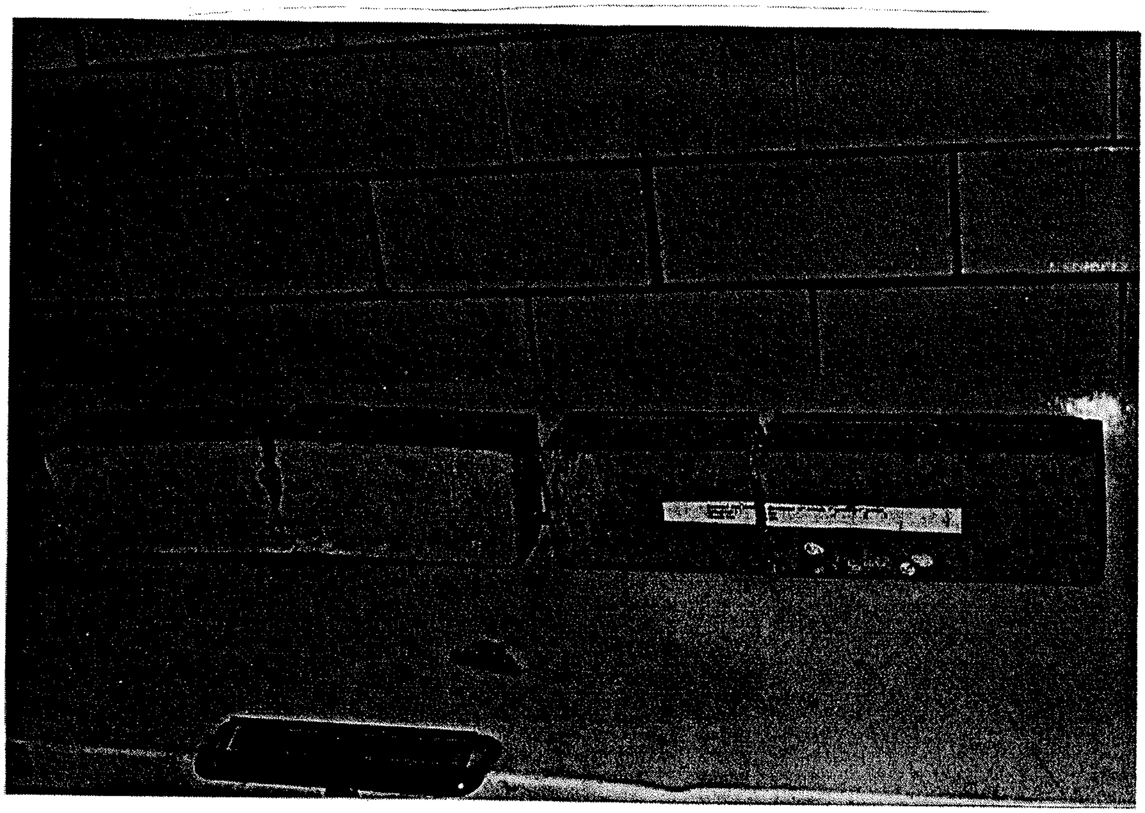

Photo 20a Comparison of Failure of Plain & Basalt Rod Reinforced Beams

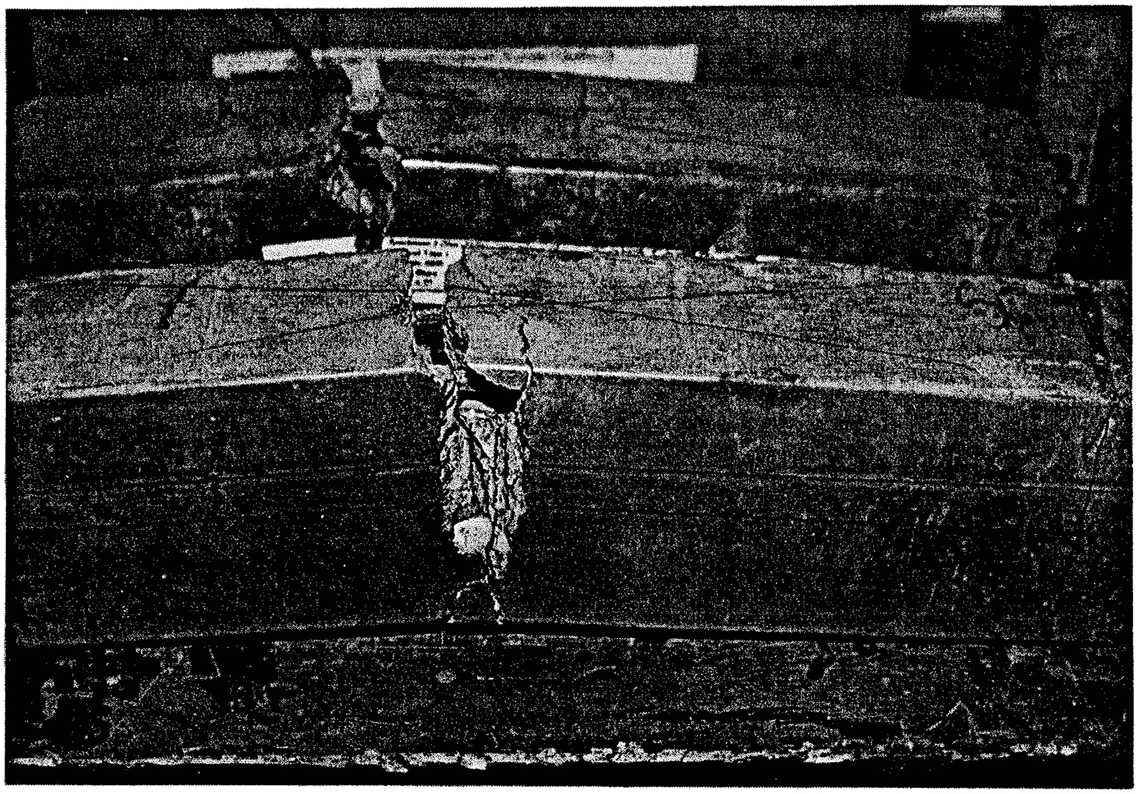

Photo 20b Close-Up of Typical Flexural Failure
The Basalt Rods are Visible in the Photograph

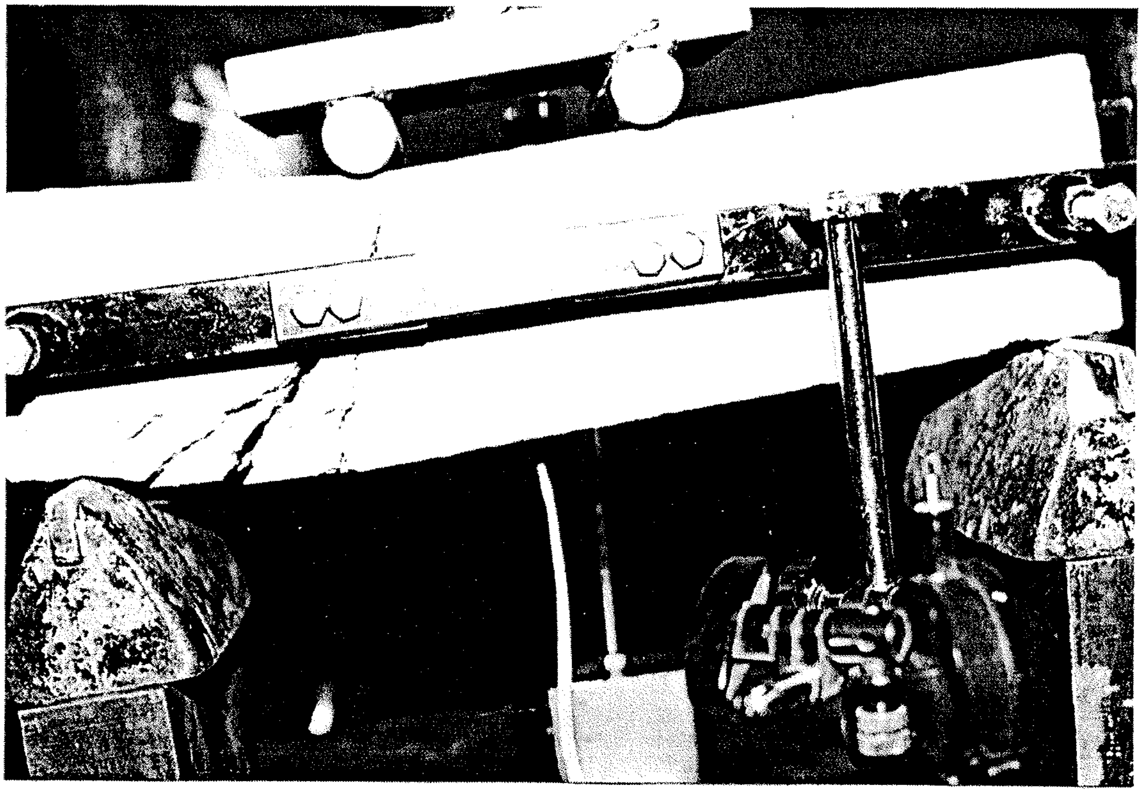

Photo 21 Close-Up of Failure in Shear Mode

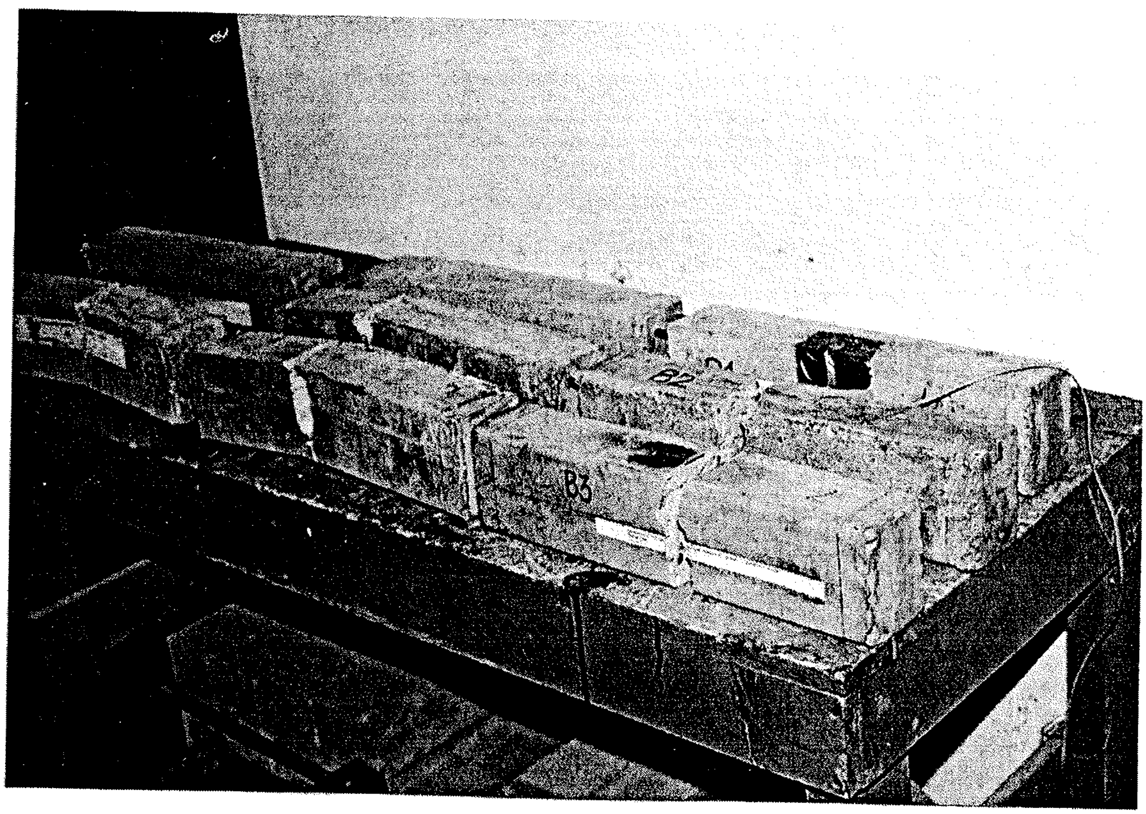

Photo 21a General View of Tested Beams

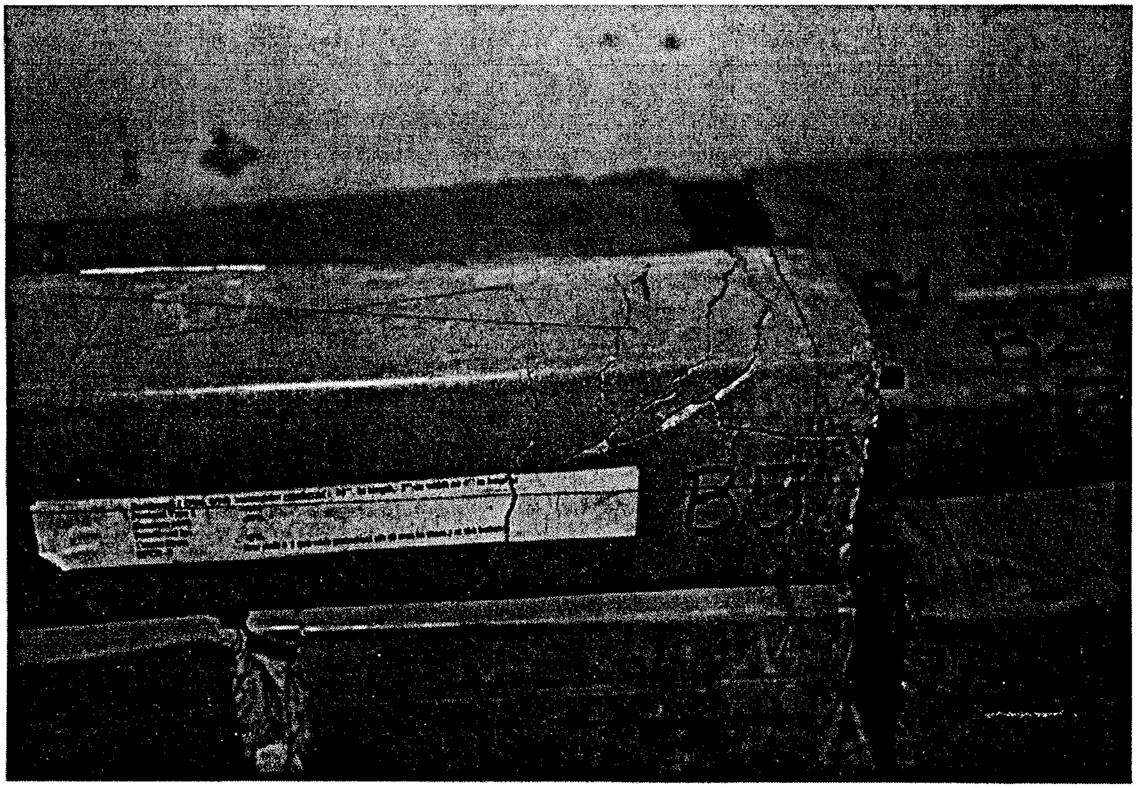

Photo 21b Close-Up of Secondary End Splitting Failure

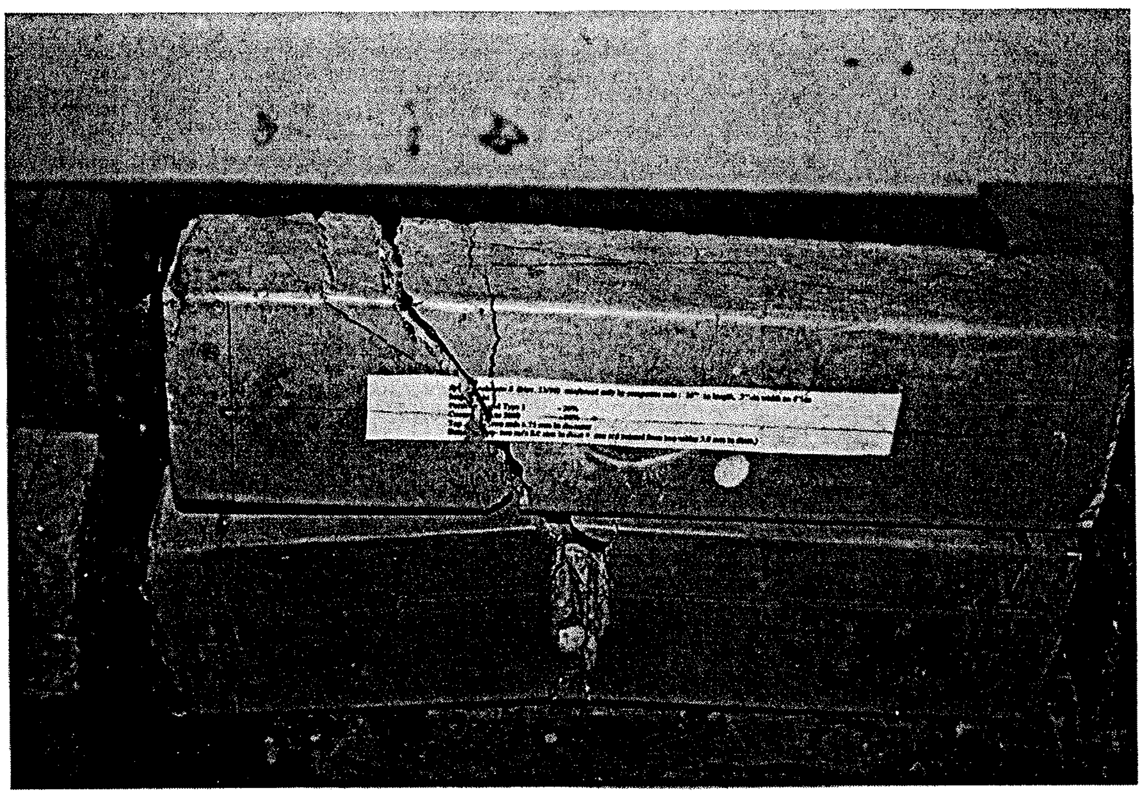

Photo 22 Close-Up of Secondary Shear Failure.

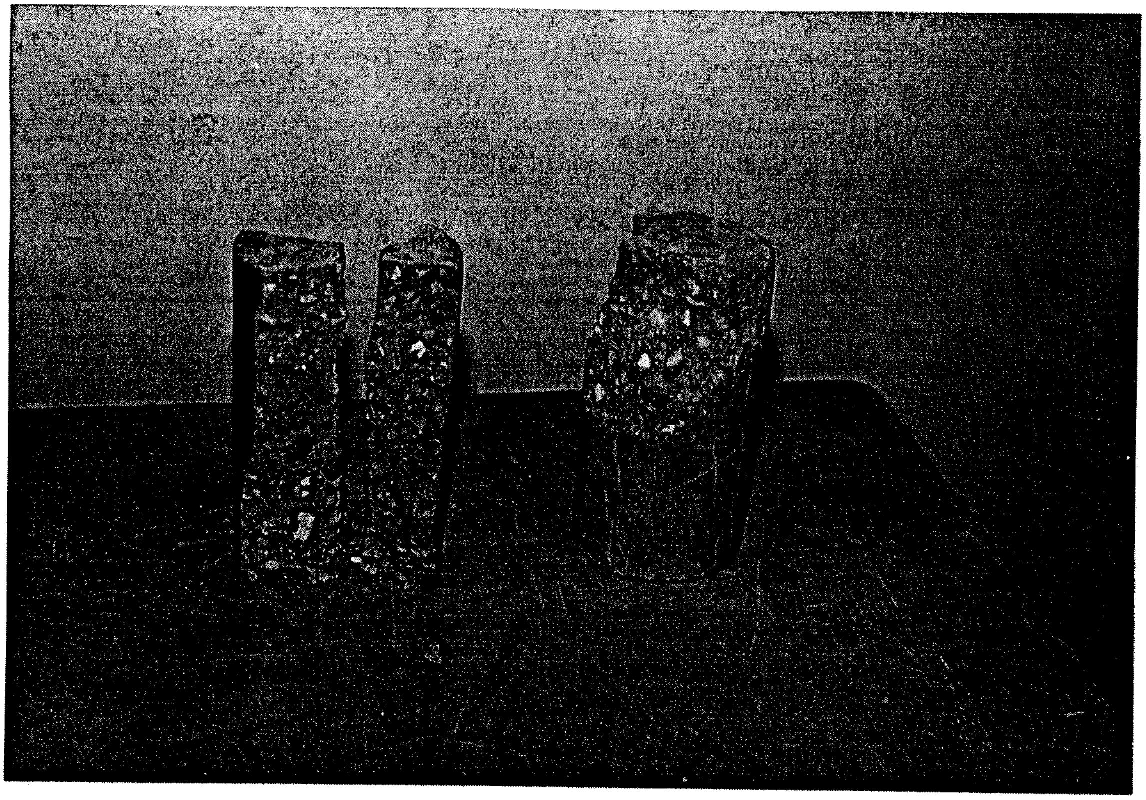

Photo 23 Comparison of Cylinder Failure in Compression

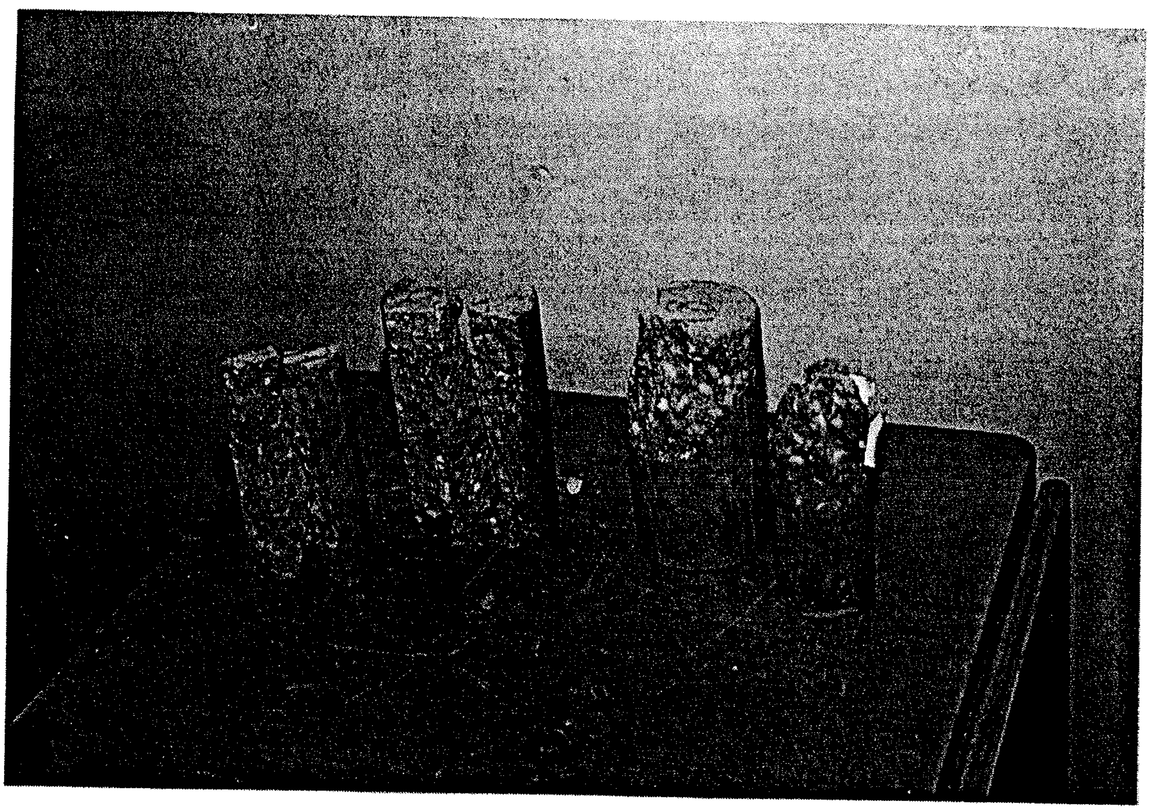

Photo 23a General View of Both Large & Small and Plain & Reinforced Cylinders (Close-Up)

SKETCH 1:

BEAM A: SPAN LENGTH = 3'6"

NO. OF BARS = 2

DIA OF BAR = 0.56"

DEVELOPMENT LENGTH = 4½" (ON EACH SIDE)

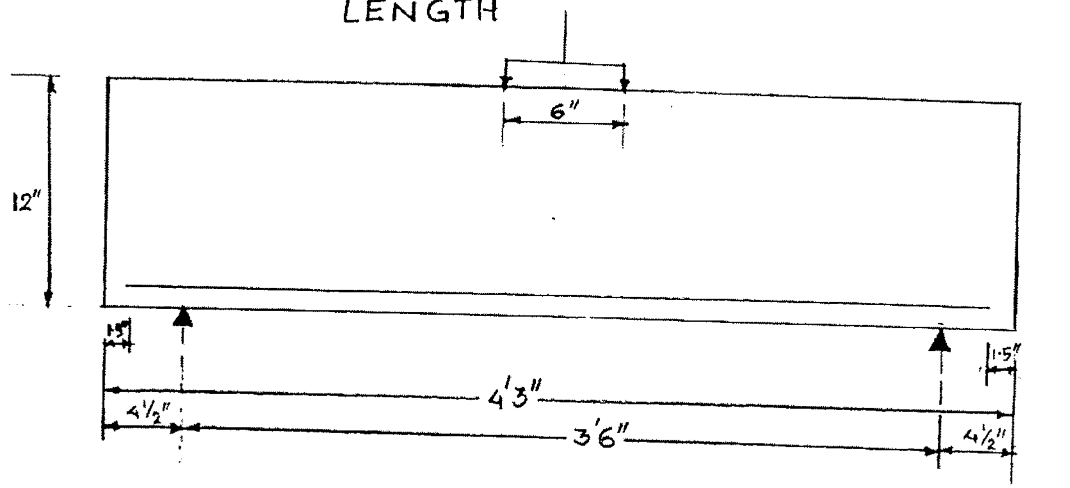

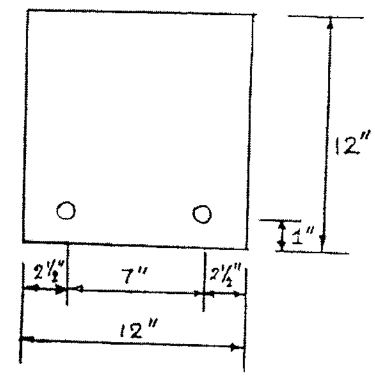

BEAM B: SPAN LENGTH = 3'6"

NO. OF BARS = 2

DIA OF BAR = 0.56"

DEVELOPMENT LENGTH = $4\frac{1}{2}$" (ON EACH SIDE)

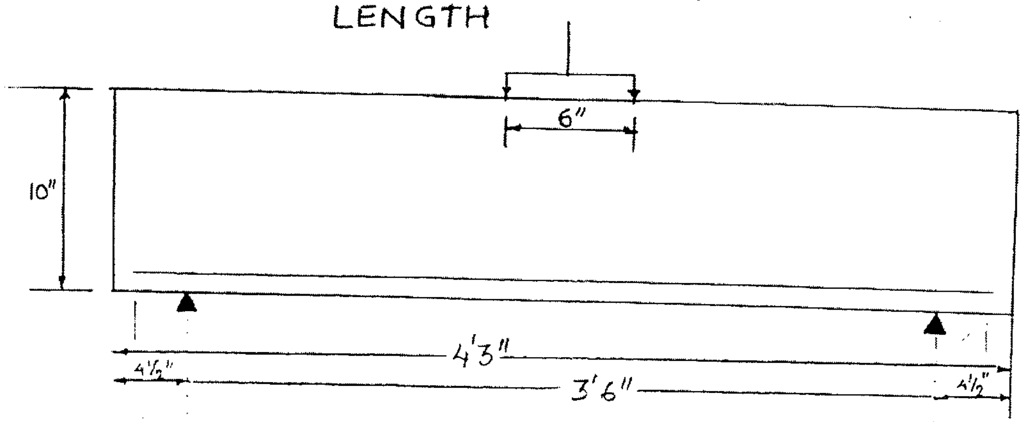

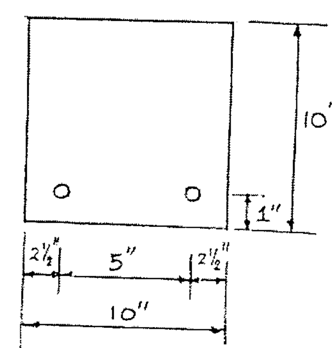

SKETCH 2:

BEAM C:

SPAN LENGTH = 3'6"
NO. OF BARS = 2
DIA OF BAR = 0·56"
DEVELOPMENT LENGTH = $4\frac{1}{2}$" (ON EACH SIDE)

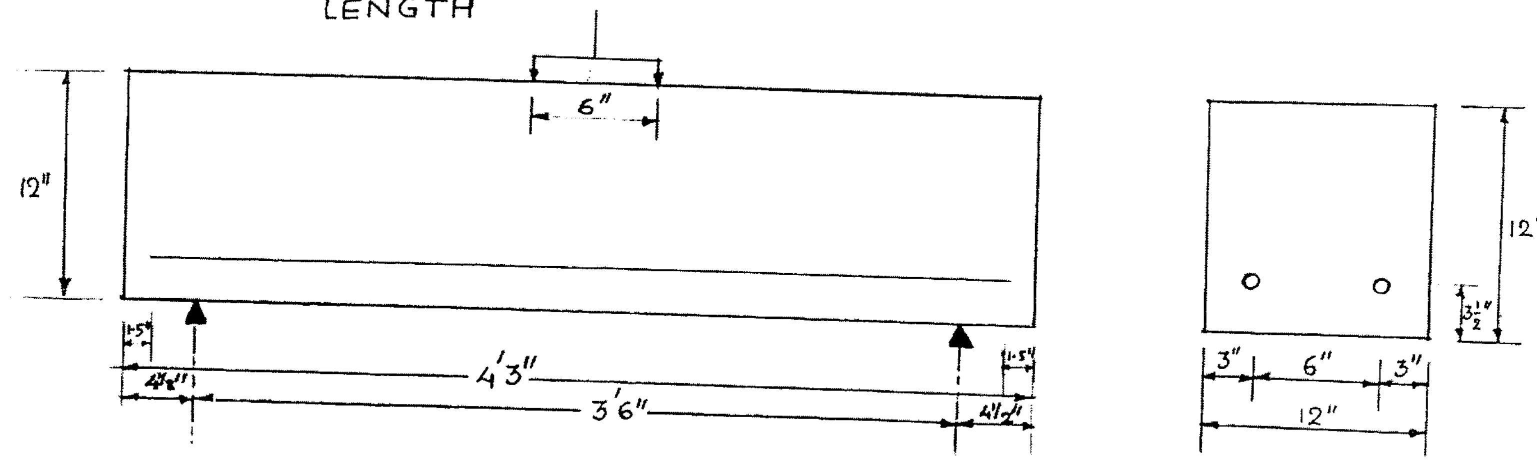

BEAM D:

SPAN LENGTH = 3'6"
NO. OF BARS = 2
DIA OF BAR = 0·56"
DEVELOPMENT LENGTH = $4\frac{1}{2}$" (ON EACH SIDE)

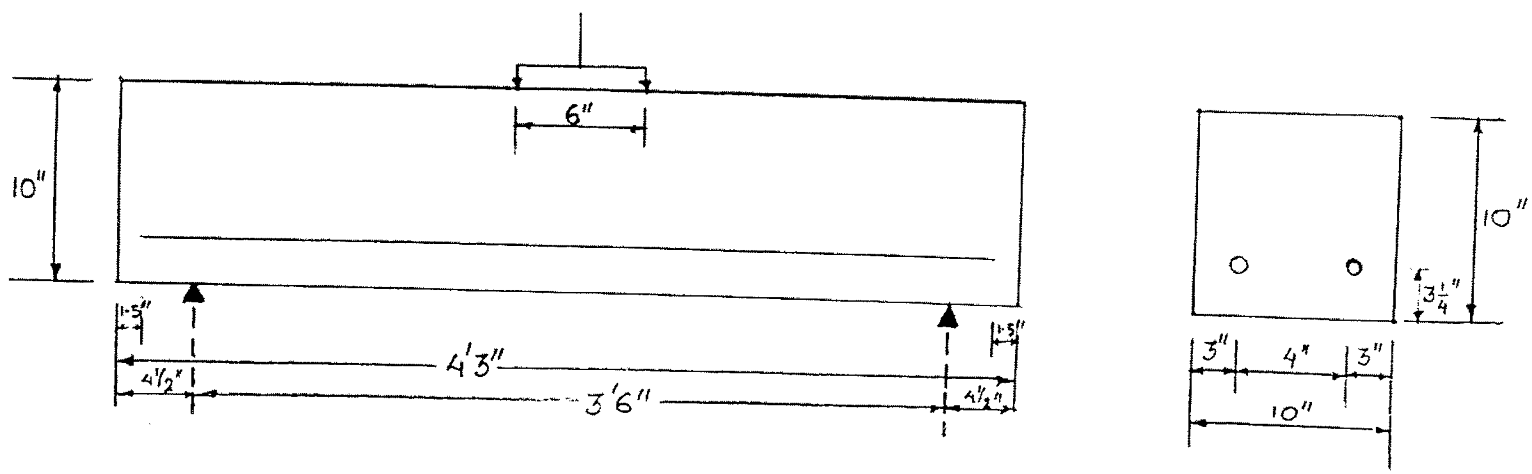

SKETCH 3:

BEAM E:
SPAN LENGTH = 2'6"
NO. OF BARS = 2
DIA OF BAR = 0.56"
DEVELOPMENT LENGTH = 1'0" (ON EACH SIDE)

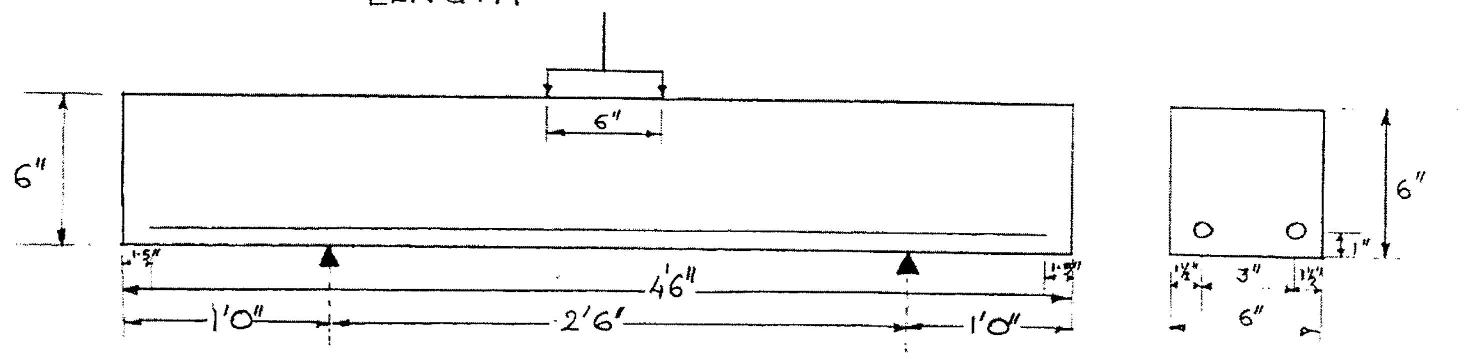

BEAM F:
SPAN LENGTH = 3'0"
NO. OF BARS = 2
DIA OF BAR = 0.2"
DEVELOPMENT LENGTH = 1'3" (ON EACH SIDE)

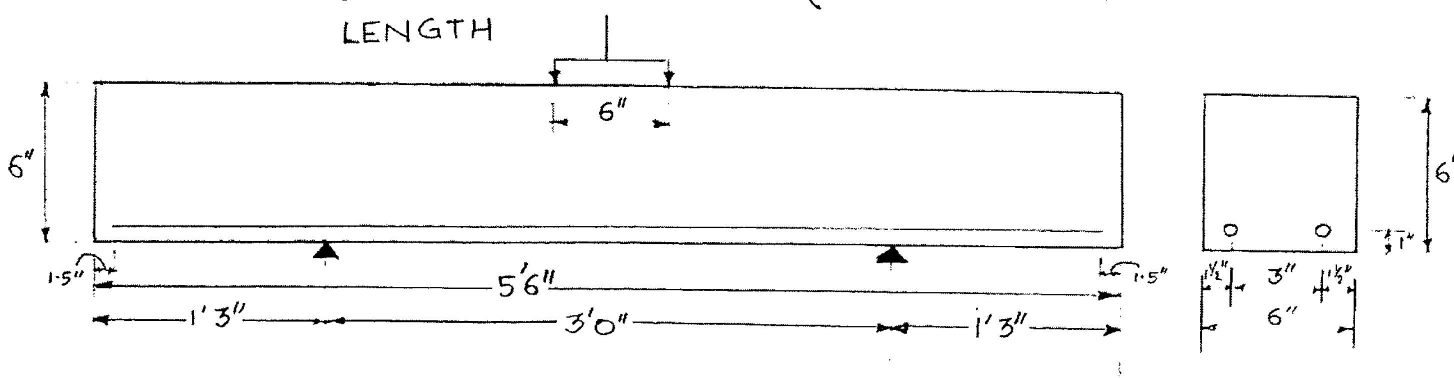

SKETCH 4:

(SIDE VIEW)

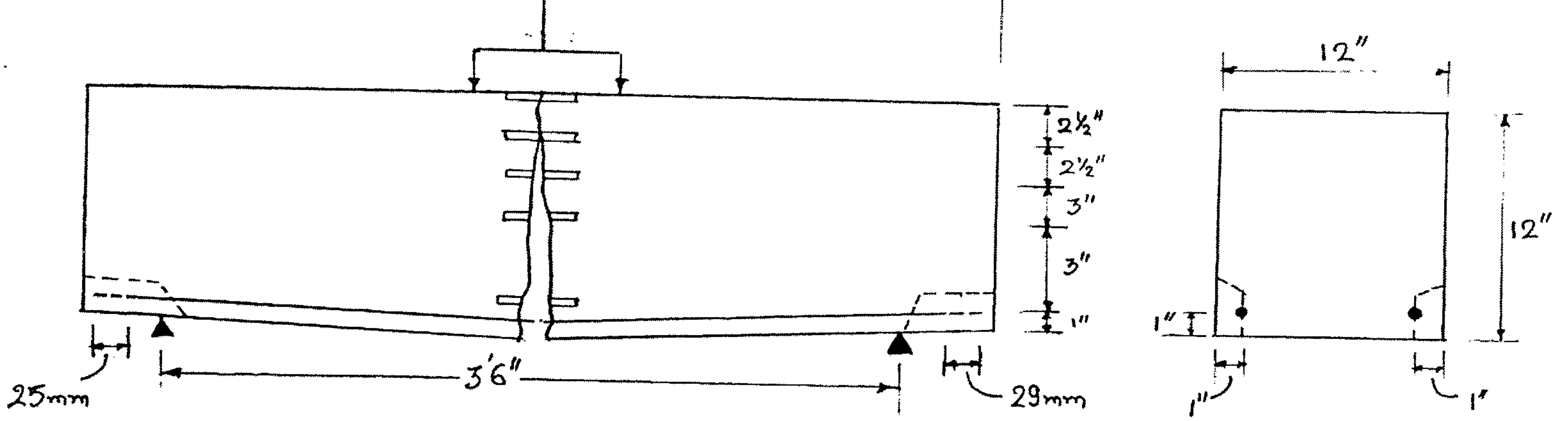

BEAM BRC-A

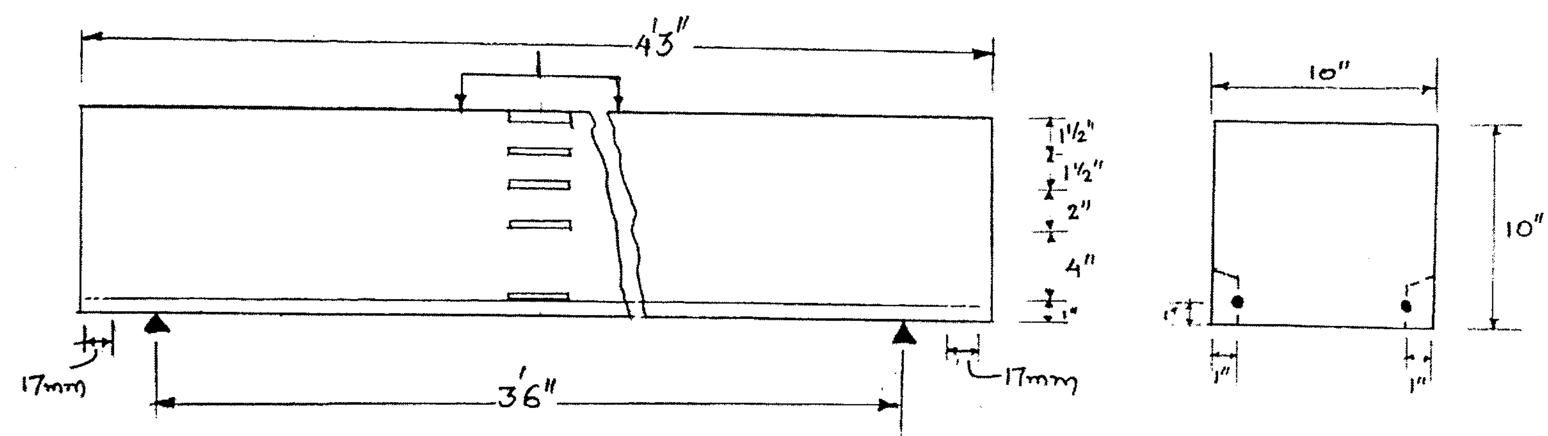

BEAM BRC-B

SKETCH 4a:

BRC-C

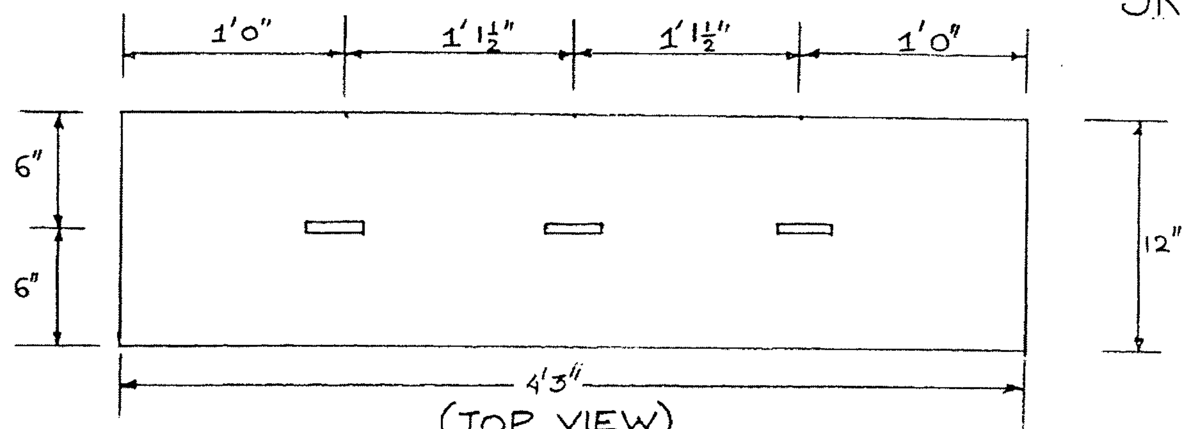

(TOP VIEW)

BRC-D

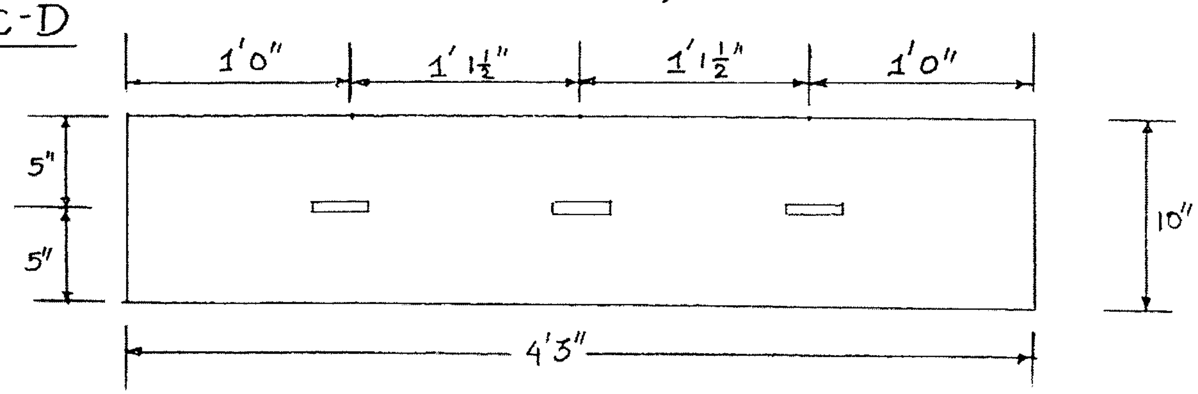

(TOP VIEW)

SKETCH 5:

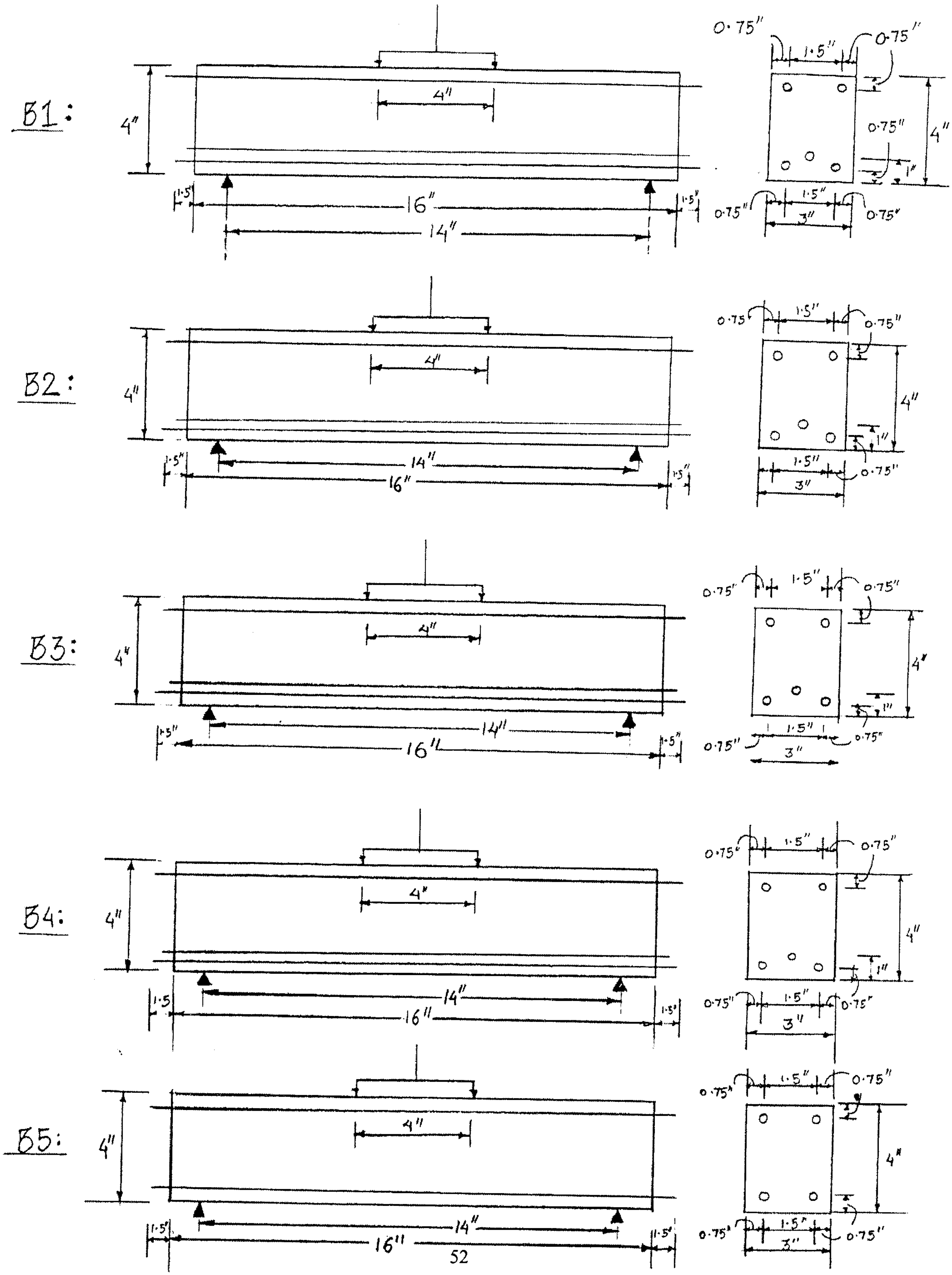
B1:
4"
4"
16"
14"
1·5"
1·5"
0·75"
1·5"
0·75"
0·75"
4"
1"
0·75"
1·5"
0·75"
3"
B2:
4"
4"
14"
16"
1·5"
1·5"
0·75
1·5"
0·75"
4"
1"
1·5"
0·75"
3"
B3:
4"
4"
14"
16"
1·5"
1·5"
0·75"
1·5"
0·75"
4"
1"
0·75"
1·5"
0·75"
3"
B4:
4"
4"
14"
16"
1·5
1·5"
0·75"
1·5"
0·75"
4"
1"
0·75"
1·5"
0·75"
3"
B5:
4"
4"
14"
16"
1·5"
1·5"
0·75"
1·5"
0·75"
4"
0·75"
1·5"
0·75"
3"

Table 9:Mix Proportions for Concrete Reinforced with Basalt Rebars (Beams Designed & Cast in the Lab)

For 0.142 m^3 (5.0 ft^3)

Specimen No.	W/C	Cement kg(lbs)	Fine Agg. kg(lbs)	Coarse Agg. kg(lbs)	Water kg(lbs)
BRC-A	0.5	51.36 (113)	133 (292.6)	133 (292.6)	25.68 (56.5)
BRC-B	0.5	51.36 (113)	133 (292.6)	133 (292.6)	25.68 (56.5)
BRC-C	0.5	51.36 (113)	133 (292.6)	133 (292.6)	25.68 (56.5)
BRC-D	0.5	51.36 (113)	133 (292.6)	133 (292.6)	25.68 (56.5)

For 0.0852 m^3 (3.0 ft^3)

BRC-E & F	0.5	30.8(67.8)	79.8(175.5)	79.8(175.5)	15.4(33.9)

Basic Mix Proportions for one m^3 (yd.^{3})

Cement kg(lbs)	Water kg(lbs)	Fine Agg. kg(lbs)	Coarse Agg. kg(lbs)	Water Cement Ratio
361.9 (610)	188 (305)	937.4 (1580)	937.4 (1580)	0.5

Table 10: Details of Beams Designed and Cast in the Lab

Beam No.	Dimensions (in)	Details of Reinforcement
BRC-A	12in x 12in x 51in	Two basalt rebars with a diameter of 0.56in and length 48in. The cover was maintained at 1in. Development length was 4.5in on each side.
BRC-B	10in x 10in x 51in	Two basalt rebars with a diameter of 0.56in and length 48in. The cover was maintained at 1in. Development length was 4.5in on each side.
BRC-C	12in x 12in x 51in	Two basalt rebars with a diameter of 0.56in and length 48in. The cover was maintained at 3.5in. Development length was 4.5in on each side.
BRC-D	10in x 10in x 51in	Two basalt rebars with a diameter of 0.56in and length 48in. The cover was maintained at 3.25in. Development length was 4.5in on each side.
BRC-E	6in x 6in x 51in	Two basalt rebars with a diameter of 0.56in and length 48in. The cover was maintained at 1in. Development length was 12in on each side.
BRC-F	6in x 6in x 66in	Two basalt rebars with a diameter of 0.2in and length 60in. The cover was maintained at 1in. Development length was 15in on each side.

Table 10a: Comparison of Calculated & Actual Moments (For Beams BRC-A to F)

Beam No.	Ultimate Load KN(lbs)	Cracking Load KN(lbs)	Actual Moments		Calculated Moments	
			Ultimate KN.m(k-ft.)	Cracking KN.m(k-ft.)	Ultimate KN.m(k-ft.)	Cracking KN.m(k-ft.)
BRC-A	71.20 (16000)	66.00 (15000)	16.27 (12.00)	15.25 (11.25)	119.80 (88.35)	17.82 (13.14)
BRC-B	44.50 (10000)	37.80 (8500)	10.17 (7.50)	8.65 (6.38)	92.60 (68.26)	9.98 (7.36)
BRC-C	68.50 (15400)	57.80 (13000)	15.66 (11.55)	13.22 (9.75)	89.60 (66.00)	17.76 (13.10)
BRC-D	43.00 (9700)	35.60 (8000)	9.87 (7.28)	8.14 (6.00)	69.69 (48.44)	9.98 (7.36)
BRC-E	45.00 (10100)	40.00 (9000)	6.85 (5.05)	6.10 (4.50)	35.90 (26.50)	2.26 (1.67)
BRC-F	12.20 (2750)	11.10 (2500)	2.33 (1.72)	2.12 (1.56)	3.57 (2.63)	2.25 (1.66)

Table 11: Details of the Basalt Rods Used for Reinforcing the Concrete

Name	Size of Beam (inches)	No. of Bars	Description of Bars	Coarse Fibers (%)
BR-1	3in x 4in x 14in	5	2 rods with 6.75mm(0.265in) in diameter(top) & 1 rod having periodical twisted ribs & made from 2 cables of 3mm(0.118in) diameter & 2 rods with 6.75mm(o.27in) in diameter at bottom.	1.5
BR-2	3in x 4in x 14in	5	2 rods with 6.75mm(0.265in) in diameter(top) & 1 rod 8mm(0.32in) in diameter & 2 rods with 6.75mm(0.27in) diameter at bottom.	2
BR-3	3in x 4in x 14in	5	2 rods with 6.75mm(0.265in) in diameter(top) & 1 rod having periodical twisted ribs & made from 2 cables of 3mm(0.118in) diameter & 2 rods with 6.75mm(0.27in) at bottom.	1.5
BR-4	3in x 4in x 14in	5	2 rods with 6.75mm(0.265in) in diameter(top) & 1 rod having periodical twisted ribs & made from 2 cables of 3mm(0.118in) diameter with 2 rods of 8mm(0.32in) diameter at bottom.	--
BR-5	3in x 4in x 14in	4	2 rods at top with 6mm(0.24in) in diameter & 2 rods at bottom with 6mm(0.24in) in diameter. Fibers were ROVING RB-15(chopped) & 10mm(0.4in) in length.	2

Details of the Plain Concrete Beams

P1	3in x 4in x 14in	--	Plain(Control) Concrete Beam	--
P2	3in x 4in x 14in	--	Plain(Control) Concrete Beam	--
P3	3in x 4in x 14in	--	Plain(Control) Concrete Beam	--

TABLE 12: TOUGHNESS INDICES

Mixture Type	Specimen #	First Crack Toughness (inch-lbs)	Toughness Indices			Toughness Ratios		Residual Strength Indices	
			I5	I10	I20	I10/I5	I20/I10	$R_{5,10}$	$R_{10,20}$
BRC	1	3.0	5.2	9.7	16.2	1.7	1.9	64.5	90.8
BRC	2	2.8	4.8	9.0	15.4	1.7	1.9	64.1	83.6
BRC	3	2.4	5.2	9.9	17.7	1.8	1.9	77.9	94.4
BRC	4	3.5	4.8	8.9	15.0	1.7	2.0	60.3	83.0
BRC	5	2.3	4.8	9.3	16.5	1.8	2.0	72.3	88.4

Japanese Toughness Index & Equivalent Flexural Strength

Mixture Type	Specimen #	Toughness (inch-lbs)	Equivalent Flexural Strength(psi)
BRC	1	154.8	469.0
BRC	2	141.2	415.5
BRC	3	138.2	407.8
BRC	4	155.2	487.9
BRC	5	137.3	404.9

Conversion Factor:
1 in-lb = 0.113 Nm

Table 13: Comparison of Calculated and Actual Moments

Beam No.	Ultimate Load (KN)	Cracking Load (KN)	Actual Moments		Calculated Moments	
			Ultimate (KN.m)	Bond Slip (KN.m)	Ultimate (KN.m)	Cracking (KN.m)
BRC-1	20.00	17.70	1.27	1.12	4.07	0.33
BRC-2	18.20	16.00	1.16	1.02	4.30	0.33
BRC-3	15.60	12.40	0.99	0.79	4.07	0.33
BRC-4	21.00	19.00	1.33	1.21	5.50	0.33
BRC-5	16.00	15.00	1.02	0.95	3.20	0.33

Conversion Factor:
25.4mm = 1in.
1 in-lb = 0.113 Nm

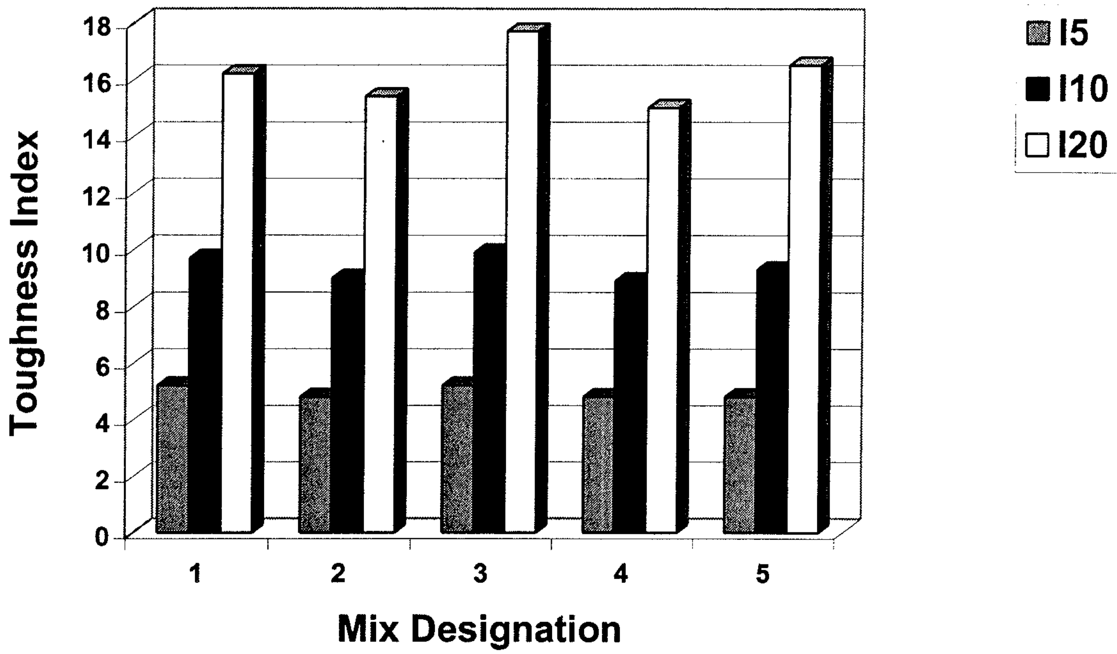

Fig. 8 Comparison of Toughness Indices for BRC-1to5

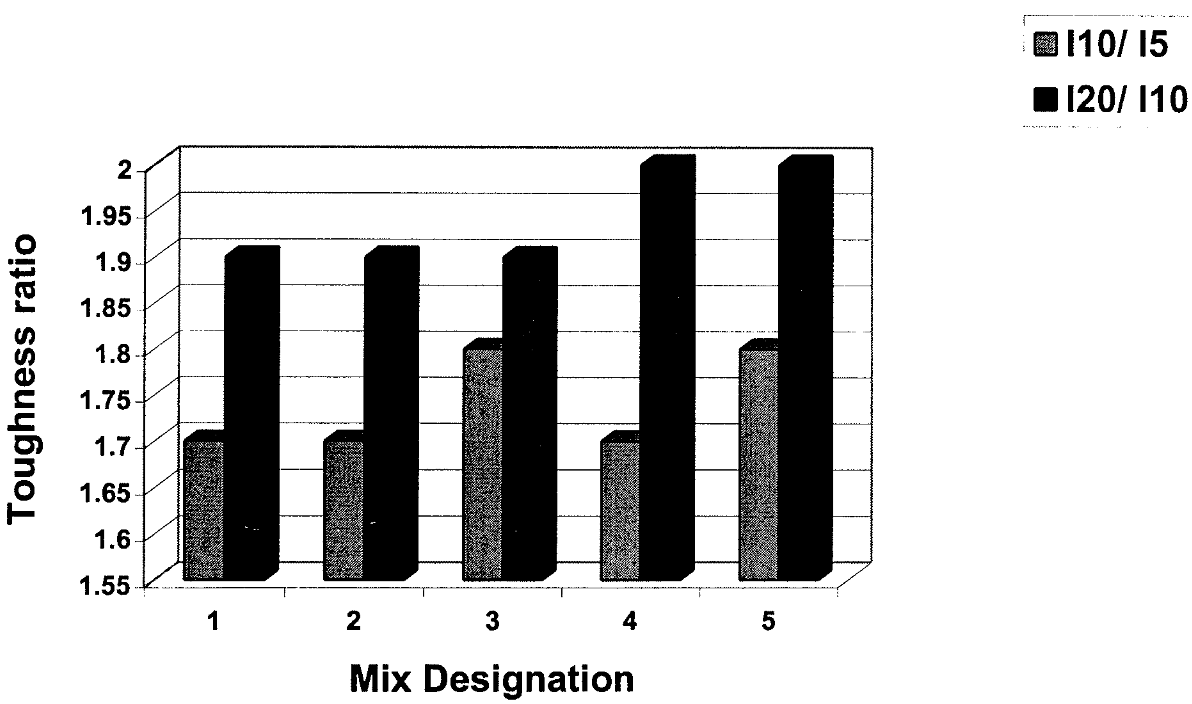

Fig. 9 Comparison of Toughness

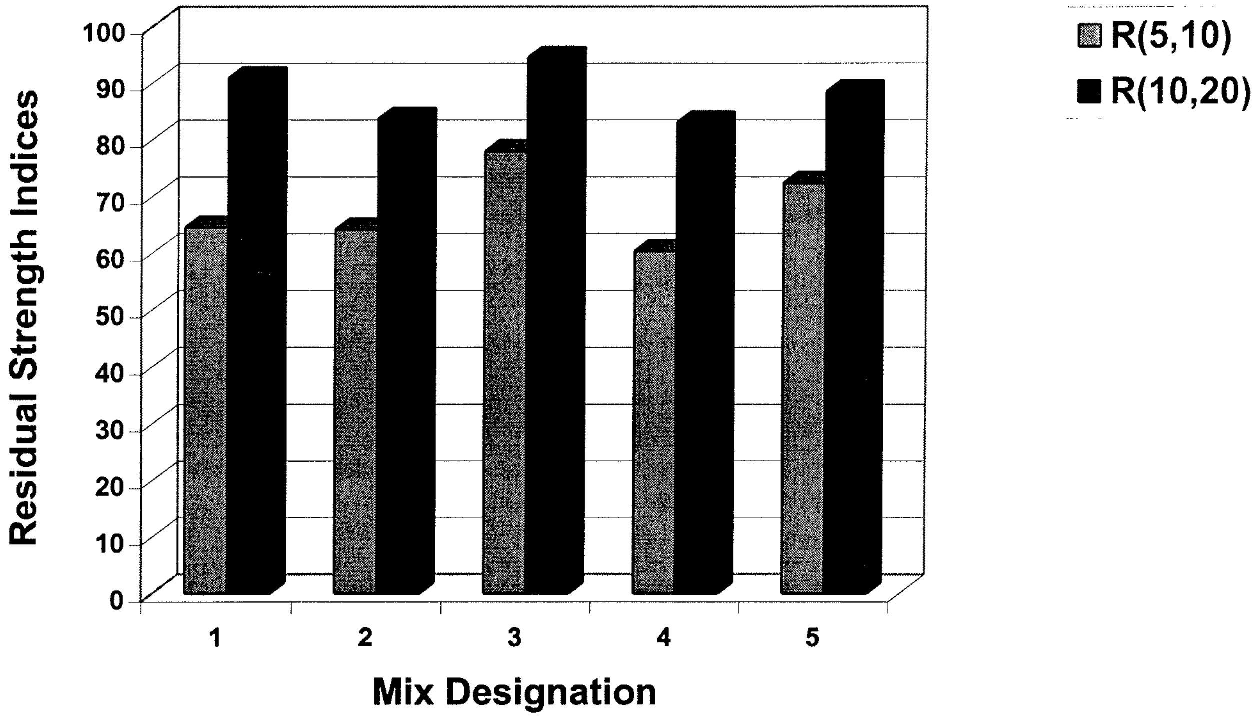

Fig. 10 Comparison of Residual Strength Indices for BRC-1to5

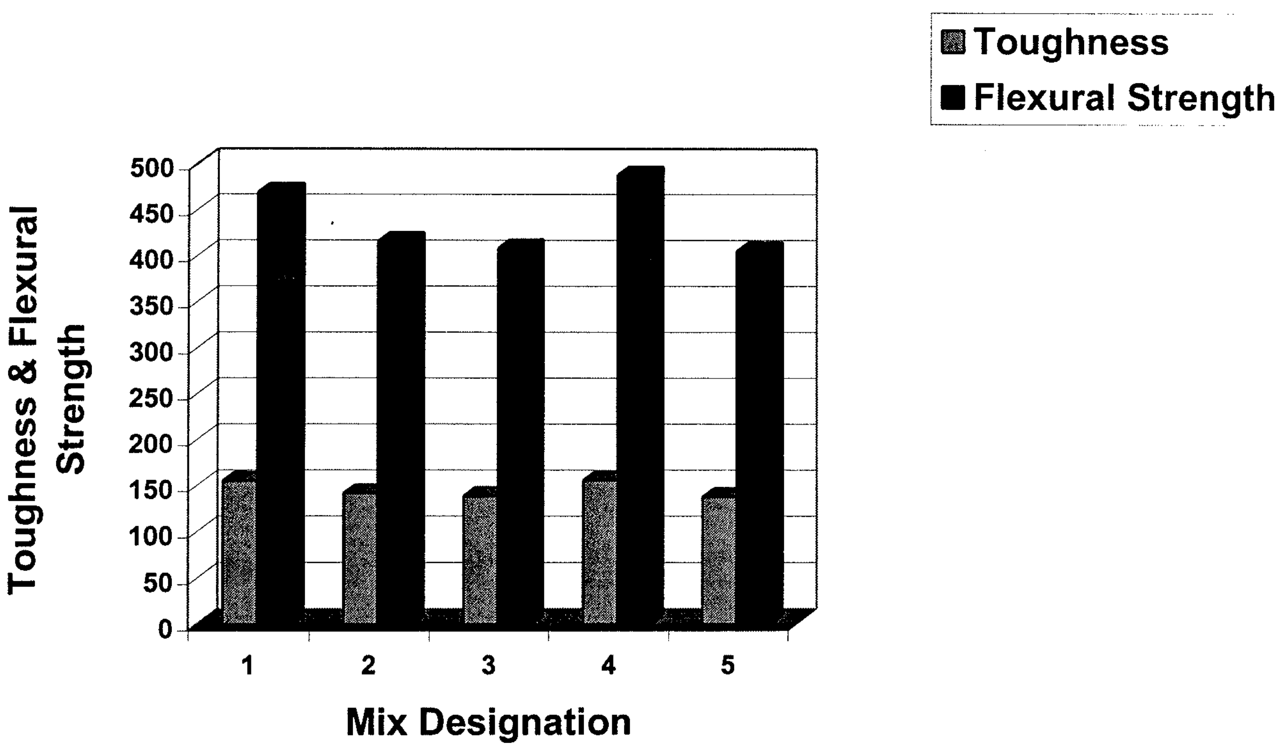

Fig. 11 Comparison of Japanese Toughness & Equivalent

6. REFERENCES

1. ACI Committee 544, "State-of-the-Art Report on Fiber Reinforced Concrete", Report ACI 544 IR-82, Concrete International Design and Construction, May 1982.
2. Ramakrishnan, V., "Recent Advancements in Concrete Fiber Composites", ACI-Singapore Chapter – Special Publication, July 19, 1993.
3. Ramakrishnan, V., "High Performance Fiber Reinforced Concretes," Application of High Performance Concrete Including Marine Structures, National Science Foundation (NSF) and Australian Research Council (ARC) – Sponsored USA-Australia Workshop, Sydney, Australia, August 20-23, 1997, pp. 2-31.
4. Ramakrishnan, V., "A New Material (Polyolefin Fiber Reinforced Concrete) for the Construction of Pavements and White-Topping of Asphalt Roads," Proceedings of the Sixth International Purdue Conference on Concrete Pavement: Design and Materials for High Performance, Indianapolis, Nov. 18-21, 1997, pp. 119-130.
5. Ramakrishnan, V., "Performance Characteristics and Applications of High – Performance Synthetic Fiber Reinforced Concretes," Proceedings of the International Workshop on High Strength Concrete and Structural Strengthening, Singapore, Nov. 29, 1997, pp. 33-54.
6. Ramakrishnan, V., "Structural Applications of Polyolefin Fiber Reinforced concrete," American Concrete Institute, Spring Convention, Session on "Structural Application of Fiber Reinforced Concrete," Seattle, Washington, April 6-11, 1997. (Accepted for publication in the proceedings.)
7. Ramakrishnan, V., "Application of a New High Performance Polyolefin Fiber Reinforced Concrete in Transportation Structures," TCDC Workshop on Advances in High Performance Concrete Technology and its Applications, Government of India, Structural Engineering Research Center and United Nations UNDP, April 16-18, 1997, Madras, India.
8. Spadea, G., and Bencardino, F., "Behavior of Fiber-Reinforced Concrete Beams under Cyclic Loading," *Journal of Structural Engineering*, Vol. 123, No. 5, May 1997, pp. 660-668.
9. Trottier, J.F., Morgan, D.R., and Forgeron, D., " Fiber Reinforced Concrete for Exterior Slabs-on-grade, part 1", Concrete International, Vol. 19, No. 6, June 1997, pp. 35-39.
10. Bakht, B., Mufti, A., "F. R. C. Deck Slabs Without Tensile Reinforcement," *Concrete International,* Feb. 1996, pp. 50-55.
11. Billy D. Neeley., and Edward F. O'Neil., "Polyolefin Fiber Reinforced Concrete," *Materials for the New Millennium*, Proceedings of the Fourth Materials Engineering Conference, Washington, D.C., November 10-14, 1996, pp. 113-122.
12. Li Fang., and Christian Meyer., "Biaxial Low-Cycle Fatigue Behavior of Steel Fiber Reinforced Concrete," *Materials for the New Millennium*, Proceedings of the Fourth Materials Engineering Conference, Washington, D.C., November 10-14, 1996, pp. 436-445.
13. Ramakrishnan,V., C.Meyer,A.E.Naaman, "Cyclic Behavior, Fatigue Strength, Endurance Limit and Models for Fatigue Behavior of FRC", Chapter 4,High Performance Fiber Reinforced Cement Composites 2,E& FN Spoon, New York,1996.
14. Adebar, P., Mindess, S., St.-Pierre, D., and Olund, B., " Shear Tests of Fiber Concrete Beams without Stirupps", *ACI Structural Journal*, Vol. 94, No. 1, Jan-Feb 1997, pp.68-76.
15. Armelin, H.S., Banthia, N., "Prediction of Flexural Post Cracking Performance of Steel Fiber Reinforced Concrete from the Pull Out of Single Fibers," *ACI Materials Journal*, Vol. 94, No. 1, Jan. – Feb. 1997, pp. 18-31.
16. Ashour, S.A., Mahmood, K., and Wafa, F.F., " Influence of Steel Fibers and Compression Reinforcement on Deflection of High-Strength Concrete Beams", *ACI Structural Journal*, Vol. 94, No. 6, Nov-Dec 1997, pp. 611-624.
17. Banthia, N.; Yan, C.; and Lee, W.Y., "Restrained Shrinkage Cracking in Fiber Reinforced Concrete with Polyolefin Fibers," Proceedings of the Fifth International Conference on Structural Failure, Durability and Retrofitting, Singapore, Nov. 27-28, 1997, pp. 456-470.
18. Casanova, P., and Rossi, P., " Analysis and Design of Steel Fiber Reinforced Concrete Beams", *ACI Structural Journal*, Vol. 94, No. 5, Sep-Oct 1997, pp. 595-602.

19. Khaloo, R., Nakseok Kim, "Influence of Concrete and Fiber Characteristics on Behavior of Steel Fiber Reinforced Concrete Under Direct Shear," *ACI Materials Journal*, Vol. 94, No. 6, Nov. – Dec. 1997, pp. 592 – 601.
20. Opara, N.K., Dogan, E., Uang, C.M., and Haghyayeghi, A.R., " Flexural Behavior of Composite R.C.-Slurry Infiltrated Mat Concrete (SIMCON) Members", *ACI Structural Journal,* Vol. 94, No. 5, Sep-Oct 1997, pp. 502-512.
21. Paskova, T., Meyer, C., "Low Cycle Fatigue of Plain and Fiber Reinforced Concrete," *ACI Materials Journal*, Vol. 94, No. 4, July – Aug. 1997, pp. 273-285.

APPENDIX A

LOAD-DEFLECTION CURVES
FOR
BASALT FIBER REINFORCED
CONCRETE BEAMS

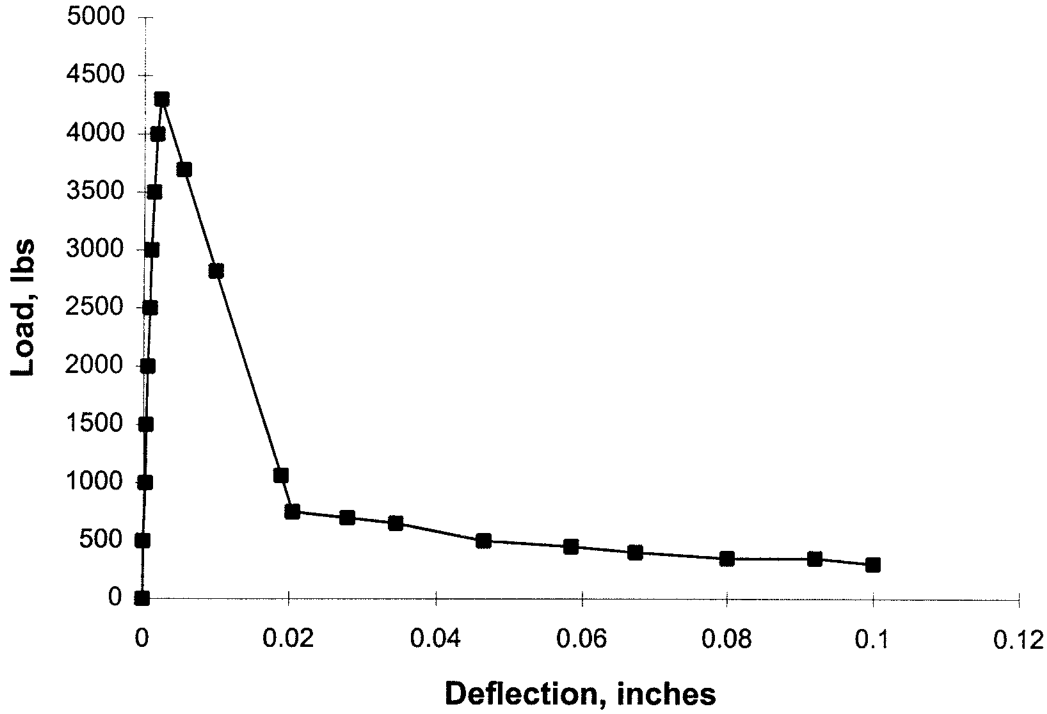

Fig. A1 LOAD DEFLECTION CURVE
Sp: BFRC2-1 (7 Day)

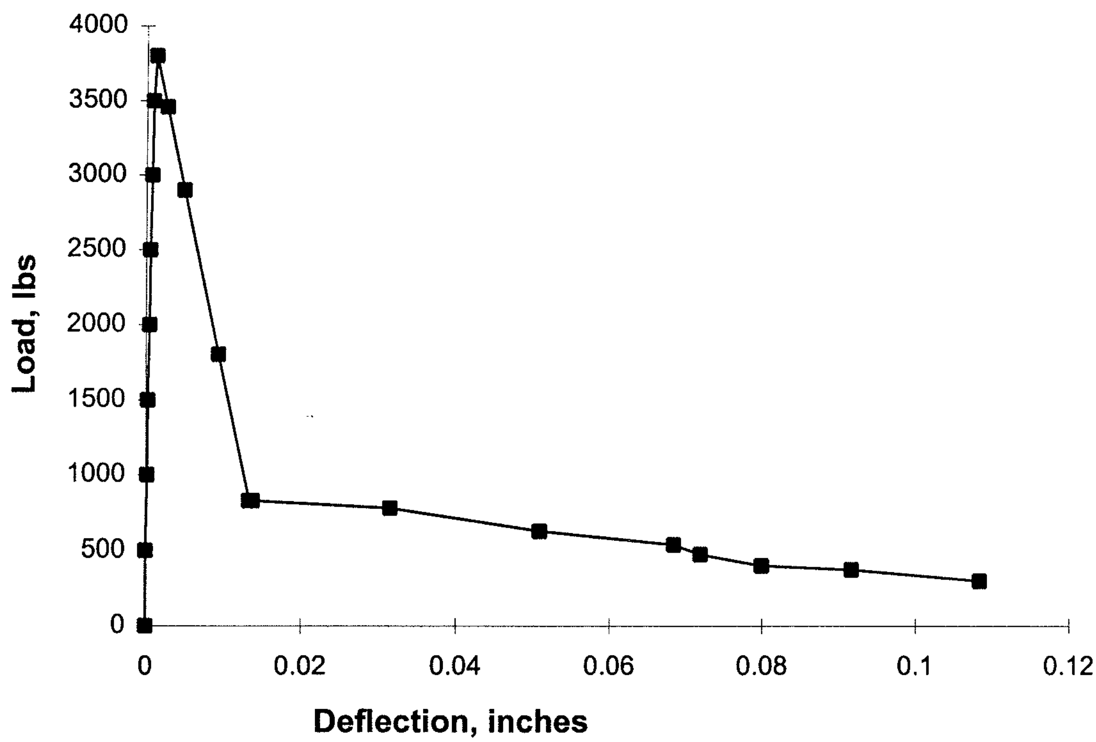

Fig. A2 LOAD DEFLECTION CURVE
Sp: BFRC2-2 (7 Day)

Conversion Factor:
25.4mm = 1in,1kg = 2.2lb

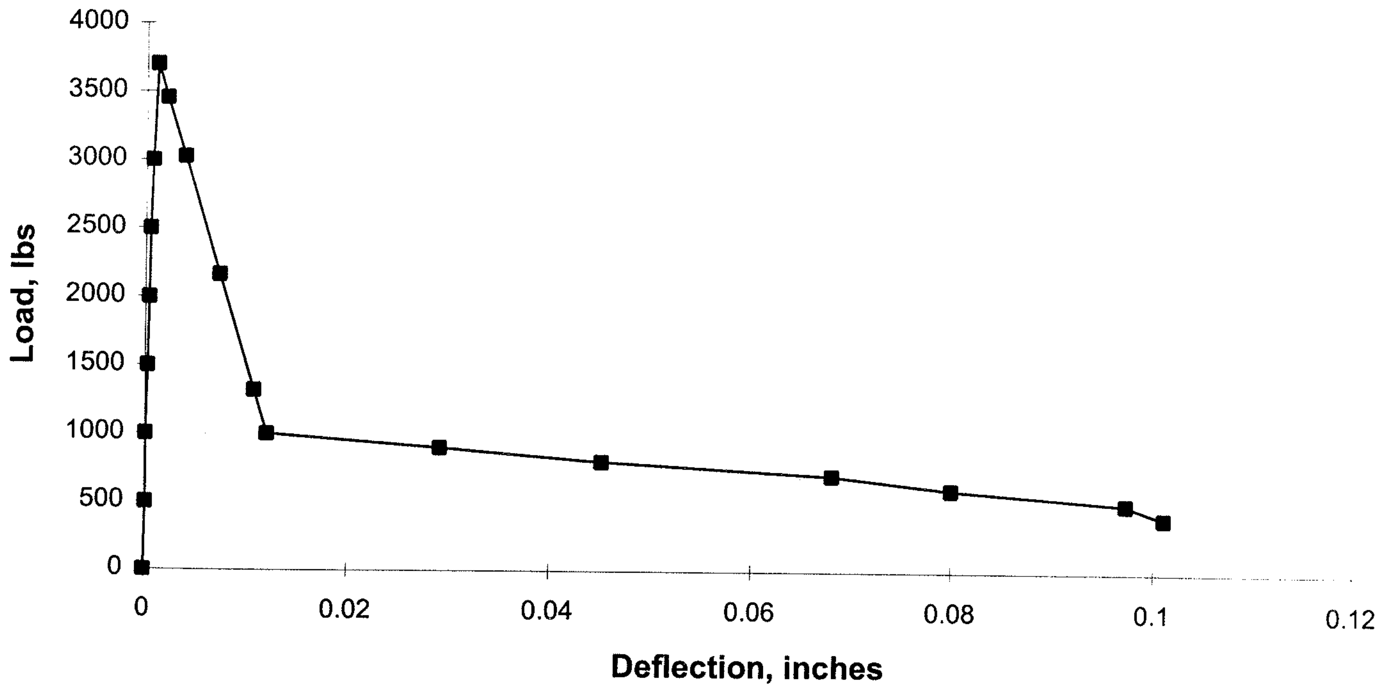

Fig. A3 LOAD DEFLECTION CURVE
Sp: BFRC2-3 (7 Day)

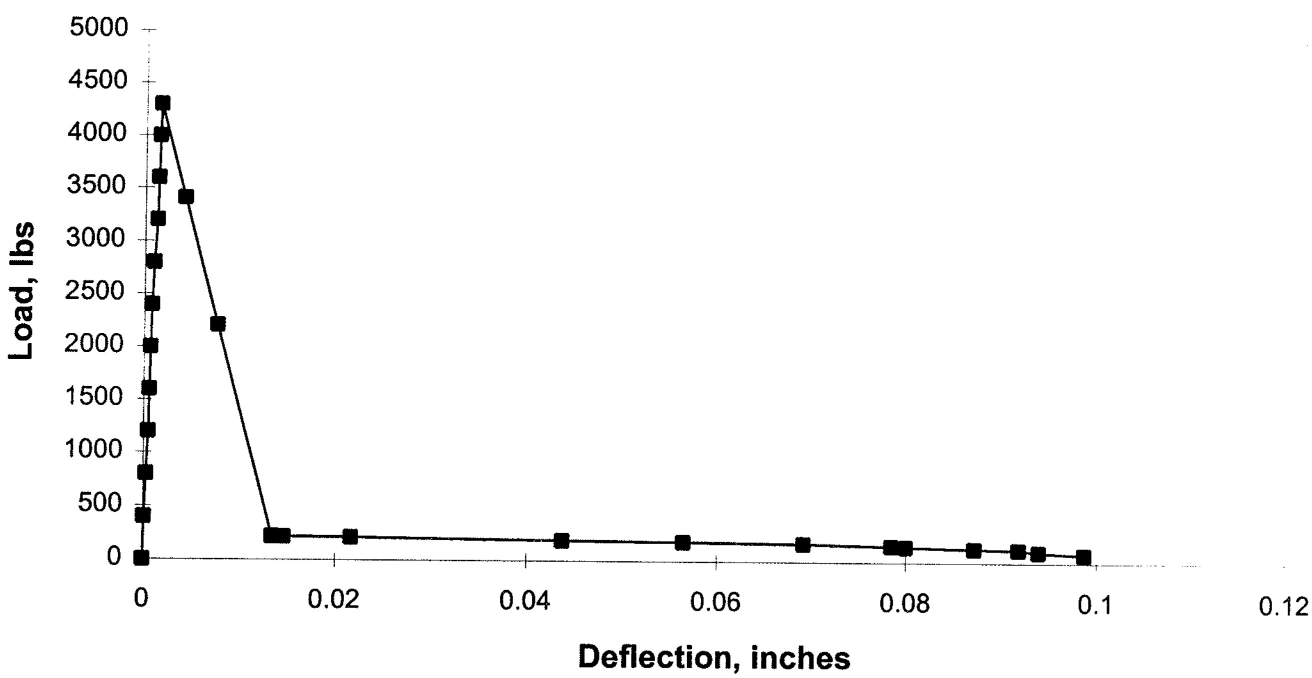

Fig. A4 LOAD DEFLECTION CURVE
Sp: BFRC2-4 (28 Day)

Conversion Factor:
25.4mm = 1in,1kg = 2.2lbs

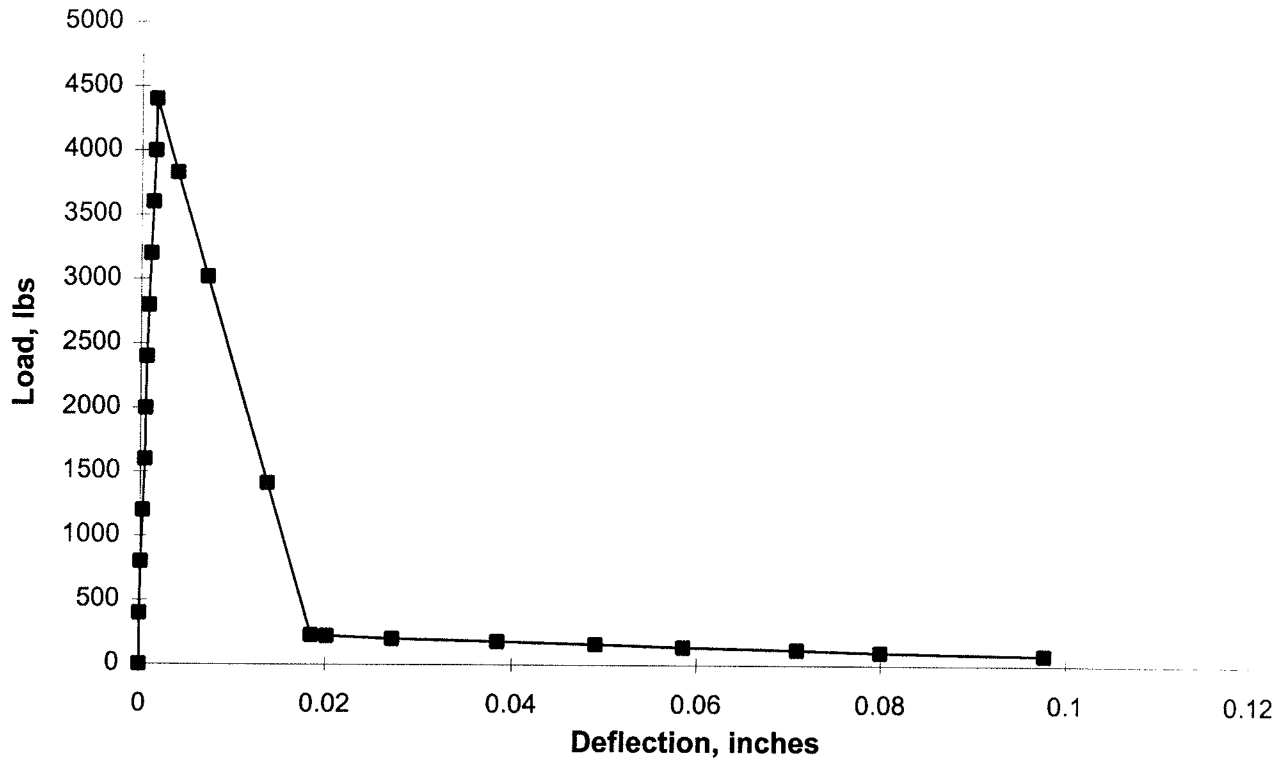

Fig. A5 LOAD DEFLECTION CURVE
Sp: BFRC2-5 (28 Day)

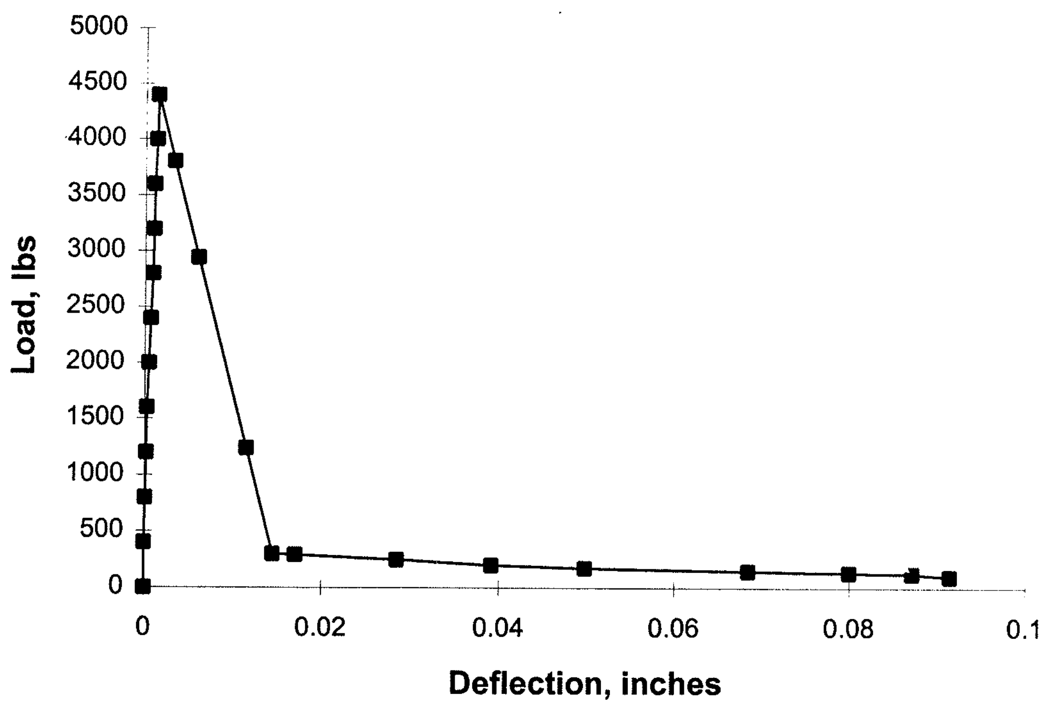

Conversion Factor:
25.4mm = 1in,1kg = 2.2lbs

Fig. A6 LOAD DEFLECTION CURVE
Sp: BFRC2-6 (28 Day)

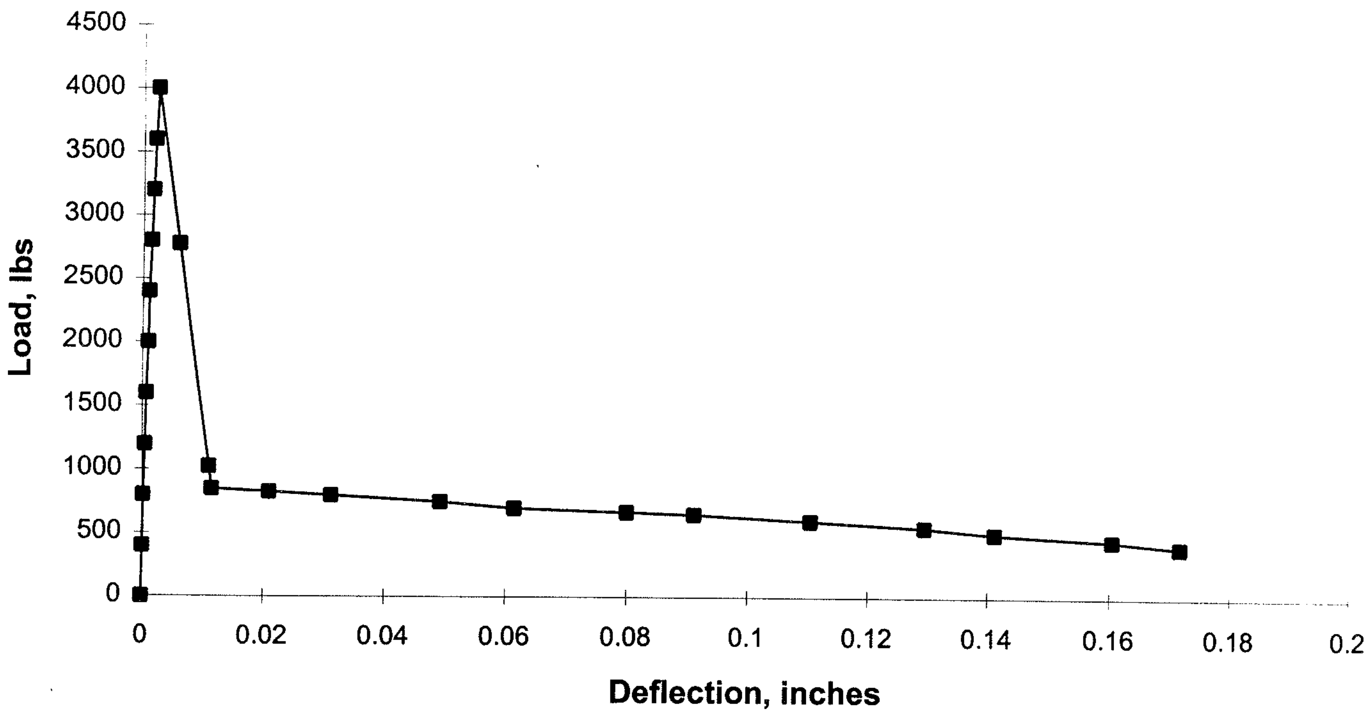

Fig. A7 LOAD DEFLECTION CURVE
Sp: BFRC3-1 (7 Day)

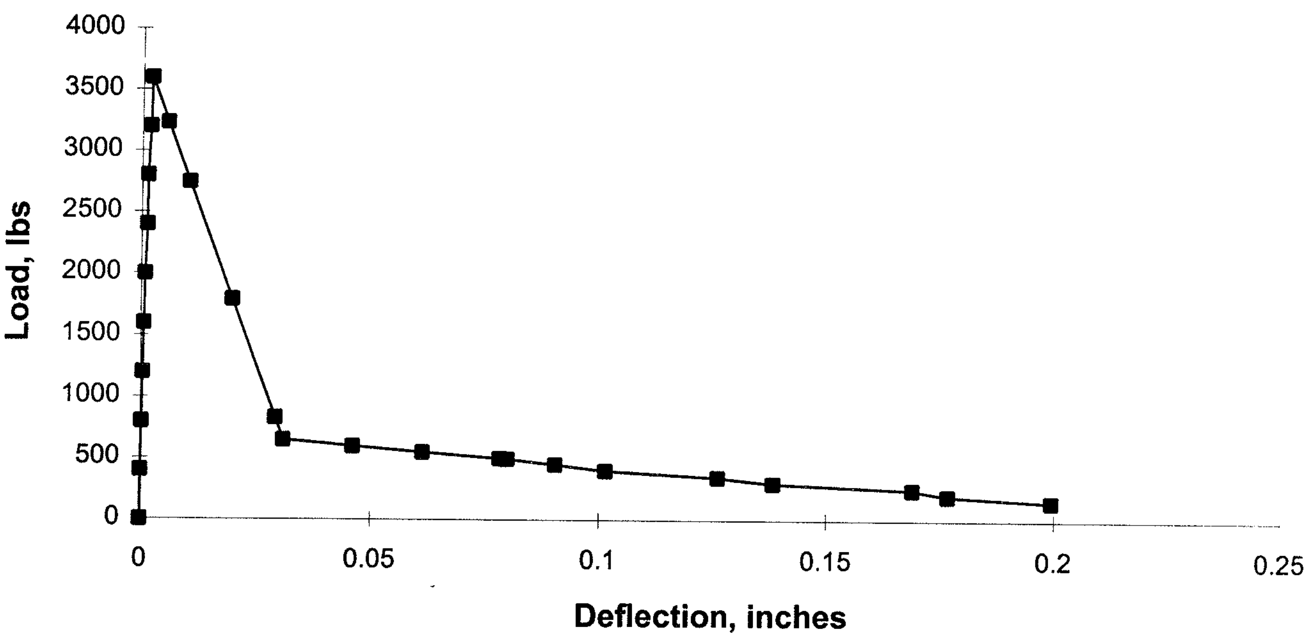

Conversion Factor:
25.4mm = 1in,1kg = 2.2lbs

Fig. A8 LOAD DEFLECTION CURVE
Sp: BFRC3-2 (7 Day)

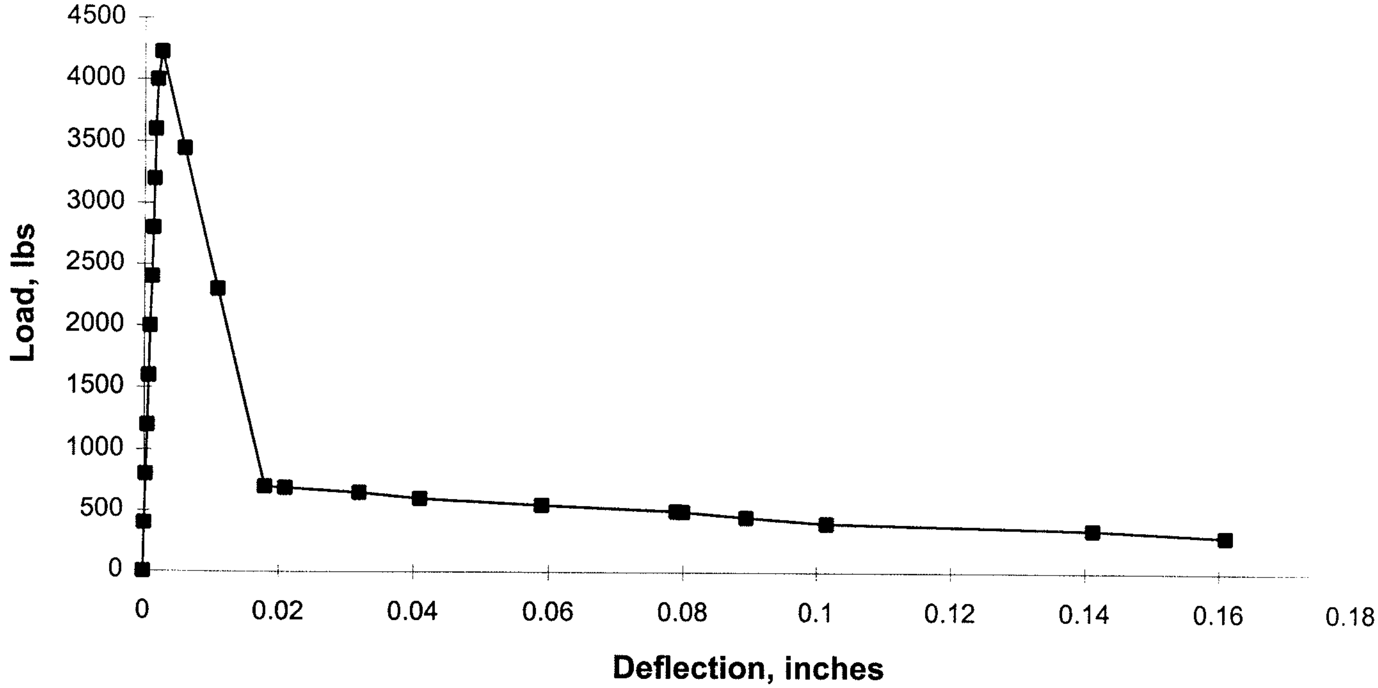

Conversion Factor:
25.4mm = 1in,1kg = 2.2lbs

Fig. A9 LOAD DEFLECTION CURVE
Sp: BFRC3-3 (7 Day)

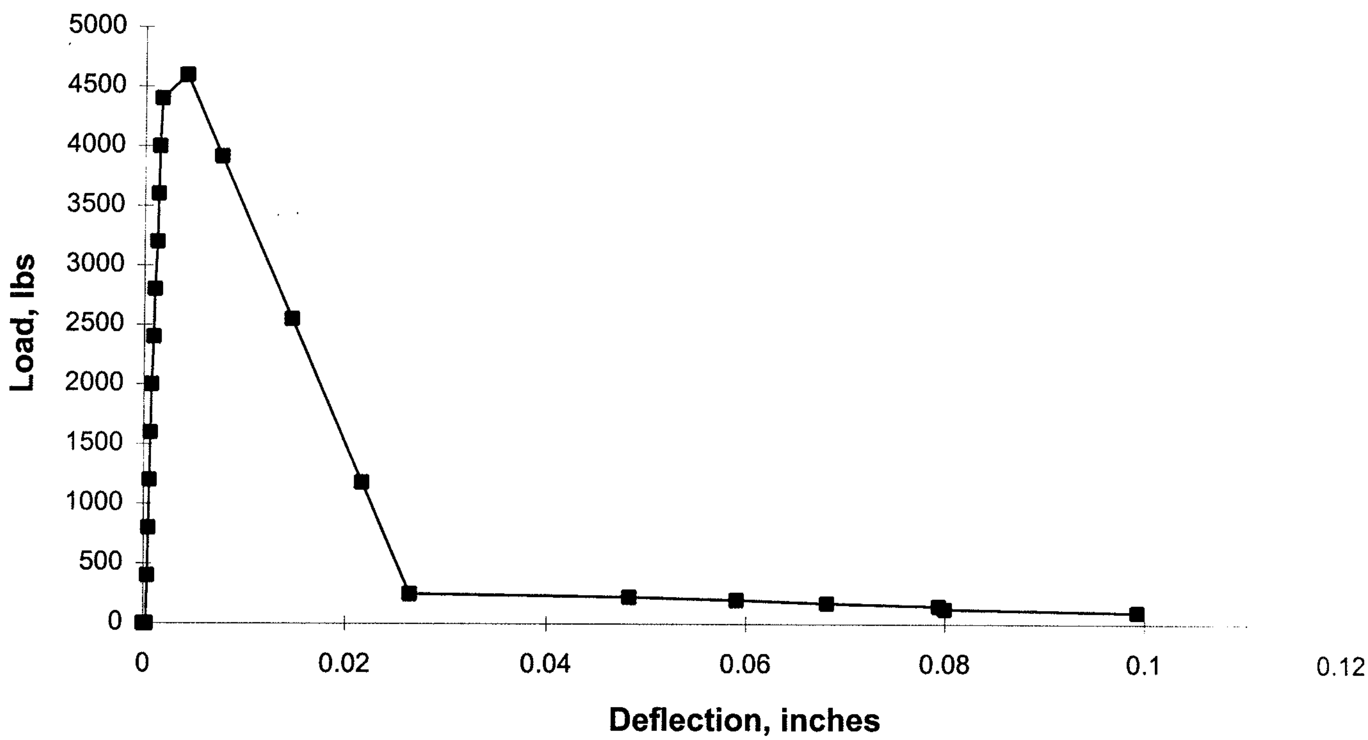

Fig. A10 LOAD DEFLECTION CURVE
Sp: BFRC3-4 (28 Day)

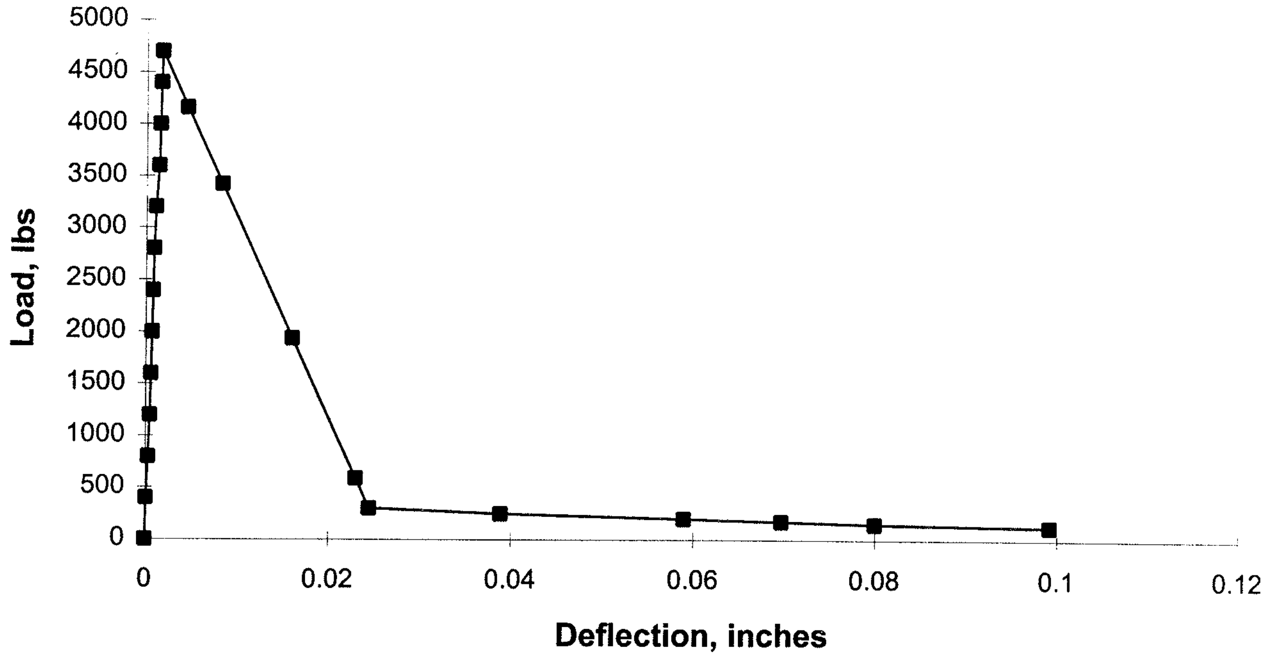

Fig. A11 LOAD DEFLECTION CURVE
Sp: BFRC3-5 (28 Day)

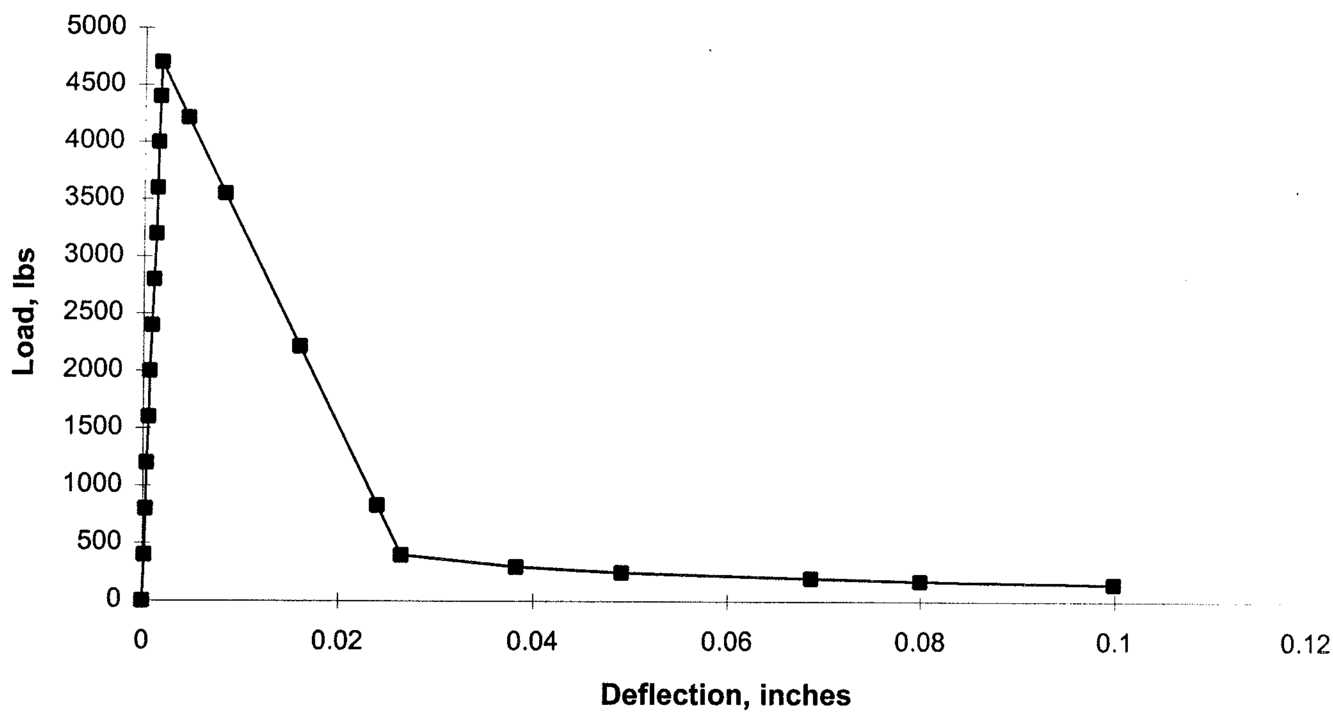

Fig. A12 LOAD DEFLECTION CURVE
Sp: BFRC3-6 (28 Day)

Conversion Factor:
25.4mm = 1in,1kg = 2.2lbs

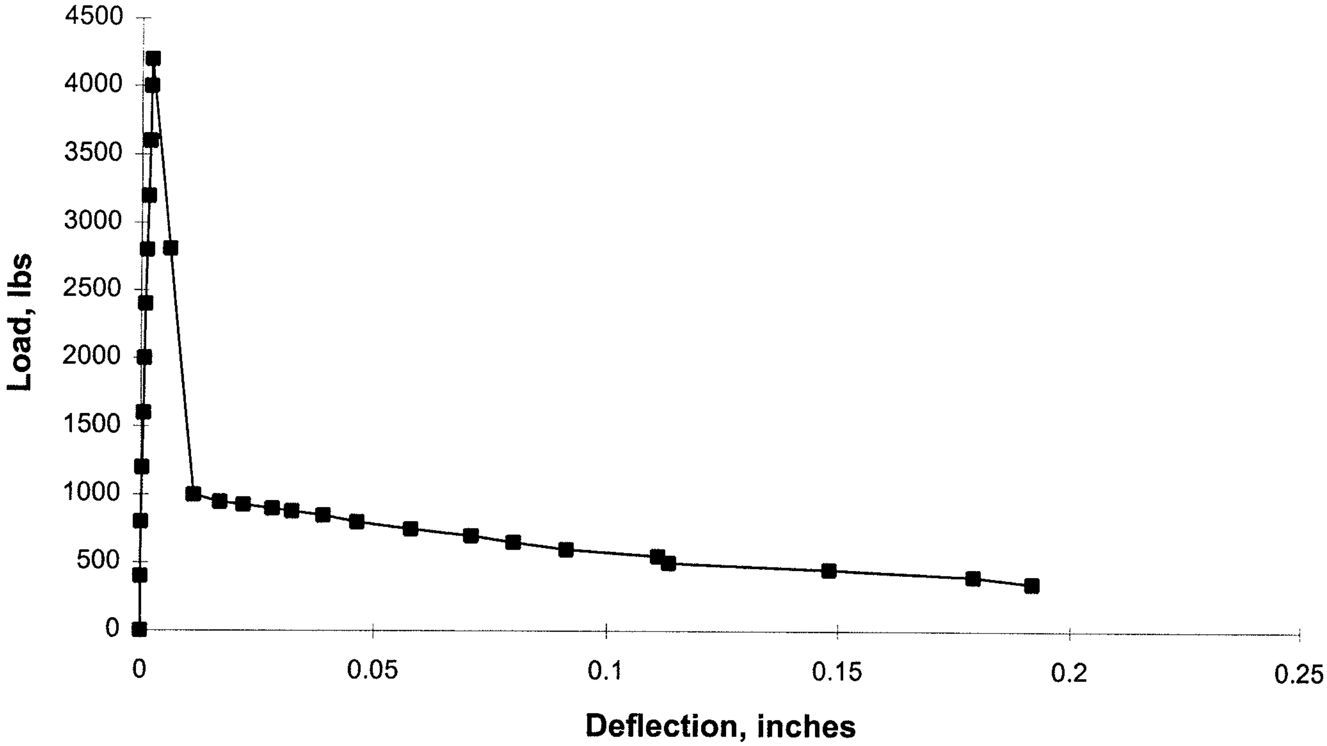

Fig. A13 LOAD DEFLECTION CURVE
Sp: BFRC4-1 (7 Day)

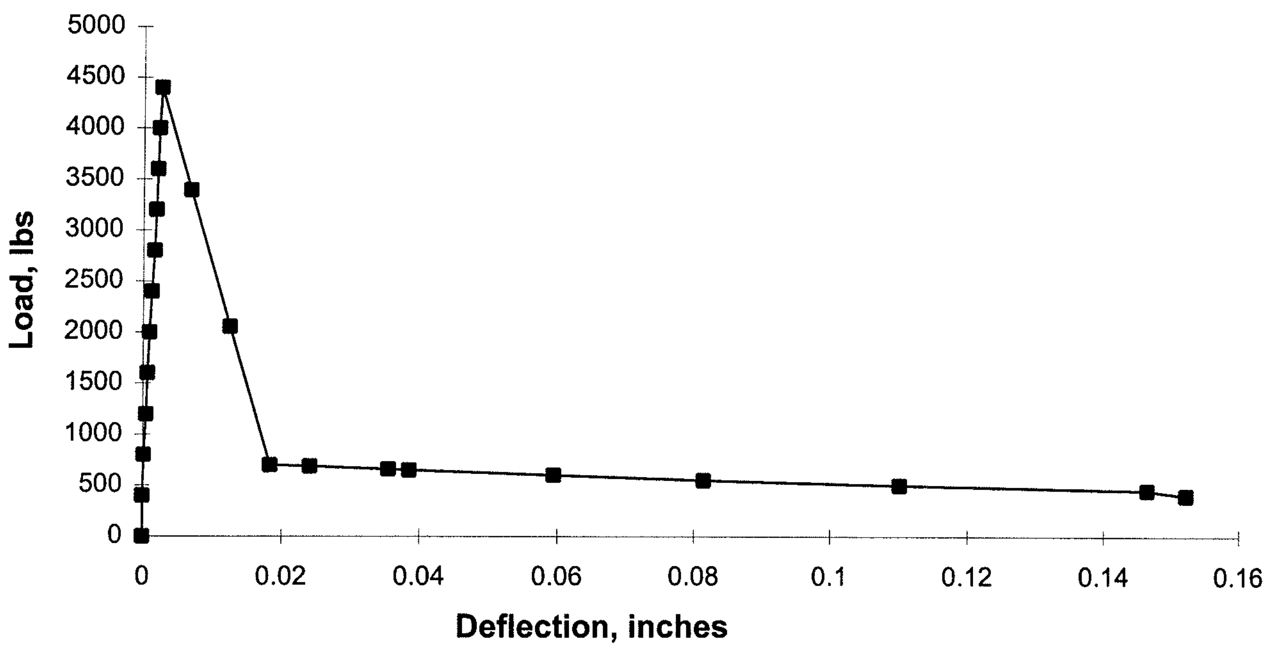

Conversion Factor:
25.4mm = 1in,1kg = 2.2lbs

Fig. A14 LOAD DEFLECTION CURVE
Sp: BFRC4-2 (7 Day)

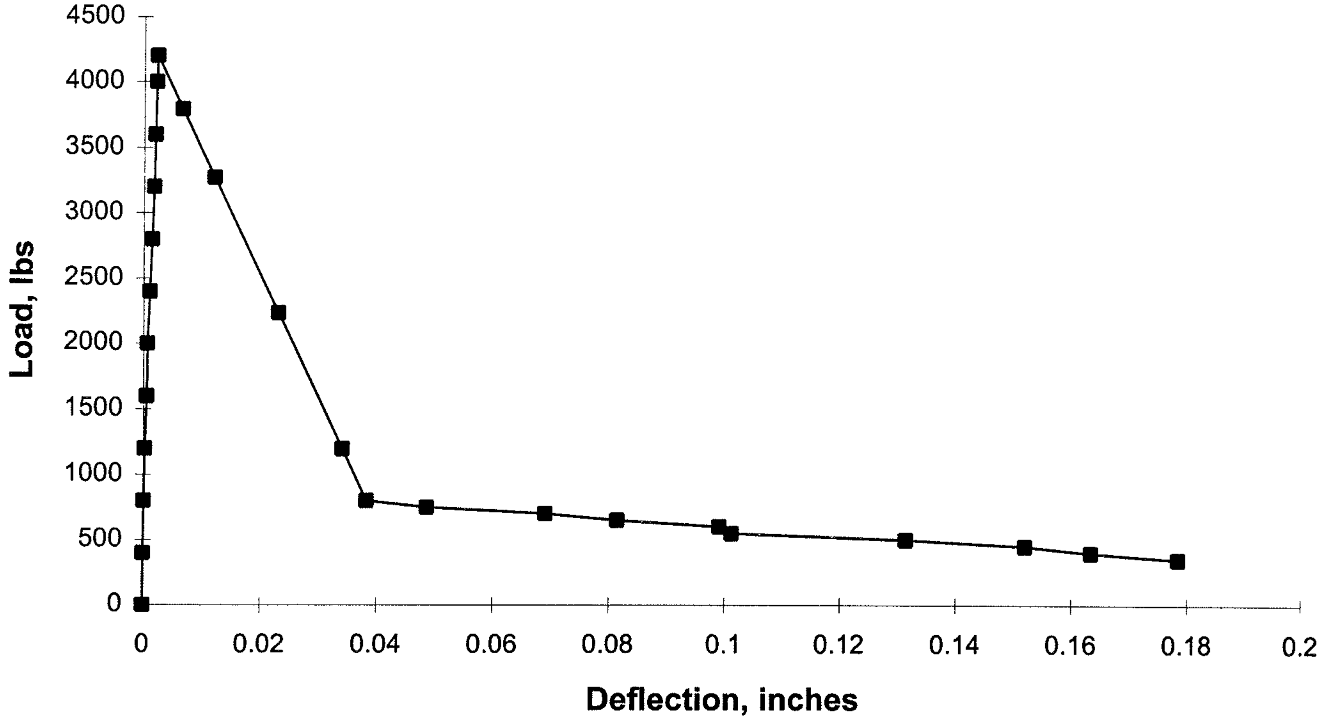

Fig. A15 LOAD DEFLECTION CURVE
Sp: BFRC4-3 (7 Day)

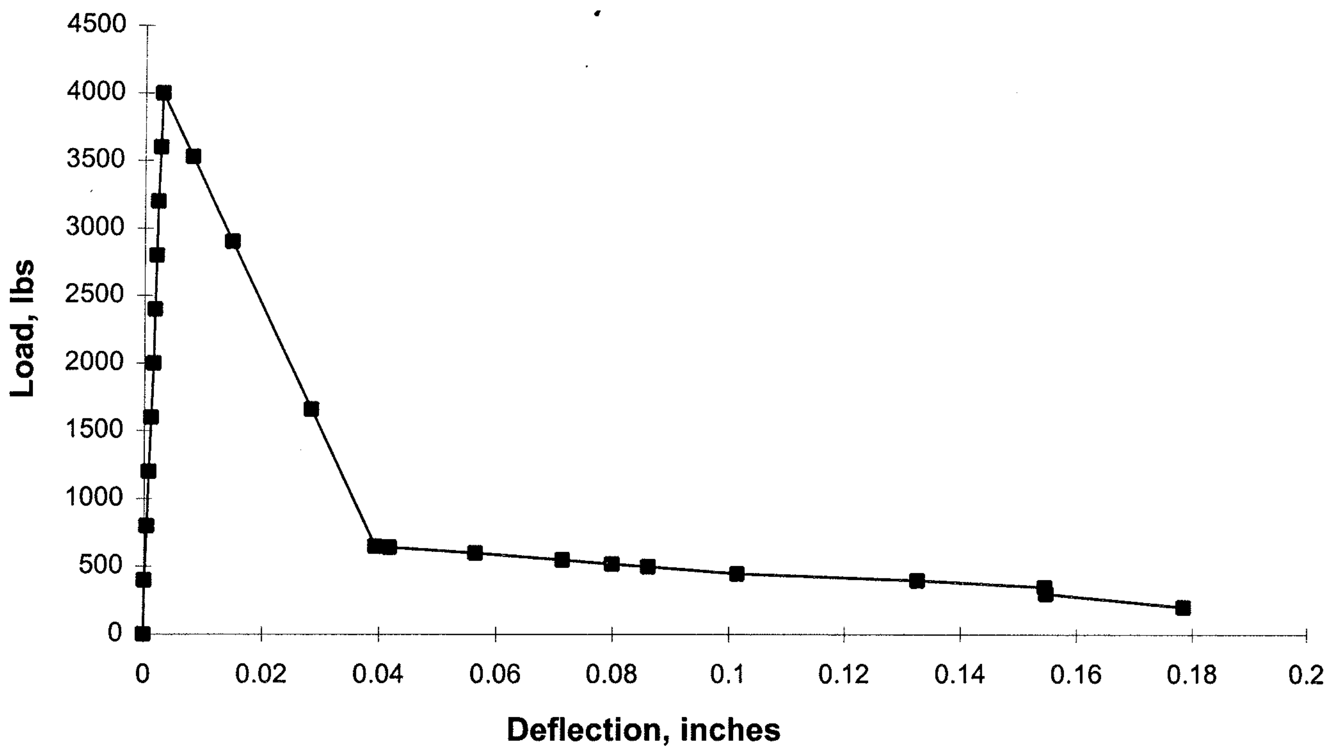

Fig. A16 LOAD DEFLECTION CURVE
Sp: BFRC5-1 (7 Day)

Conversion Factor:
25.4mm = 1in,1kg = 2.2lbs

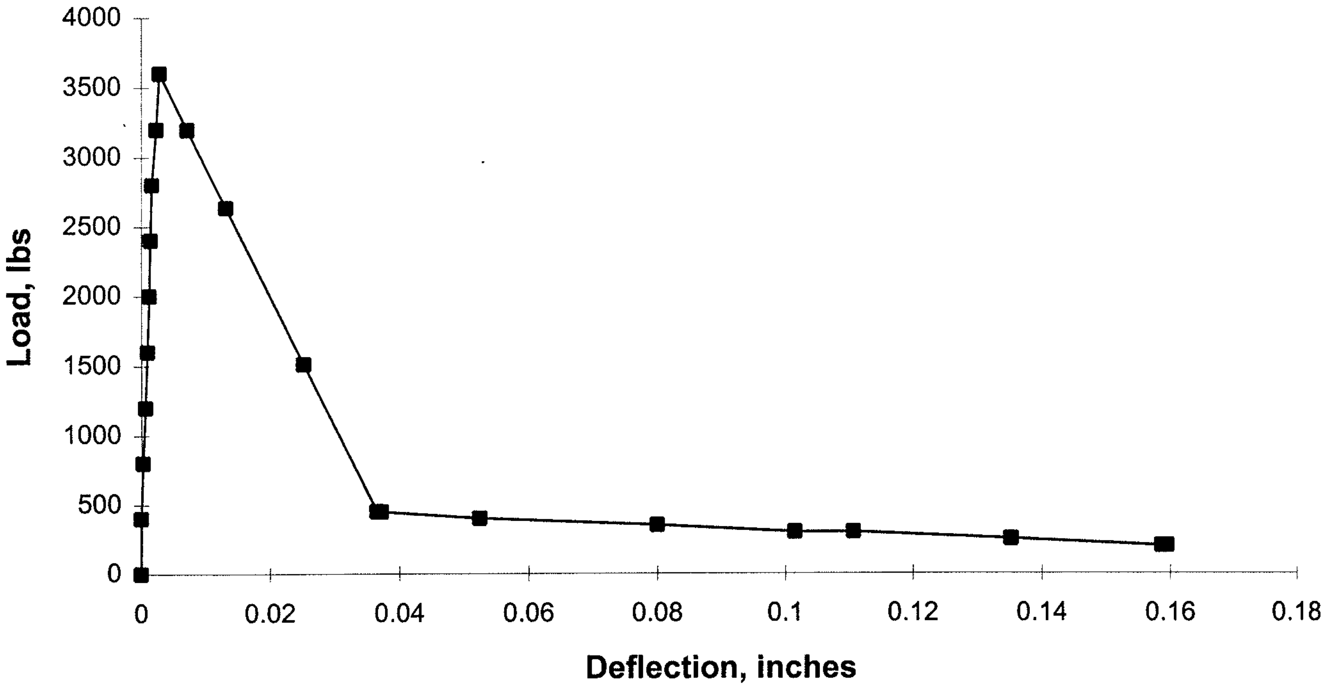

Fig. A17 LOAD DEFLECTION CURVE
Sp: BFRC5-2 (7 Day)

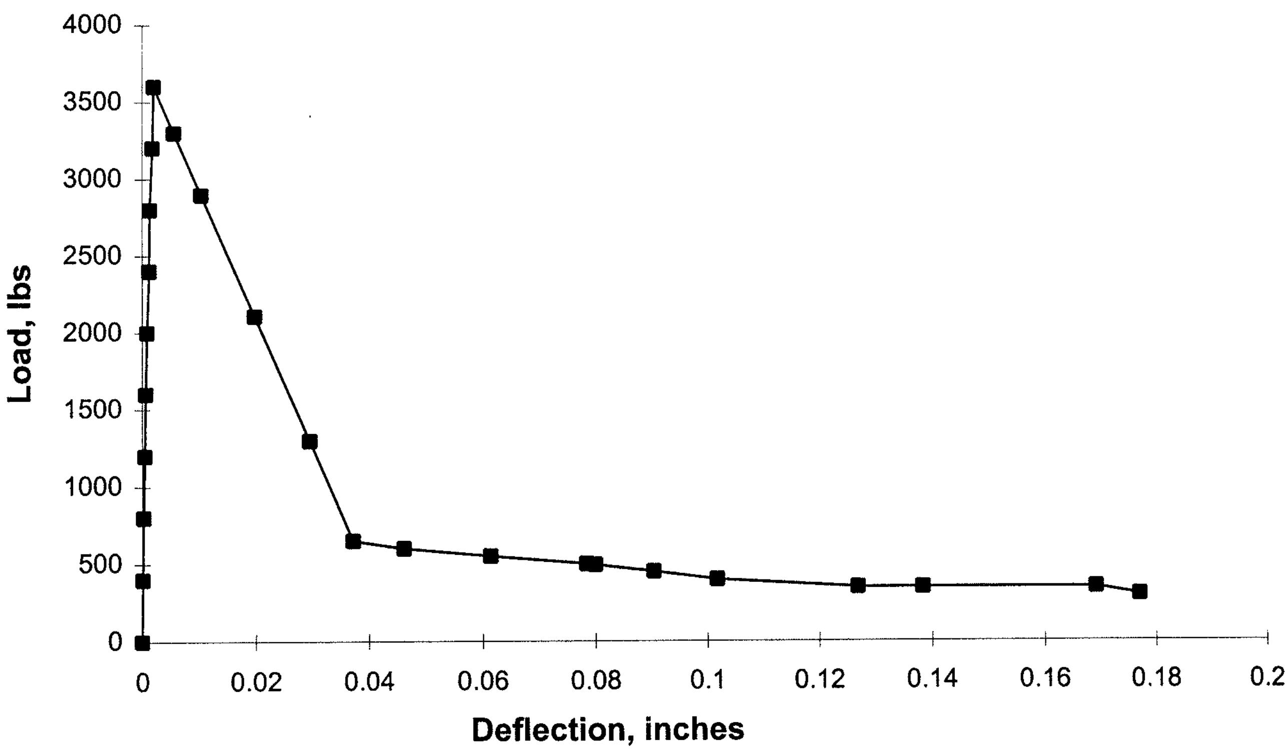

Conversion Factor:
25.4mm = 1in.1kg = 2.2lbs

Fig. A18 LOAD DEFLECTION CURVE
Sp: BFRC5-3 (7 Day)

APPENDIX B

LOAD-DEFLECTION CURVES FOR BEAMS BRC-A TO F

Table B1: Deflection Measurements for Beams BRC-A to C

BRC-A		BRC-B		BRC-C	
Load (lbs)	Deflection (in)	Load (lbs)	Deflection (in)	Load (lbs)	Deflection (in)
0	0	0	0	0	0
1000	0.0006	1000	0.0001	500	0.0003
2000	0.0013	2000	0.0017	1000	0.0048
3000	0.0020	3000	0.0023	2000	0.0055
4000	0.0026	4000	0.0027	3000	0.0059
5000	0.0032	5000	0.0032	4000	0.0062
6000	0.0037	6000	0.0037	6000	0.0068
7000	0.0041	7000	0.0041	7000	0.0072
8000	0.0045	8000	0.0043	8000	0.0075
9000	0.0048	9000	0.0107	9000	0.0078
10000	0.0050	8699	0.0129	10000	0.0082
11000	0.0053	7237	0.0236	11000	0.0086
12000	0.0057	6800	0.0268	12000	0.0088
13000	0.0059	7900	0.0394	13000	0.0090
14000	0.0060	8300	0.0452	14000	0.0091
15000	0.0061	8900	0.0561	15000	0.0095
16000	0.0063	9500	0.0667	11893	0.0273
9500	0.0189	9900	0.0800	7000	0.0386
10000	0.0298	10000	0.0983	5752	0.0500
10289	0.0346			5000	0.0689
10500	0.0419			4000	0.0800
11000	0.0586			3775	0.0955
11383	0.0662			3000	0.1000
12000	0.0800				
12500	0.0977				
13000	0.1123				

Conversion Factor:
25.4mm = 1in
1 kg = 2.2 lbs

Table B2: Deflection Measurements for Beams BRC-D to F

BRC-D		BRC-E		BRC-F	
Load (lbs)	Deflection (in)	Load (lbs)	Deflection (in)	Load (lbs)	Deflection (in)
0	0	0	0	0	0
1000	0.0006	500	0.0004	500	0.0010
2000	0.0010	1000	0.0007	1000	0.0015
3000	0.0014	1500	0.0009	1500	0.0020
4000	0.0025	2000	0.0011	2000	0.0025
5000	0.0041	2500	0.0013	2500	0.0030
6000	0.0053	3000	0.0016	2264	0.0090
7000	0.0062	3500	0.0019	1969	0.0165
8000	0.0068	4000	0.0020	1380	0.0315
9000	0.0072	4500	0.0022	1000	0.0412
7981	0.0204	5000	0.0041	1500	0.0663
6669	0.0374	5500	0.0050	2000	0.0800
6500	0.0396	6000	0.0056	2500	0.0880
5000	0.0512	6500	0.0060	2700	0.0920
4000	0.0696	7000	0.0069		
3826	0.0714	7500	0.0076		
3000	0.0800	8000	0.0083		
2000	0.0982	8500	0.0090		
1000	0.1080	9000	0.0100		
		9500	0.0109		
		10000	0.0120		
		8474	0.0105		
		7000	0.0591		
		7800	0.0792		
		8345	0.0822		
		9000	0.0863		
		9400	0.0882		
		9800	0.09		

Conversion Factor:
25.4mm = 1in
1 kg = 2.2 lbs

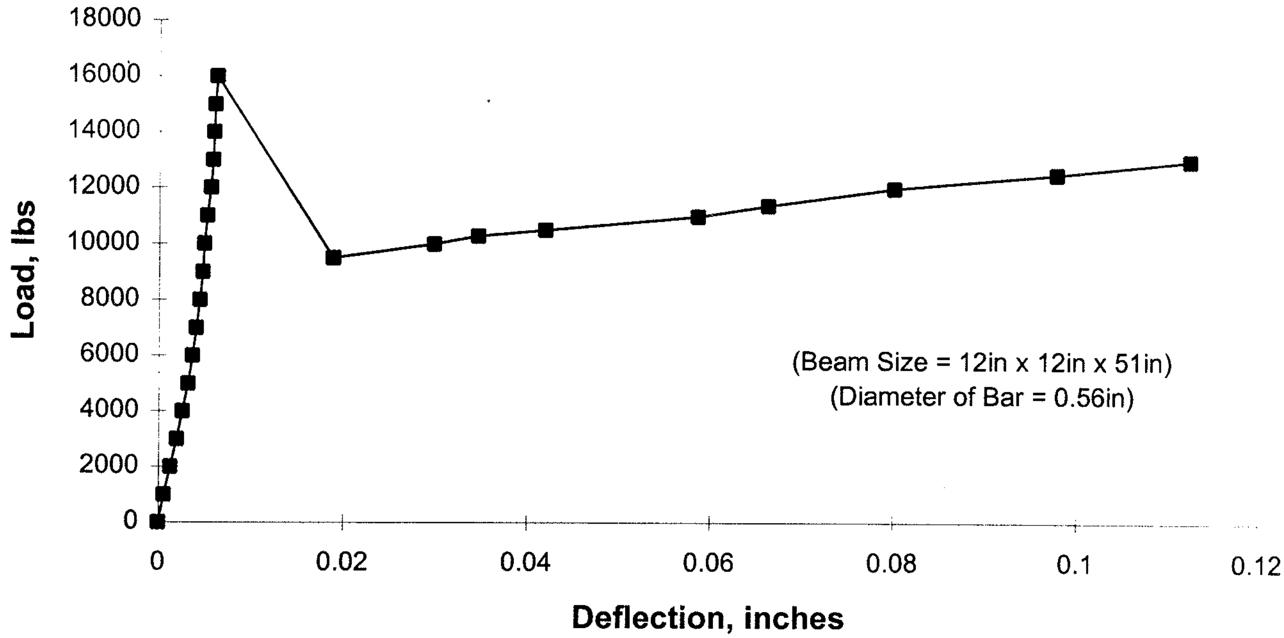

Conversion Factors:
1kg=2.2lbs,25.4mm=1in.

Fig. B1 LOAD DEFLECTION CURVE
Sp:BRC-A

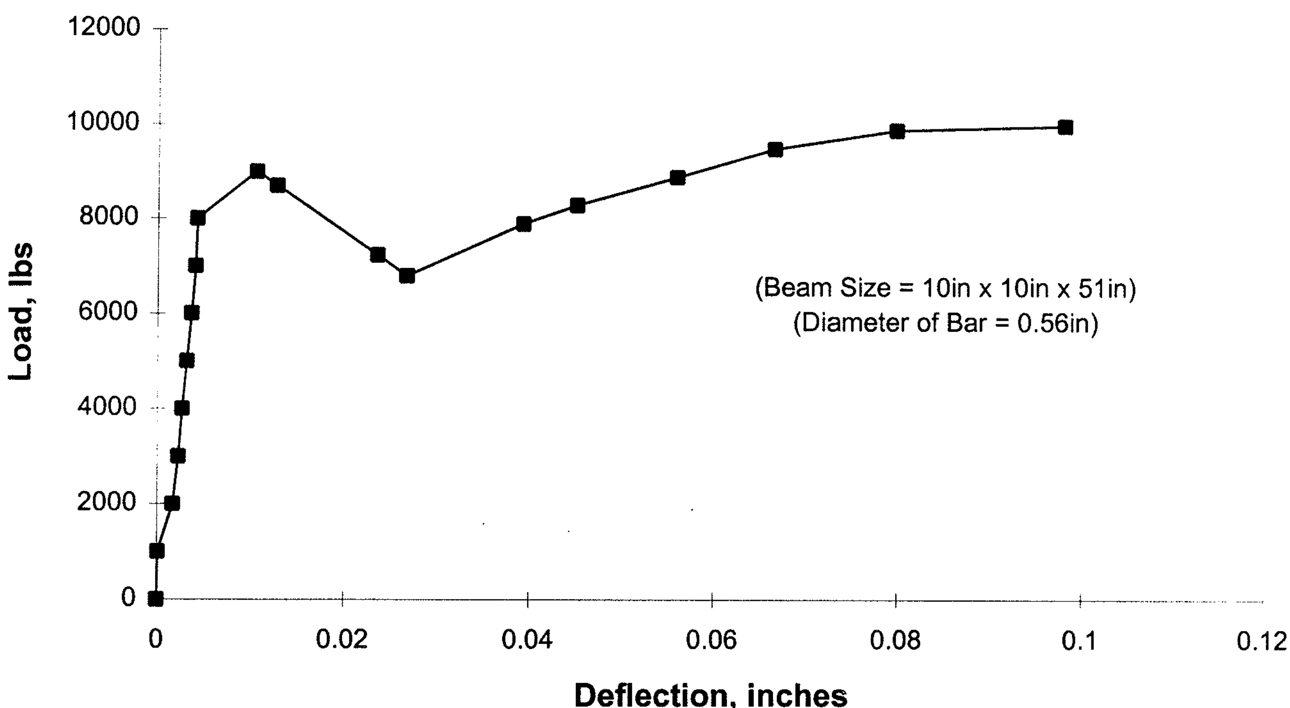

Conversion Factors:
1kg=2.2lbs,25.4mm=1in.

Fig. B2 LOAD DEFLECTION CURVE
Sp:BRC-B

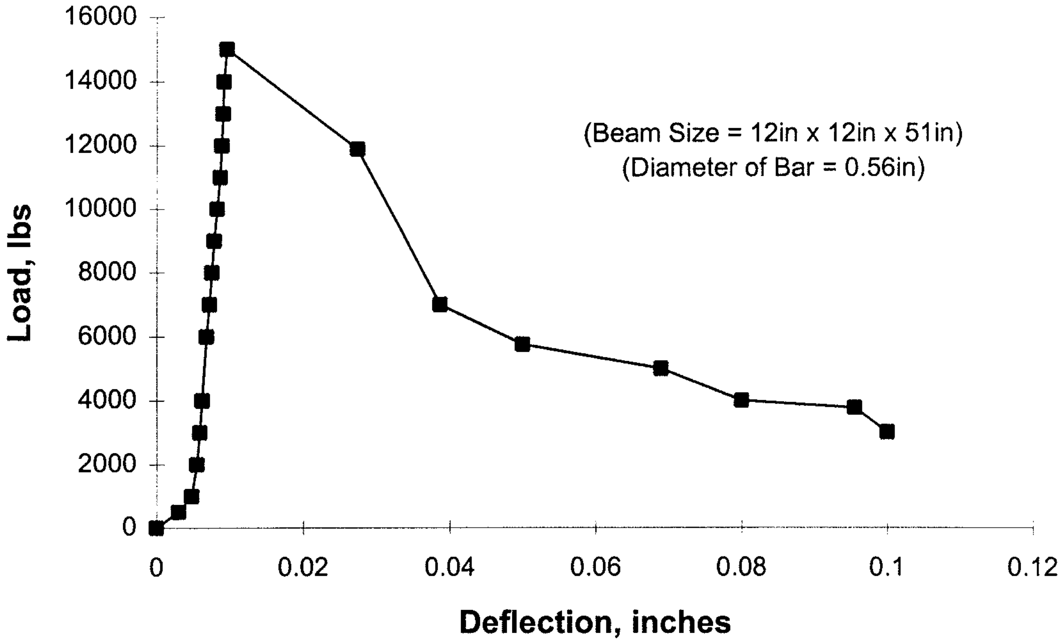

Conversion Factors:
1kg=2.2lbs,25.4mm=1in.

Fig. B3 LOAD DEFLECTION CURVE
Sp:BRC-C

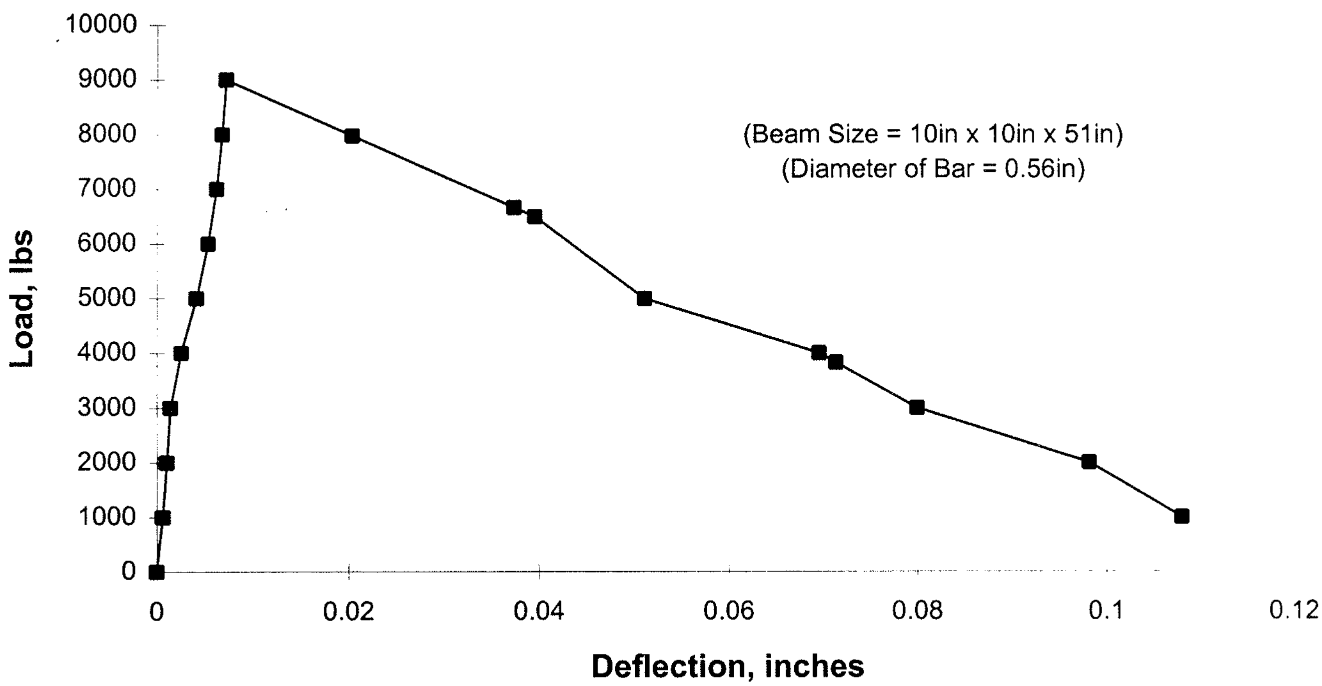

Conversion Factors:
1kg=2.2lbs,25.4mm=1in.)

FIg. B4 LOAD DEFLECTION CURVE
Sp:BRC-D

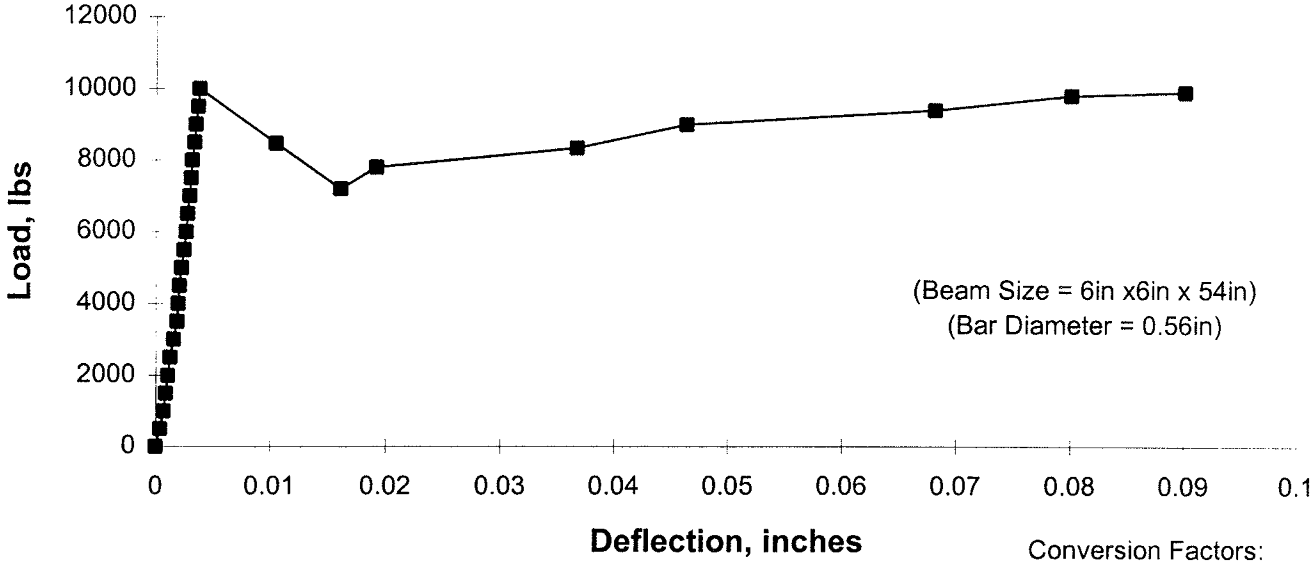

Conversion Factors:
1kg=2.2lbs,25.4mm=1in.

Fig. B5 LOAD DEFLECTION CURVE
Sp:BRC-E

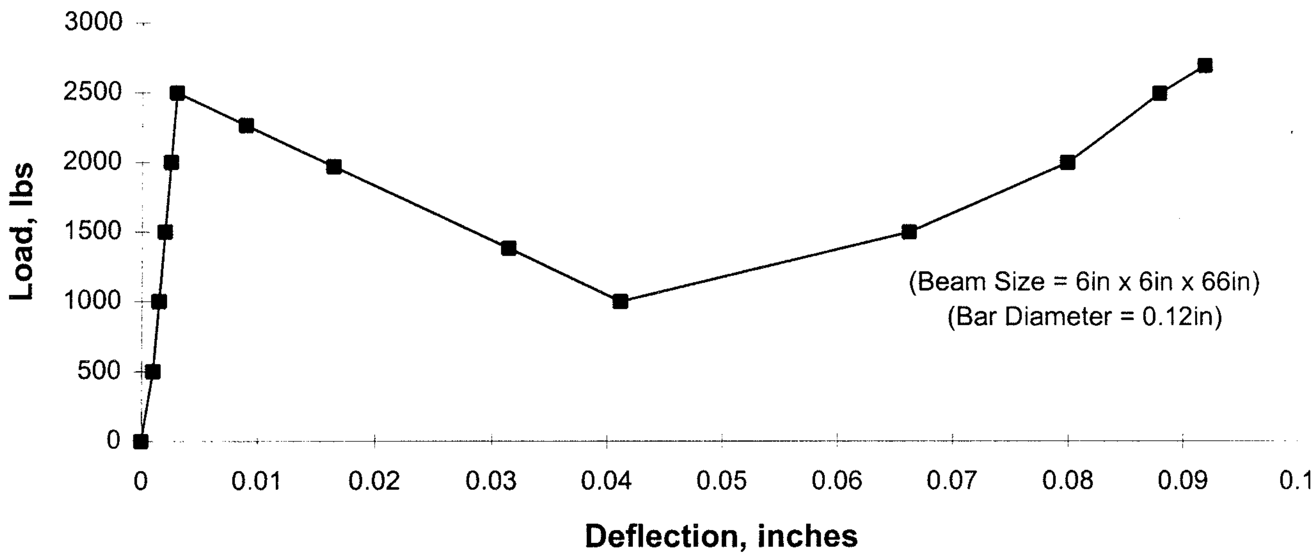

Fig. B6 LOAD DEFLECTION CURVE
Sp:BRC-F

Conversion Factors:
1kg=2.2lbs,25.4mm=1in.

APPENDIX C

LOAD-DEFLECTION CURVES
FOR
BEAMS BRC-1 TO 5

Table C1: Deflection Measurements for Beams BRC-1 to 5

BRC-1		BRC-2		BRC-3		BRC-4		BRC-5	
Load (lbs)	Deflection (in)	Load (lbs)	Deflection (in)	Load (lbs)	Deflection (in)	Load (lbs)	Deflection (in)	Load (lbs)	Deflection (in)
0	0	0	0	0	0	0	0	0	0
400	0.0001	400	0.0001	400	0.0001	400	0.0001	400	0.0001
800	0.0003	800	0.0002	800	0.0004	800	0.0002	800	0.0003
1200	0.0004	1200	0.0004	1200	0.0006	1200	0.0003	1200	0.0005
1600	0.0006	1600	0.0005	1600	0.0008	1600	0.0005	1600	0.0006
2000	0.0007	2000	0.0007	2000	0.0010	2000	0.0006	2000	0.0007
2400	0.0009	2400	0.0009	2400	0.0014	2400	0.0008	2400	0.0009
2800	0.0011	2800	0.0010	2800	0.0016	2800	0.0009	2800	0.0010
3200	0.0013	3200	0.0011	3200	0.0017	3200	0.0011	3400	0.0013
3600	0.0014	3600	0.0014	3300	0.0018	3600	0.0012	3500	0.0015
4000	0.0015	3800	0.0015	3048	0.0048	4000	0.0014	3244	0.0039
4400	0.0016	4000	0.0016	2712	0.0088	4400	0.0015	2893	0.0072
3890	0.0045	3611	0.0042	2040	0.0168	4600	0.0017	2200	0.0137
3221	0.0083	3088	0.0077	1000	0.0292	4108	0.0045	1200	0.0231
1903	0.0158	2041	0.0147	1350	0.0497	3440	0.0083	1400	0.0498
1200	0.0198	1100	0.0210	1800	0.0681	2123	0.0158	1600	0.0682
1400	0.0314	1385	0.0398	2100	0.0800	1000	0.0222	2000	0.0800
1600	0.0528	1500	0.0510	2265	0.1281	1400	0.0487	2400	0.1021
2000	0.0692	1700	0.0712	2672	0.1422	2000	0.0612	2800	0.1451
2400	0.0800	2000	0.0800	2934	0.1617	2300	0.0800	3300	0.1683
2800	0.1121	2300	0.0992	3128	0.1821	2800	0.1121		
3200	0.1348	2600	0.1181	3200	0.1973	3100	0.1392		
3500	0.1562	2900	0.1434			3600	0.1498		
3900	0.1783	3400	0.1683			4100	0.1681		
4300	0.1897	3985	0.1892			4500	0.1797		

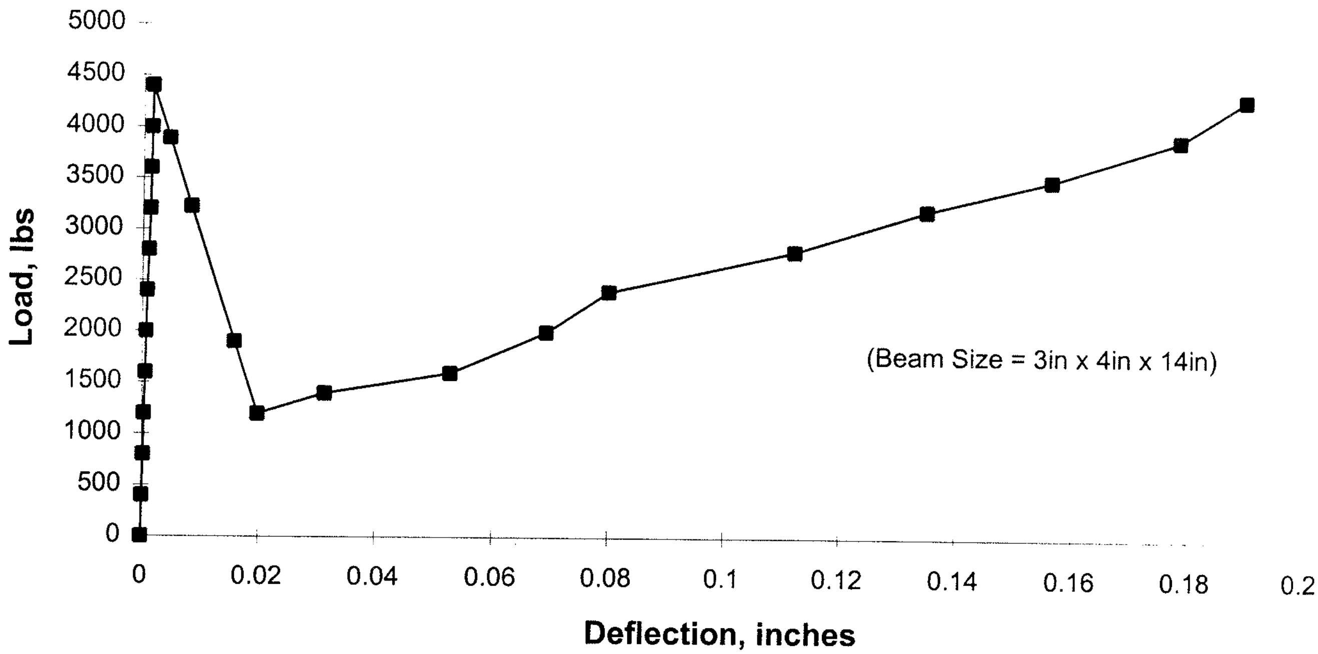

Conversion Factors:
1kg=2.2lbs,25.4mm=1in.

Fig. C1 LOAD DEFLECTION CURVE
Sp: BRC1

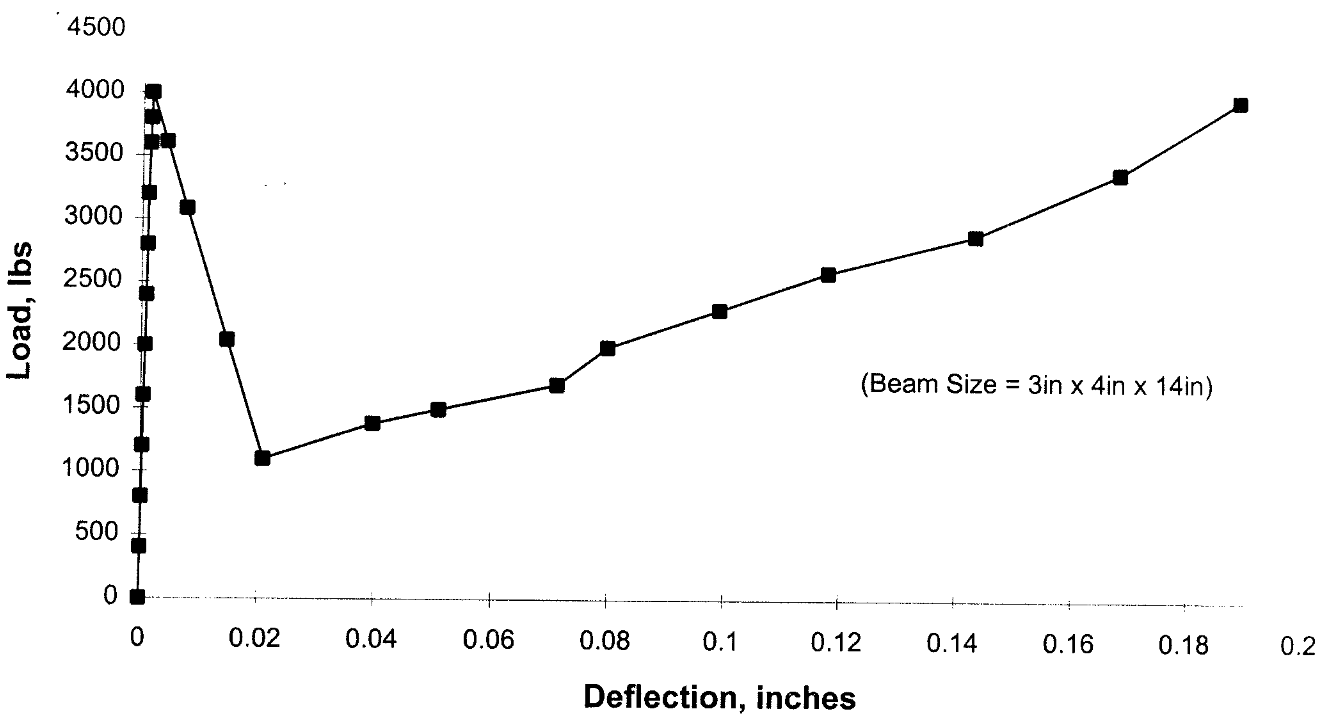

Conversion Factors:
1kg=2.2lbs,25.4mm=1in.

Fig. C2 LOAD DEFLECTION CURVE
Sp:BRC2

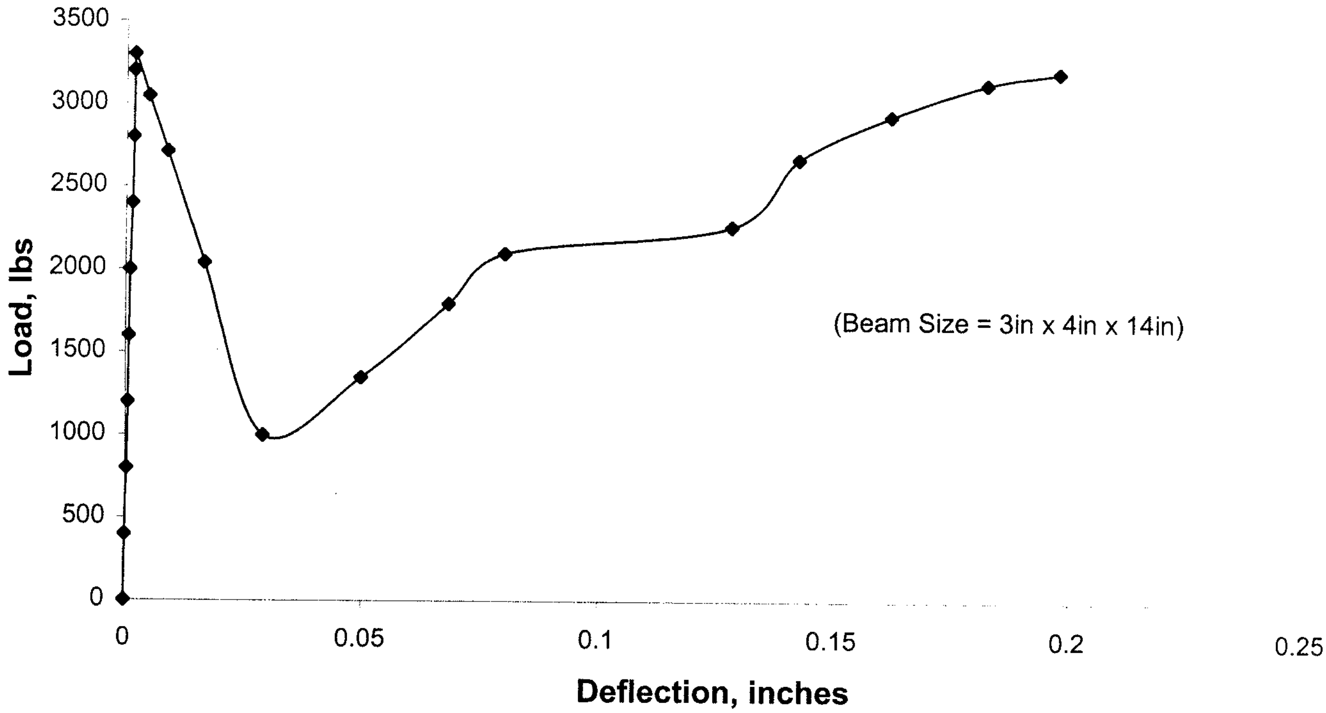

Fig. C3 LOAD DEFLECTION CURVE
Sp:BRC3

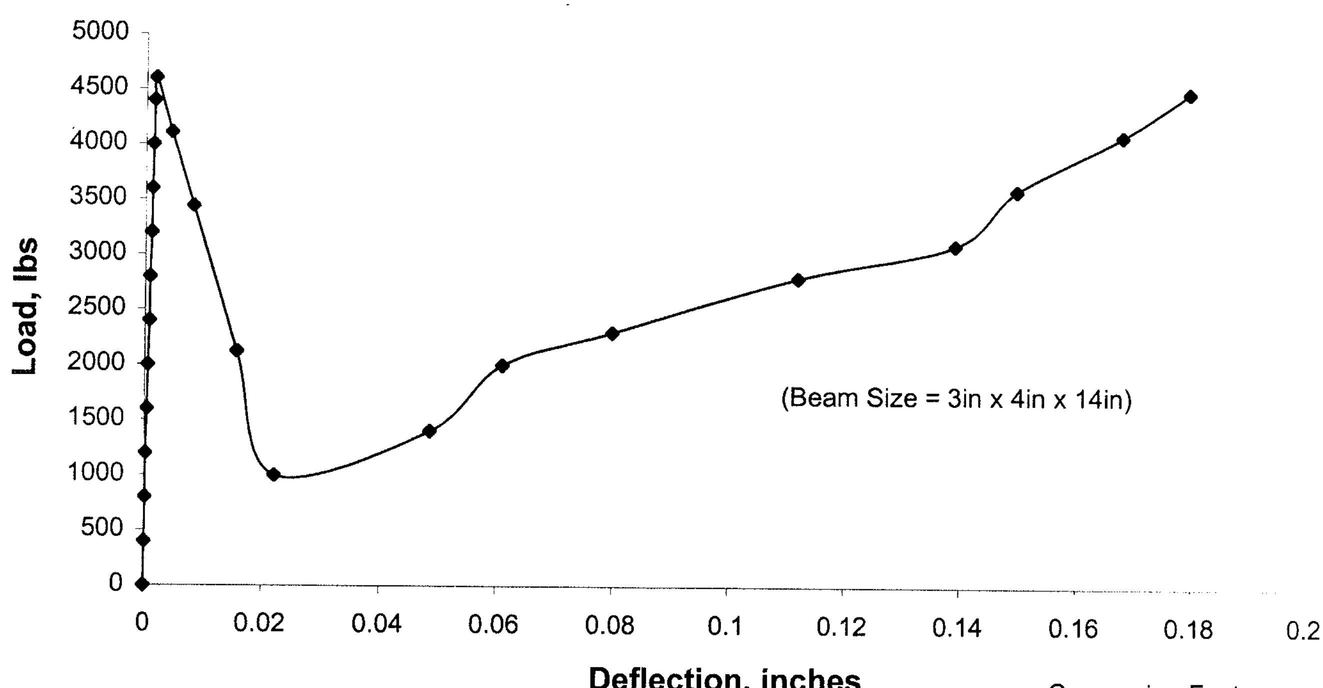

Conversion Factors:
1kg=2.2lbs,25.4mm=1in.

Fig. C4 LOAD DEFLECTION CURVE
Sp:BRC4

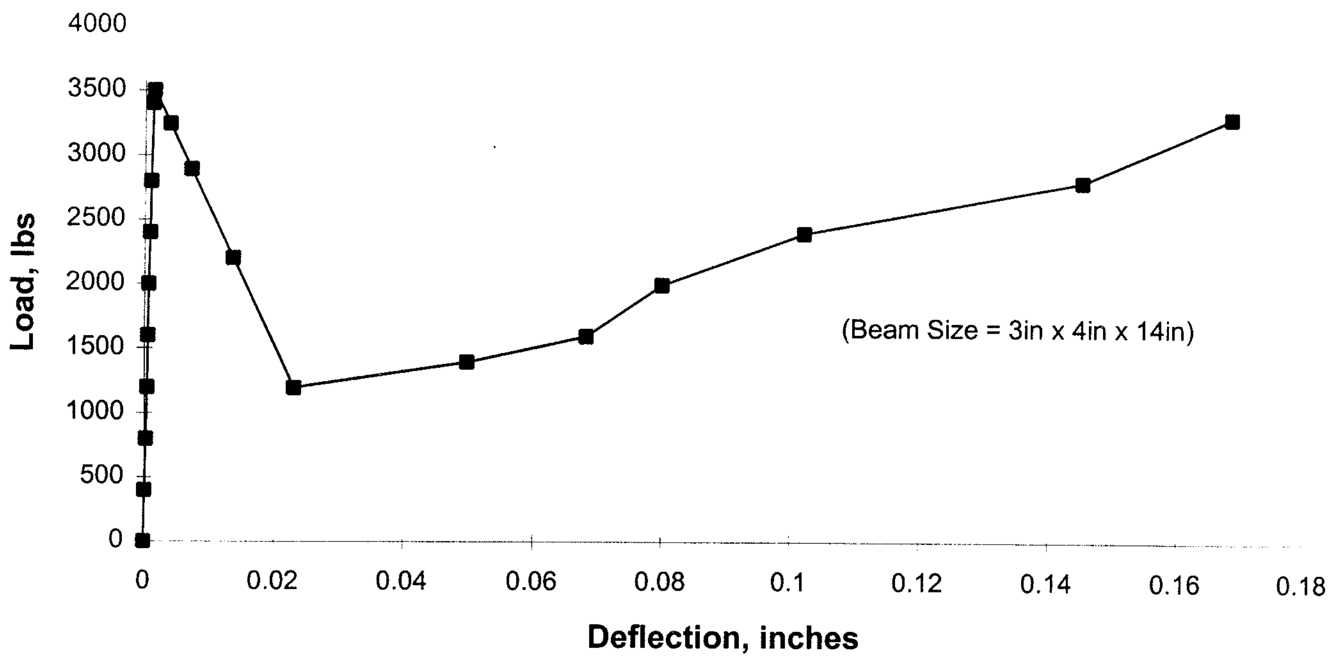

Conversion Factors:
1kg=2.2lbs,25.4mm=1in.

Fig. C5 LOAD DEFLECTION CURVE
Sp:BRC5